Technische Universität München

Institute for Diabetes and Obesity (IDO)

Helmholtz Zentrum München

Post-transcriptional regulation by RNA-binding proteins in CD4$^+$ T helper cells

Christian Alexander Johannes Gallus

Vollständiger Abdruck der von der Fakultät für Medizin der Technischen Universität München zur Erlangung des akademischen Grades eines **Doktors der Naturwissenschaften (Dr. rer. nat.)** genehmigten Dissertation.

Vorsitzender:	Prof. Dr. Percy A. Knolle
Prüfer der Dissertation:	1. Prof. Dr. Matthias Tschöp
	2. Prof. Dr. Michael Sattler

Die Dissertation wurde am 26.11.2018 bei der Technischen Universität München eingereicht und durch die Fakultät für Medizin am 15.05.2019 angenommen.

1. Abstract

Post-transcriptional gene regulation is an essential layer to control cellular development, identity and function. Although there are a multitude of studies concerning post-transcriptional regulation in different types of immune cells, many questions remain unanswered.

In this thesis, we investigated proteins as well as mechanisms of post-transcriptional regulation in *in vitro* generated primary T effector (T_{eff}) and Foxp3 expressing regulatory T (Treg/T_{Foxp3+}) cells. To this end, we employed a technique recently developed by Landthaler and Hentze termed "interactome capture", which allows capture of all RNA-binding proteins (RBPs) bound to the total mRNA in a cell (the "RBPome"). We identified the RBPome of two T helper cell subsets, namely T_{eff} as well as T_{Foxp3+} cells. From this we could determine the overlapping $CD4^+$ RBPome present in both subsets with 240 proteins as well as 57 and 6 preferentially bound RBPs in T_{eff} and T_{Foxp3+} cells respectively. We analyzed the biochemical as well as structural properties of these proteins and showed that our data are in line with previously published RBPome datasets. Additionally, we generated RNA sequencing and proteome data for the two cell types and their integration resulted in identification of different promising subgroups of proteins with potentially important functions in T helper cell stability and/or function. Furthermore, when we compared the identified proteins with other datasets we found 14 proteins, which were previously not detected in any mammalian RBPome. Of these proteins, especially the identification of known transcription factors Stat1, Stat4 and Vav1 as mRNA-binding proteins illustrates the extensive and so far still insufficiently studied multifunctionality of proteins as well as their ability to cross-connect different types of signaling pathways.

In a following approach we specifically focused the analysis on Treg cells, which are crucial for the maintenance of immune homeostasis and investigated a possible post-transcriptional regulatory mechanism of their lineage defining transcription factor Foxp3. Again, we tried to identify the responsible RBPs as well as the inducing external conditions of this regulatory process. Although we were able to capture *Foxp3* mRNA via a specific pull down assay, due to technical limitations it was not possible to identify the respective bound RBPs. However, we revealed the presence of different isoforms of *Foxp3* mRNA, which further substantiates our hypothesis of its post-transcriptional regulation.

Altogether, we provide a resource of post-transcriptional factors likely having important regulatory functions in T cells, which can be utilized as a starting point for a multitude of promising follow-up studies of gene regulation in T helper cells.

2. Zusammenfassung

Posttranskriptionelle Genregulation ist eine essentielle Kontrollebene bei der Entwicklung, Differenzierung und Funktion von Zellen. Trotz einer Vielzahl von Studien bezüglich posttranskriptioneller Regulation in verschiedenen Immunzellen bleiben weiterhin viele Fragen unbeantwortet.

Das Ziel dieser Doktorarbeit war die Identifizierung von Proteinen sowie eine Untersuchung ihrer Funktionsmechanismen in der posttranskriptionellen Regulation in *in vitro* generierten T effektor (T_{eff}) und Foxp3 exprimierenden regulatorischen T (Treg/T_{Foxp3+}) Zellen. Dazu verwendeten wir die kürzlich von Landthaler und Hentze entwickelte Methode "interactome capture" zur Bestimmung aller RBPs, die an die gesamte mRNA in einer Zelle gebunden sind (das sog. "RBPome"). Daraufhin konnte das RBPome von zwei Unterklassen von T-Helferzellen (T_{eff} und T_{Foxp3+} Zellen) ermittelt werden. Hieraus ließ sich das "$CD4^+$ RBPome" ableiten, welches aus den 240 überschneidenden Proteine besteht. Außerdem wurden 57 bzw. 6 RBPs jeweils ausschließlich in T_{eff} oder T_{Foxp3+} Zellen gemessen. Eine Analyse der biochemischen sowie strukturellen Eigenschaften der Proteine zeigte große Gemeinsamkeiten mit bereits publizierten RBPome Datensets. Zusätzlich wurden durch RNA Sequenzierung und Proteome Messung weitere Daten für die beiden Zellunterklassen generiert. Nach deren Eingliederung konnten die Proteine in verschiedene vielversprechende Gruppen eingeteilt werden, die potentiell Einfluss auf die T-Helferzellstabilität und/oder –funktion ausüben. Ein Vergleich mit anderen RBPome Datensets ergab, dass 14 der Proteine bisher noch unentdeckt waren. Besonders die Identifizierung der bekannten Transkriptionsfaktoren Stat1, Stat4 und Vav1 als mRNA-bindende Proteine zeigt, dass die Multifunktionalität von Proteinen sowie deren Fähigkeit verschiedene Signaltransduktionswege zu vernetzen weiterhin offene Fragen beinhaltet.

In einem darauf folgenden Ansatz wurde der Fokus speziell auf regulatorische T Zellen gelegt, welche für die Aufrechterhaltung des Immungleichgewichts verantwortlich sind. Dabei sollte ein möglicher posttranskriptioneller Regulationsmechanismus des identitätsbestimmenden Transkriptionsfaktors Foxp3 untersucht werden. Dementsprechend sollten wieder die daran beteiligten RNA-bindenden Proteine (RBPs), sowie die extrazellulären Bedingungen identifiziert werden, welche für diesen regulatorischen Prozess verantwortlich sind. Obwohl es gelang mithilfe eines Pulldown-Assays spezifisch *Foxp3* mRNA anzureichern, war es aufgrund von technischen Schwierigkeiten nicht möglich, daran gebundene RNA-bindende Proteine nachzuweisen. Es konnten allerdings mehrere unterschiedliche Isoformen von *Foxp3* mRNA in T_{Foxp3+} Zellen nachgewiesen werden, was die Hypothese hinsichtlich der posttranskriptionellen Regulation dieser mRNA zusätzlich unterstützt.

Zusammenfassend stellen wir einen Fundus an posttranskriptionellen Faktoren mit höchstwahrscheinlich wichtigen regulatorischen Funktionen in T Zellen zur Verfügung, der als Ausgangspunkt für eine Vielzahl von weiterführenden Untersuchungen zur Genregulation verwendet werden kann.

Table of Contents

.....1

1. Abstract 2

2. Zusammenfassung.....3

3. Introduction.....6
3.1 The immune system 6
3.2 Regulatory T cells and their function.....7
3.3 The transcription factor Foxp3 and the Treg cell signature.....11
3.4 Regulation of gene expression by RNA-binding proteins.....12
3.5 Characteristics of RNA-binding proteins.....16
3.6 Regulation of development and function of immune cells via RBPs 17
3.7 Aim of the study.....19

4. Materials..... 21
4.1 Antibodies 21
4.2 Cytokines.....21
4.3 Oligonucleotides 22
4.4 Buffers.....24
4.5 Mice 26
4.6 Chemicals, enzymes, devices and kits.....26

5. Methods 29
5.1 Bacterial culture 29
5.1.1 Bacterial culture 29
5.1.2 Transformation of bacteria..... 29
5.2 Cell culture and viral transduction.....29
5.2.1 T cell isolation and *in vitro* differentiation 29
5.2.2 Cell culture conditions 30
5.2.3 Storage of cells 30
5.2.4 Calcium Phosphate transfection 30
5.2.5 Retroviral T cell transduction..... 31
5.2.6 FACS analysis and sorting..... 31
5.3 Molecular methods for analysis of nucleic acids 32
5.3.1 PCR and generating target constructs..... 32
5.3.2 Plasmid purification..... 34
5.3.3 Ligation of DNA fragments..... 34
5.3.4 Total RNA isolation 34
5.3.5 RNA purification from cell lysates 34
5.3.6 cDNA synthesis and Real-Time PCR..... 34
5.3.7 RNA sequencing..... 35
5.4 Total and specific mRNA pull down.....35
5.4.1 Total mRNA pull down/RBPome capture..... 35
5.4.2 Generation of antisense oligonucleotides..... 36
5.4.3 Specific mRNA pull down..... 37
5.5 Molecular methods for analysis of proteins.....38
5.5.1 SDS-PAGE and western blot for analysis of pull downs..... 38
5.5.2 Silver staining..... 38
5.6 Mass spectrometry and analysis.....39
5.6.1 Sample preparation for mass spectrometry..... 39
5.6.2 LC-MS/MS analysis..... 39

5.6.3 Computational MS-data analysis ... 39
5.6.4 Statistical analyses of MS-data ... 40
5.6.5 Whole proteome analysis ... 40
5.7 Validation of RNA binding ability ... 41
5.8 Bioinformatics and statistical analysis ... 41
5.9 Human orthologs ... 42

6. Results ... 43
6.1 Establishment of total mRNA pull down in CD4$^+$ T cells ... 43
6.2 Validation of mRNA binders ... 46
6.3 Analysis of identified RNA-binding proteins ... 47
6.3.1 Functional and biophysical analysis of RBPome ... 47
6.3.2 CD4$^+$ RBPome in context to published datasets ... 51
6.4 Pull down of one specific mRNA ... 56
6.5 Reporter assays for Foxp3 regulation ... 58
6.6 Different isoforms of *Foxp3* mRNA ... 62

7. Discussion ... 65
Identification and characterization of mRNA-binding proteins in CD4$^+$ T cells ... 65
7.1 Discussion of experimental aspects: RBPome capture in CD4$^+$ T cells ... 65
7.2 Discussion of experimental aspects: Attempt to identify and characterize *Foxp3* mRNA binding factors and their regulatory role for *Foxp3* ... 66
7.2.1 Specific pull down of one mRNA and identification of bound RBPs ... 66
7.2.2 Analysis of Foxp3 regulation by retroviral reporter assays ... 67
7.3 Discussion of biological results: RBPome capture of primary mouse T helper cells ... 68
7.4 Discussion of biological results: Expanding the knowledge on primary mouse RNA-binding proteins ... 70
7.5 Discussion of biological results: Attempt to identify and characterize Foxp3 mRNA binding factors and their regulatory role for *Foxp3* ... 73

8. Outlook and future directions ... 75
8.1 Extending the analyses of mRNA-binding proteins and their function in CD4$^+$ T cells ... 75
8.2 Post-transcriptional regulation of *Foxp3* ... 75

9. Conclusion ... 77

10. Contributions and Acknowledgements ... 78

11. Literature ... 79

12. Supplements ... 92
12.1 List of Figures ... 92
12.2 List of tables ... 92
12.3 List of supplementary tables ... 93
12.4 List of abbreviations and scientific notation ... 93

3. Introduction

3.1 The immune system

The immune system is necessary to protect the host from a variety of pathogenic organisms which it is constantly exposed to. Mounting of an immune response against an invading pathogen or toxic or allergenic substances is based on the immune system's capacity to distinguish self from non-self (Chaplin 2010). It consists of two parts, termed the innate and the adaptive immune system (Figure 1). The innate immune system is responsible for an immediate immune response and composed of cells (e.g. neutrophils, monocytes and macrophages) as well as proteins (e.g. the complement system, cytokines and acute phase proteins). It is highly conserved and found in organisms from plants, fungi, and insects to mammals. The second part, the adaptive immune system, is highly specialized and composed of B- and T-lymphocytes.

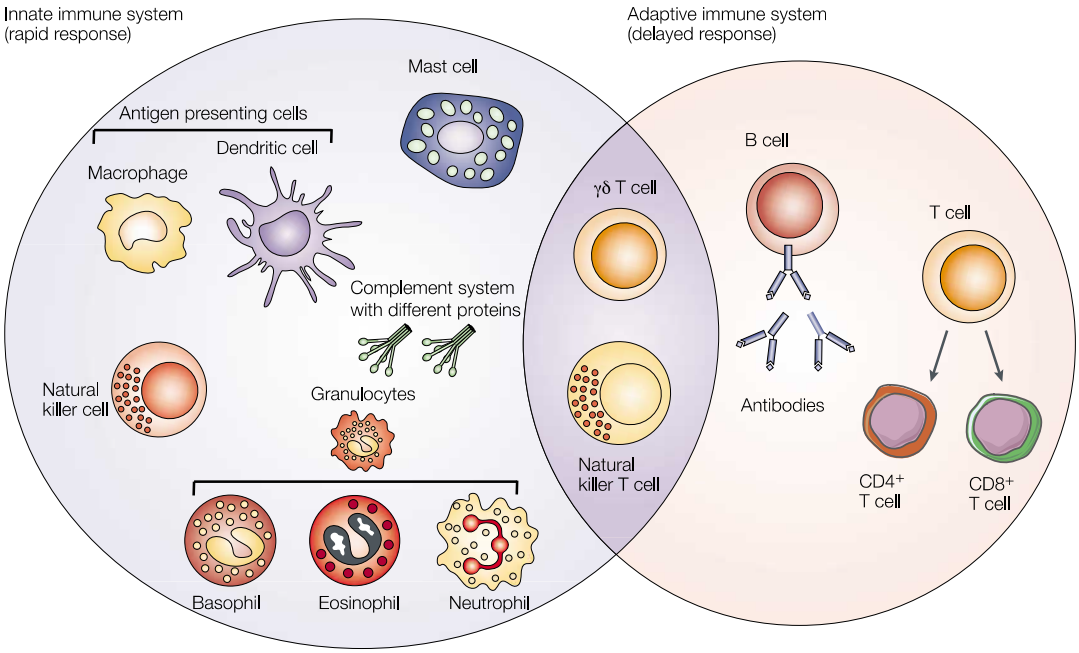

Figure 1: Components of innate and adaptive immunity (modified from Dranoff 2004)
The innate immune system employs pattern-recognition receptors (PRRs) and other surface molecules to identify constituents common to many pathogens. Its activation results in a quick immune response characterized by inflammation or phagocytosis, which is mediated by soluble factors such as proteins of the complement system or cellular effectors including granulocytes, macrophages, dendritic cells (DCs) or natural killer (NK) cells. In contrast, the adaptive immune system is slower to mount a response, since it includes the expansion of lymphocytes, which are able to specifically recognize one particular pathogen or its processed constituents. Its responses are mediated by antibodies or $CD4^+$ and $CD8^+$ T cells. Additionally, NKT cells and γδ T cells belong to the class of cytotoxic T lymphocytes and exert their function at the intersection of innate and adaptive immunity.

They are able to specifically recognize a pathogen and mount an immune response towards it but in contrast to the innate immune system it takes from days to weeks to develop this response. Also, after clearance of the infection, it provides long-lasting immunity to this pathogen by generation of memory cells (Parkin and Cohen 2001).
B- and T cells develop from common hematopoietic precursor cells in the bone marrow. These hematopoietic stem cells (HSCs) either stay in the bone marrow and develop to B cells or they migrate as T progenitors through the blood into the thymus, where T lymphocyte development occurs (Fast 2013). Both of these cells generate antigen-specific receptors (B- and T cell receptors respectively) by random rearrangement of DNA segments called V(D)J recombination, which results in a repertoire of ~10^8 T-cell receptors (TCRs) and ~10^{10} antibody specificities for B cells (Arstila, Casrouge et al. 1999). After generation of a functioning receptor these cells are called naïve B- and T cells. They can now be activated by encountering their cognate antigen, which is presented on the surface of specialized antigen presenting cells (APCs) such as dendritic cells or macrophages. This encounter usually takes place in secondary lymphoid organs, for example lymph nodes, spleen or tonsils.
T cells are divided into two classes. Cytotoxic T cells express CD8 on their surface and are responsible for antiviral and antitumor activity. On the other hand, CD4 expressing T helper cells regulate a variety of other immune cells by secretion of cytokines and can also activate B cells. $CD4^+$ T cells are again subdivided into two antagonistic types, namely effector and regulatory T cells. Effector T cells (T_{eff}) such as Th1, Th2 or Th17 cells, to name only a few, are activated after infection with different kinds of pathogens. They produce specific proinflammatory cytokines (e.g. IFN-γ, IL-4 and IL-17 respectively) to activate and stimulate other immune cells (Zhu, Yamane et al. 2010). This encompasses the activation of macrophages, which in turn kill intracellular pathogens or stimulation of B cells to produce antibodies. In contrast, regulatory T cells, characterized by the expression of the transcription factor Foxp3 (Treg/T_{Foxp3+} cells) are responsible for maintaining immune homeostasis, dampening of overexuberant immune responses and preventing autoimmune diseases, such as type 1 diabetes (Sakaguchi, Sakaguchi et al. 2001, Feuerer, Hill et al. 2009). Conversely, they can also prevent the immune system from exerting its antitumor activity, as has been seen in some forms of cancer (Zou 2006) or hinder the development of sterilizing immunity towards various pathogens (Rouse, Sarangi et al. 2006, Belkaid 2007).

3.2 Regulatory T cells and their function

The pivotal role of regulatory T cells for the immune system is seen when mutations in *Foxp3* render Treg cells non-functional. In this case, mice suffer from a lethal autoimmune syndrome, which is characterized by multi-organ inflammation and death at around four weeks of age (Fontenot, Gavin et al. 2003). Likewise, if human FOXP3 is not functional, patients suffer from fatal immunodysregulation polyendocrinopathy enteropathy X-linked (IPEX) syndrome (Bennett, Christie et al. 2001).

These severe consequences of Treg cell absence occur, because they mediate two crucial aspects, namely immune tolerance and immune homeostasis. Immune tolerance can be divided into central and peripheral tolerance. In central tolerance, lymphocytes with receptors specific for self-antigens die via apoptosis (a process called clonal deletion) at an immature stage of their development. Alternatively, some of them are able to replace these self-reactive receptors by receptor editing (Sakaguchi, Yamaguchi et al. 2008). However, a small population of those self-reactive cells starts expressing the transcription factor Foxp3 and is then called thymic Treg cells (tTreg cells) (Figure 2). If self-reactive cells escape into the periphery, damage to the host is prevented by establishing peripheral tolerance. Here, the autoreactive cells are either deleted by apoptosis, rendered anergic to their respective antigen (e.g. still alive but unable to respond to antigen stimulation) or they develop into a second type of regulatory cells, called peripheral Treg cells (pTreg cells) (Figure 2) and (Li and Rudensky 2016).

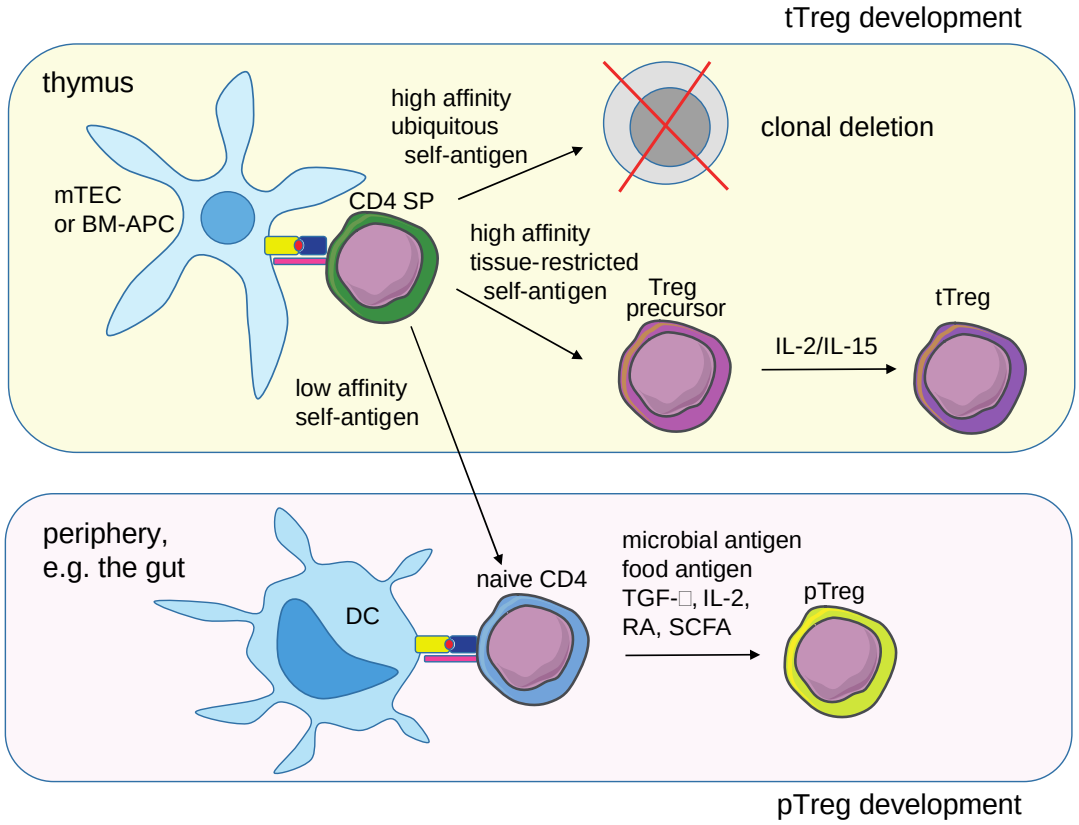

Figure 2: Regulatory T cell development (modified from Lee and Lee 2018)
tTreg cell development takes place in the thymus, where medullary thymic epithelial cells (mTECs) or bone marrow derived antigen-presenting cells (BM-APCs) present high affinity tissue-restricted self-antigens to single-positive (SP) T cells, thus inducing differentiation, which is later finalized by the effects of IL-2 and IL-15. pTreg cells on the other hand, develop in the periphery, by encountering for example antigens of colonic commensal microbiota or food antigens, which are presented by tissue-resident dendritic cells. Additionally, several factors such as TGF-β, IL-2, retinoic acid and short chain fatty acids are required for the development of pTreg cells.

Although both types of Treg cells are responsible for immune tolerance and homeostasis, they differ in a variety of characteristics (Shevach and Thornton 2014).

The exact differences in their differentiation processes are still to be determined, but it is thought that for tTreg cells high affinity interactions with the TCR are of great importance, while for pTreg cell generation, the cytokine TGF-β as well as stimulation with lower affinity TCR signal are crucial (Horwitz, Zheng et al. 2008, Gao, Lin et al. 2012). It has been shown that Treg cells can be reprogrammed into proinflammatory cells (Zhou, Bailey-Bucktrout et al. 2009, Esposito, Ruffini et al. 2010) and although some of the conversion mechanisms have been studied, it is still under debate in which way and to what degree the stability of Foxp3 expression is affecting or influenced by these reprogramming processes. Also it is still not entirely clear if this is mainly related to tTreg or pTreg cells, even though some studies suggest that tTreg cells have a more stable Foxp3 expression (Gao, Lin et al. 2012).

The prime function of regulatory T cells, the suppression of other immune cells such as B cells, NK cells, $CD4^+$ and $CD8^+$ T cells, is mediated via various mechanisms, namely suppression by inhibitory cytokines, cytolysis, metabolic disruption and suppression by modulation of dendritic-cell (DC) maturation or function (Figure 3) (Vignali, Collison et al. 2008).

The three inhibitory cytokines IL-10, IL-35 and TGF-β are key mediators of Treg cell function. However, even though especially the suppressive effects of IL-10 and TGF-β are well known, their specific role for tTreg and pTreg cells and their function is still controversially debated as there are various conflicting *in vitro* and *in vivo* studies (Takahashi, Kuniyasu et al. 1998, Thornton and Shevach 1998, Dieckmann, Plottner et al. 2001, Jonuleit, Schmitt et al. 2001, Annacker, Asseman et al. 2003, Hawrylowicz and O'Garra 2005). Nonetheless it has been shown, that prevention of colitis in a mouse model is dependent on IL-10 produced by Treg cells (Asseman, Mauze et al. 1999) and membrane-bound TGF-β is required for their maximal regulatory activity (Nakamura, Kitani et al. 2001). More recently, a study found IL-35 to be necessary to cure IBD in mice (Collison, Workman et al. 2007).

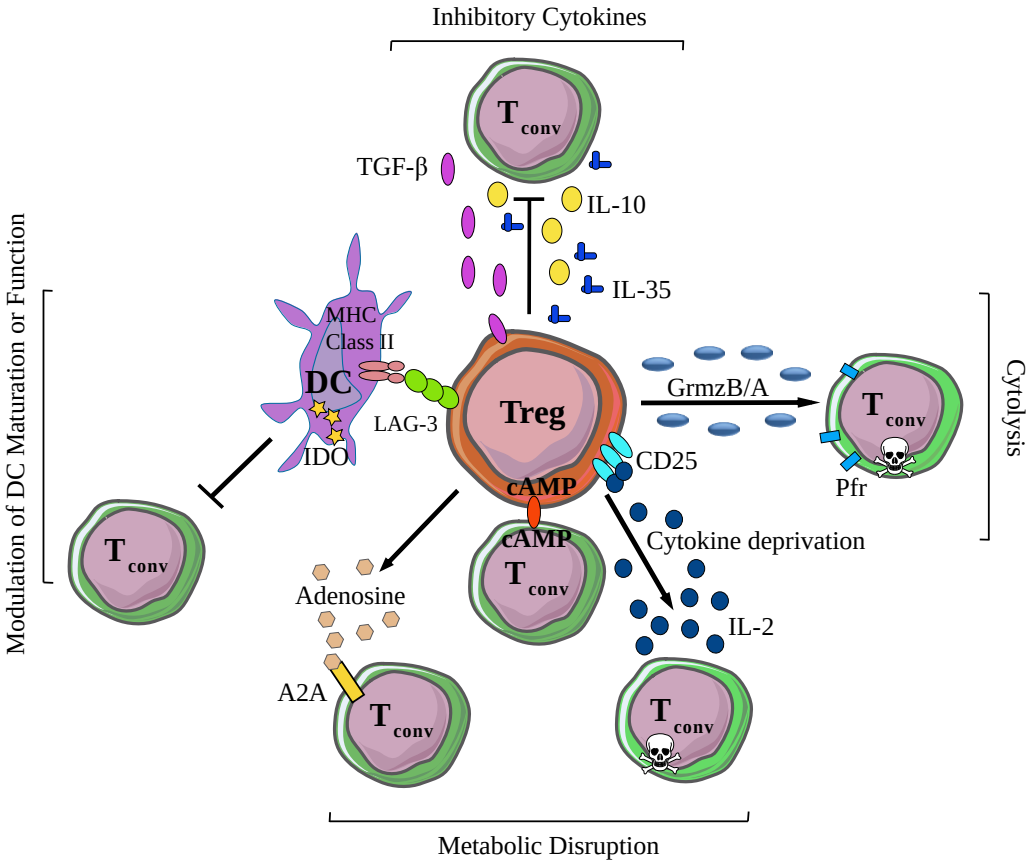

Figure 3: Mechanisms of suppression by regulatory T cells (modified from Workman, Szymczak-Workman et al. 2009)
Treg cells can suppress effector cells by a variety of mechanisms. One of them is mediated via the inhibitory cytokines TGF-β, IL-35 and IL-10. They are also able to secrete the proteins granzyme A and B as well as perforine, which mediate cytolysis of the target effector cell. Additionally, they are able to inhibit growth or function or induce apoptosis by metabolic disruption. Here, they starve target cells by consumption of IL-2 or cause inhibition by cAMP and /or adenosine production. Furthermore, Treg cells can interact with APCs, thus reducing their ability to activate conventional T cells (T_{conv}). Moreover, they have been shown to mediate production of indoleamine 2,3-dioxygenase **(**IDO) in DCs, which also results in reduced T cell responses.

Another means of Treg cell mediated suppression is cytolysis of the respective target cells. It was shown, that mouse Treg cells have upregulated granzyme B expression (McHugh, Whitters et al. 2002), and use this to induce apoptosis in effector T cells (Gondek, Lu et al. 2005) or B cells (Zhao, Thornton et al. 2006). Furthermore, they are able to "metabolically disrupt" their target cells, thus inhibiting their growth and function. Especially the consumption of IL-2 by Treg cells via their highly expressed IL-2 receptor CD25 and thereby starving effector T cells is believed to be one of those mechanisms. However, the extend and importance of this is still under debate, as it has been shown to be utilized by mouse (Pandiyan, Zheng et al. 2007) but being insufficient for suppression by human Treg cells (Oberle, Eberhardt et al. 2007). Additionally, several studies found the production of adenosine, which is bound to the adenosine receptor 2A ($A_{2A}R$) on target cells (Kobie, Shah et al. 2006) or the direct transfer of the second messenger cAMP via gap junctions and thus inhibition of effector T cell function (Bopp, Becker et al. 2007) to be important mechanisms.

An indirect mechanism of suppression is mediated via the effect on APCs. Here, cell surface molecules on Treg cells like cytotoxic T-lymphocyte-associated protein 4 (CTLA-4) or lymphocyte activation gene 3 (LAG-3) are interacting with CD80/CD86 and MHC class II on the APC surface, thus resulting in a reduced ability of the APC to activate T effector cells (Sojka, Huang et al. 2008, Tang and Bluestone 2008, Vignali, Collison et al. 2008). Furthermore, it has been shown that Treg cells mediate the production of indoleamine 2,3-dioxygenase (IDO) in DCs, whose activity correlates with reduced T cell-mediated responses in mouse systems (Mellor and Munn 2004).

3.3 The transcription factor Foxp3 and the Treg cell signature

Treg cells constitutively express the transcription factor Foxp3, which is required for their development and function and therefore is often referred to as 'lineage-specifying transcription factor' or 'master regulator'. *Foxp3* and its regulation have been intensively studied and many different transcriptional and post-translational regulatory mechanisms have been discovered. There are four conserved non-coding DNA sequence (CNS) elements located in the *Foxp3* gene locus, which determine various characteristics of the Treg cell population (Lee and Lee 2018). Interestingly, the *Foxp3* promoter has relatively low transcriptional activity, emphasizing the importance of other regulatory elements. CNS1 for example is not required for tTreg cell generation, as it acts as a TGF-β sensor, which is only crucial for the induction of pTregs. Therefore, deletion of CNS1 has been shown to result in a strong decrease in Treg cell presence in gut-associated lymphoid tissue (Zheng, Josefowicz et al. 2010). Deletion of CNS3 however, has been shown to strongly reduce tTreg cell numbers and is therefore considered essential for the generation of tTregs (Lee and Lee 2018). CNS2, also known as the Treg cell-specific demethylated region (TSDR), is composed of CpG islands, whose demethylation strongly facilitates transcription of *Foxp3* mRNA. This results in increased lineage stability of Treg cells, and is considered one of the strongest indicators of commitment to the Treg cell lineage and characteristic of tTregs (Gao, Lin et al. 2012, Li, Li et al. 2015, Lee and Lee 2018). CNS0 has only recently been discovered and characterized as a Satb1 dependent super-enhancer, which is required for Treg cell lineage specification in the thymus (Kitagawa, Ohkura et al. 2017).

Additionally, Foxp3 protein can be post-translationally regulated by ubiquitination, acetylation or phosphorylation. For example, it has been shown that a decrease in Foxp3 acetylation by inhibiting the acetyltransferase p300 results in a decreased Treg cell activity in mice (Liu, Wang et al. 2013). Conversely, knockdown of HDAC9 and Sirt1, which are responsible for Foxp3 acetylation, enhances Treg cell function (de Zoeten, Wang et al. 2010, Beier, Wang et al. 2011). However, whether or to what extent *Foxp3* is post-transcriptionally regulated is still unknown.

Despite its significance, Foxp3 expression alone is not sufficient to fully characterize the regulatory T cell lineage. For example, studies in mice where the *Foxp3* gene has been disrupted by insertion of GFP show that these $Foxp3^{-}GFP^{+}$ T cells are in many ways similar

to wild type Treg cells. They show an inability to produce IL-2, have an elevated expression of CD25, exhibit low proliferation *in vitro* and are able to express other Treg signature genes such as *Ctla4* or *Il2ra* (Gavin, Rasmussen et al. 2007, Lin, Haribhai et al. 2007, Zheng and Rudensky 2007). It thus became apparent that additional mechanisms, especially epigenetic changes such as histone modifications or DNA methylation, are of great importance for Treg development and maintenance. Studies have shown, that several genes exhibit Treg-cell-specific hypomethylation (e.g. *Foxp3*, *Ctla-4* or *Eos*) (Ohkura, Hamaguchi et al. 2012) and differences in nucleosome positioning and chromatin accessibility result from altered histone modifications in Treg cells (Schmidl, Klug et al. 2009, Samstein, Arvey et al. 2012). The establishment of this Treg-specific epigenetic pattern is Foxp3-independent and it is believed that Foxp3-dependent gene regulation and Treg-cell-epigenome-dependent regulation are distinct but work in concert to set up the Treg-specific gene expression pattern (Ohkura, Kitagawa et al. 2013).

Additionally, it has been shown that there is a variety of Treg cell subsets which express transcription factors normally characterizing for different T helper cell types such as T-bet or Irf4. For example, T-bet$^+$ Treg cells develop in response to IFN-γ produced by effector cells like Th1 and are then able to migrate to type 1 inflammatory sites where they suppress the local immune response (Koch, Tucker-Heard et al. 2009, Hall, Beiting et al. 2012). The same mechanism is found in Irf4$^+$ Treg cells, which correspondingly suppress type 2 inflammation and prevent uncontrolled Th2 immune responses (Zheng, Chaudhry et al. 2009).

As well as in mice, it was shown in humans that CD4$^+$CD25$^+$ T cells express FOXP3 and act as suppressors of T_{eff} cells (Ziegler 2006). However, there were also several differences found between human and murine Treg cells. In contrast to murine cells, activated human conventional T cells (T_{conv}) cells express FOXP3 without having suppressive activity (Allan, Crome et al. 2007). Furthermore, ectopic expression of FOXP3 in human CD4$^+$CD25$^-$ cells did not elicit the same suppressive capacity as in their murine counterparts (Walker, Kasprowicz et al. 2003). It was also shown that only in human cells, additionally to full length FOXP3 protein, there are two isoforms generated by alternative splicing, which lack either exon 2 or exon 2 and exon 7 (Allan, Passerini et al. 2005, Smith, Finney et al. 2006). Interestingly, roughly 70% of *FOXP3* transcript in CD4$^+$CD25$^+$ T cells is expressed lacking exon 2 (Aarts-Riemens, Emmelot et al. 2008, Mailer, Falk et al. 2009, Mailer, Joly et al. 2015). Compared to *FOXP3* full length, the isoform lacking exon 2 is found more often in the nucleus and thought to primarily maintain the suppressive capacity of Treg cells, whereas the isoform lacking exon 2 and 7 is insufficient to elicit the Treg cell phenotype (Mailer, Falk et al. 2009).

3.4 Regulation of gene expression by RNA-binding proteins

The processes responsible for the development and function of immune cells involve dynamic changes in transcript and protein levels. Many of these changes are regulated by the activity of RNA-binding proteins (RBPs) (Figure 4). There are a multitude of steps where RBPs can

act with a variety of different outcomes. For example they can regulate transcription itself or many of the following RNA processing steps like 5´end capping or RNA stability and decay and thus determine the abundance of gene transcripts (Kelley, Hendrickson et al. 2014). They are also responsible for mRNA export and localization, which enables transcripts to be transported outside of the nucleus and to the appropriate intracellular environment. Additionally, they influence transcript structure and quality by enabling (alternative) splicing and (alternative) polyadenylation (APA) events (Shi 2012, Fu and Ares 2014). Furthermore, they take part in the regulation of translation, starting from initiation over elongation to termination (Szostak and Gebauer 2013).

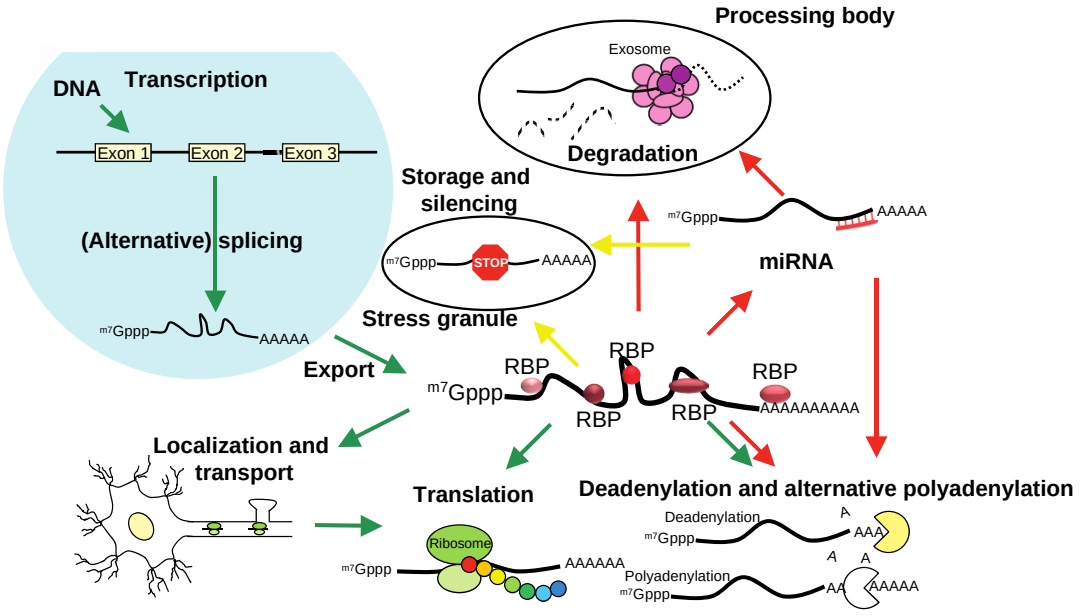

Figure 4: Mechanisms of post-transcriptional gene regulation (modified from Kojima, Shingle et al. 2011)
After transcription from DNA, mRNA can be post-transcriptionally regulated by a variety of processes. These include splicing/alternative splicing, export from the nucleus to the cytoplasm, storage and silencing, mRNA degradation, localization and transport to specific cellular compartments, (alternative) polyadenylation and finally translation. Many of these mechansims are regulated via miRNAs or RNA-binding proteins. miRNA, microRNA

RBPs exert their regulatory functions by binding to their target and forming RNA-protein complexes. These complexes are classified as heterogeneous nuclear ribonucleoprotein particles (hnRNPs) consisting of nuclear pre-mRNA and the associated RBPs or messenger ribonucleoprotein complexes (mRNPs) consisting of mature mRNA and bound RBPs (Muller-McNicoll and Neugebauer 2013). hnRNP proteins, such as hnRNPC are very important for packaging of RNA in the nucleus after transcription by forming multimers around which the RNA is wrapped (Konig, Zarnack et al. 2010). The packaging is strongly influencing alternative splicing by making strong or weak splice sites differentially accessible. Additionally, it has been shown, that some hnRNP proteins such as hnRNPA1 and PTB directly regulate alternative splicing (Treiber, Treiber et al. 2017). In humans, more than

90% of genes are subject to alternative splicing and ~70% have alternative polyadenylation sites (Tian, Hu et al. 2005, Wang, Sandberg et al. 2008, Derti, Garrett-Engele et al. 2012).
For most genes, polyadenylation takes place co-transcriptionally and requires a poly(A) signal sequence, the most common one being AAUAAA (Shi and Manley 2015). However, many other signal sequences have been found with varying frequencies (Neve, Burger et al. 2016). APA can take place when the cleavage and polyadenylation machinery is able to choose between proximal and distal polyadenylation sites. Alternative splicing and APA therefore lead to a multitude of mRNA isoforms per gene, which can encode different protein isoforms or differ in length of their 3´UTRs. Since there are many regulatory elements commonly found in 3´UTRs, such as binding sites for RBPs or miRNAs (Mu, Lu et al. 2011, Lu and Clark 2012), these isoforms are likely to be regulated differentially. The physiological relevance of this effect can be seen for example in a single nucleotide variant (SNV) in the *IRF5* gene that shifts polyadenylation from the proximal to the distal site and is thought to increase risk for systemic lupus erythematosus (SLE) (Manning and Cooper 2017).
Simultaneously to splicing and polyadenylation the nascent transcript is also prepared for nuclear export by binding of certain RNA-binding proteins. One prominent example of this nuclear export machinery is the RBP nuclear RNA export factor 1 (Nxf1), which shuttles between nucleus and cytoplasm. It can either directly bind its target RNA or be linked to it via a variety of adaptor proteins with different specificities (Muller-McNicoll and Neugebauer 2013). One of these adaptors recruited to the transcript is the multi-protein complex transcription export complex 1 (TREX1) (Lueong, Merce et al. 2016).
After transport to the cytoplasm mRNA is subject to regulatory processes that determine its turnover and stability. These are crucial for the cell to dispose of transcripts it does no longer require or aberrant transcripts potentially resulting in toxic proteins. Also, it is necessary to stabilize or destabilize certain mRNAs to allow dynamic fine-tuning of gene expression (Borbolis and Syntichaki 2015). mRNA degradation is mostly dependent on the 5´cap, which is added to the RNA shortly after initiation of transcription and composed of a methylated or trimethylated guanine as well as the poly(A) tail. For most degradation processes, deadenylation is the rate-limiting step. It is induced by the action of deadenylation complexes PAN2/PAN3 and CCR4/NOT forming mRNPs with the target mRNA (Wahle and Winkler 2013). Subsequently, mRNA can undergo exonucleolytic decay by the gradual removal of the poly(A) tail by deadenylation complexes. mRNA will then be degraded in 3´to 5´direction by the cytoplasmic RNA exosome or after removal of the 5´cap by decapping enzymes such as Dcp2 in 5´ to 3´ direction by the exonuclease Xrn1, with the latter mechanism being more predominantly used (Garneau, Wilusz et al. 2007). Binding of RBPs can differentially regulate mRNA stability. Zfp36 and Regnase-1 for example destabilize transcripts via recruitment of the deadenylation complex or direct cleavage, respectively (Sandler, Kreth et al. 2011, Mino, Murakawa et al. 2015). On the other hand, HuR binding leads to increased stability of mRNA (Brennan and Steitz 2001).
To prevent the production of truncated proteins, mutations in the RNA, which lead to premature termination codons (PTCs), errors in mRNA splicing or improper translation result in activation of the RNA quality control mechanism nonsense-mediated decay (NMD) where

a multiprotein complex is responsible for degrading aberrant mRNA (Lykke-Andersen and Jensen 2015). The RBPs up-frameshift protein 1, 2 and 3 (UPF1, UPF2 and UPF3) are crucial for NMD and mediate exo- or endonucleolytic mRNA degradation (Serdar, Whiteside et al. 2016) and NMD plays a vital role in embryo and neuronal development as well as hematopoiesis and T cell development (Weischenfeldt, Damgaard et al. 2008, Wittkopp, Huntzinger et al. 2009). In eukaryotic cells, mRNA turnover is often found to localize to subcellular compartments termed processing bodies (PBs). Here, translationally repressed mRNAs are stored and await their degradation via deadenylation and decapping complexes (Cougot, Babajko et al. 2004, Teixeira, Sheth et al. 2005). Another type of cytoplasmic RNA storage foci are named stress granules (SGs). As PBs they contain non-translating mRNAs but lack the mRNA deadenylation and degradation machinery (Kimball, Horetsky et al. 2003, Kedersha, Stoecklin et al. 2005). In fact, the function of SGs is to protect stored mRNA from degradation when the cell is experiencing environmental stress and translation initiation is inhibited (Buchan and Parker 2009). However, the two types of granules are very dynamic and share many common proteins, are able to interact and exchange their content cargo and even mature into their counterpart (Kedersha, Stoecklin et al. 2005, Wilczynska, Aigueperse et al. 2005, Buchan, Muhlrad et al. 2008, Decker and Parker 2012).

Additionally, mRNA stability and turnover is strongly influenced by microRNAs (miRNAs). They are small non-coding RNAs, which together with RBPs of the Argonaute family form the miRNA-induced silencing complex (miRISC). They bind to complementary mRNA targets and promote their degradation via decapping and deadenylation (Jonas and Izaurralde 2015). miRNA function is essential for many cellular processes such as differentiation or homeostasis, exemplified by the inhibition of lymphoid development and differentiation in the absence of DICER, an RBP necessary for the biogenesis of most miRNAs (Muljo, Ansel et al. 2005, Koralov, Muljo et al. 2008). Additionally, RBPs can dampen or enhance miRNA-mediated degradation processes. For example, dampening of target mRNA degradation takes place, when Lin28 binds to *let-7* miRNA precursors, blocking their maturation and thus enabling embryonic stem cell renewal (Viswanathan, Daley et al. 2008, Piskounova, Polytarchou et al. 2011, Bin, Jiarong et al. 2012). Furthermore, RBPs can directly compete with miRNAs for binding sites in their respective targets, as is the case for ELAVL1, which thus enhances stability of certain mRNAs in macrophages (Lu, Chang et al. 2014). On the other hand, ZFP36 is able to promote mRNA degradation by interacting with the miRISC and Pum1 and Pum2 have been shown to alter mRNA secondary structure, thus facilitating miRNA binding and subsequent degradation (Jing, Huang et al. 2005, El Gazzar and McCall 2010, Kedde, van Kouwenhove et al. 2010, Qi, Wang et al. 2012).

The last step at which post-transcriptional regulation can take place is the process of translation itself, affecting either translation initiation, elongation or termination. Again, all these processes are influenced by a variety of RBPs, such as PABP, which impacts cap-dependent translation initiation by interacting with the eIF4F cap-binding complex, thus enhancing pre-initiation complex assembly and post-termination ribosome recycling (Tarun and Sachs 1996, Rajkowitsch, Vilela et al. 2004). LARP1 on the other hand can both positively and negatively regulate translation of its targets. By binding to the 5´cap it is

blocking the assembly of the eIF4F complex (Lahr, Fonseca et al. 2017), while after phosphorylation, it is also able to bind to sequences in 3´UTRs of ribosomal proteins, thus increasing total protein synthesis in the cell (Hong, Freeberg et al. 2017). It has also been shown, that by binding, PTBP1, ELAVL1 and TIA1 allow for the recognition and usage of alternative start codons within the mRNA, thus generating different open reading frames (ORFs) resulting in the translation of different protein isoforms (Ingolia 2014).

3.5 Characteristics of RNA-binding proteins

In contrast to the variety of functions of RBPs, their structure is characterized by a relatively limited set of RNA-binding domains (RBDs) responsible for RNA recognition (Lunde, Moore et al. 2007). There are many well known RBDs such as RNA recognition motifs (RRMs), K-homology domains (KH domains) or CCCH zinc finger domains to name but a few. RNA sequences and secondary structures can often be bound by many different RBDs, thus leading to a variety of possible regulatory effects and outcomes for RNA fate (Newman, McHugh et al. 2016).

To enable binding to the structural diversity of substrates, RBPs employ two different mechanisms. They can possess multiple copies of one RBD or use a variety of combinations of them (Burd and Dreyfuss 1994). By utilizing multiple copies of one RBD, they increase affinity and specificity for their targets and by distributing the domains throughout the RBP they allow for recognition of spatially separated sites, thus enabling the induction of conformational changes in the RNA target (Sawicka, Bushell et al. 2008). By combining different RBDs in one protein, they are also able to greatly enhance binding specificity, as is the case for the RBP CPEB (Afroz, Skrisovska et al. 2014). Furthermore, RBPs are usually characterized by a modular structure, meaning they often have additional binding sites for proteins or other molecules (Lunde, Moore et al. 2007). These additional binding sites allow them to connect their RNA regulatory function with a variety of intracellular pathways such as signal transduction or metabolism. Especially metabolic enzymes that exert their so-called moonlighting function as RBPs are more and more recognized and provide interesting links between metabolism and post-transcriptional regulatory processes (Castello, Hentze et al. 2015). Exemplary for this are ACO1 (aconitase 1) and GAPDH (glyceraldehyde phosphate dehydrogenase), enzymes participating in the tricarboxylic acid (TCA) cycle and glycolysis, which have been shown to regulate various mRNAs (Chang, Curtis et al. 2013, Castello, Hentze et al. 2015).

In general, RNA-binding of RBPs can be sequence or structure specific. On the one hand they can recognize for example AU-rich elements (AREs), GU-rich elements (GREs) or polypyrimidine tracts (Turner, Galloway et al. 2014). Prominent examples for ARE-binding proteins are ELAV family and ZFP36 family proteins (Mukherjee, Jacobs et al. 2014). On the other hand they are also able to bind RNA by recognizing secondary structures like stem-loops or bulges (Kafasla, Skliris et al. 2014) as is the case for the RBPs Roquin-1 and Roquin-2, which bind a constitutive decay element (CDE) folding into a stem-loop that is

located in the 3´UTR of *tumor necrosis factor-α* (*TNF-α*) mRNA, thus promoting the mRNAs degradation (Leppek, Schott et al. 2013). The importance of these motifs for regulatory processes in immune cells is shown in mice deficient of AREs in *TNF-α* mRNA, which consequently suffer from inflammatory disease (Kontoyiannis, Pasparakis et al. 1999). Furthermore, RBPs are able to bind RNA through intrinsically disordered protein regions (IDRs). These regions are predominated by the presence of small, polar and/or charged amino acids and low occurrence of bulky hydrophobic amino acids (Hentze, Castello et al. 2018). The importance of this mode of RNA-binding was recently shown in HeLa cells, where around 50% of the reported binding sites were located in IDRs and some RBPs exhibited binding solely through IDRs (Castello, Fischer et al. 2016).

3.6 Regulation of development and function of immune cells via RBPs

There are many examples of RBPs fulfilling essential functions in various cells of the immune system, for example in their development, activation and/or function (Newman, McHugh et al. 2016).

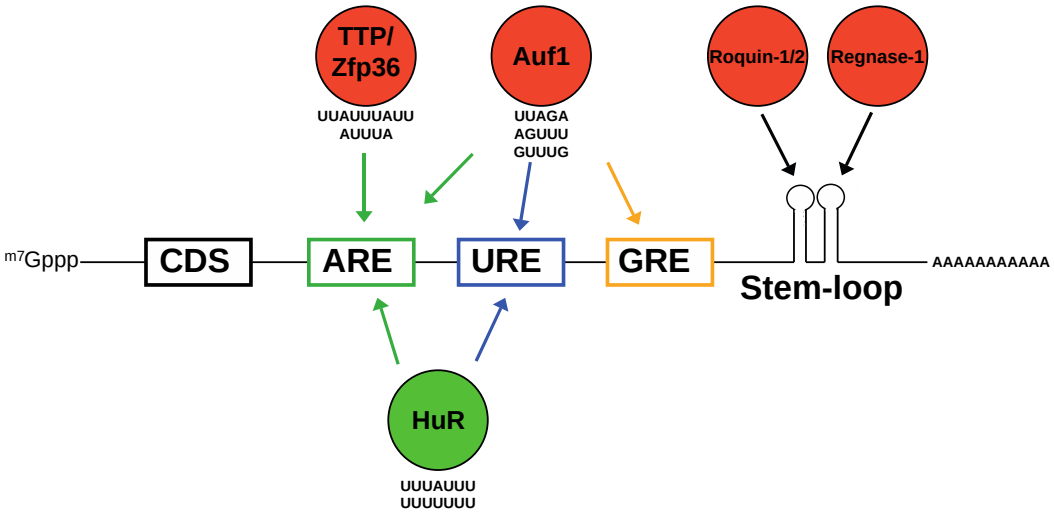

Figure 5: Prominent RNA-binding proteins regulating mRNA stability (modified from Kovarik, Ebner et al. 2017)
RBPs bind predominantly to regulatory elements located in the 3´UTR of mRNA. These elements include AU-rich elements (AREs), U-rich elements (UREs), GU-rich elements (GREs) and/or stem-loop structures. Binding can have either a stabilizing (e.g. HuR) or a destabilizing (e.g. TTP) effects on the mRNA. CDS, coding sequence; ^{m7}Gppp, 7-methylguanosine-triphosphate

Among these is the RBP tristetraprolin (Ttp/Zfp36), which preferentially binds to AREs in mRNAs, thus destabilizing them (Figure 5) (Blackshear, Lai et al. 2003). Knockout of *Zfp36* in mice results in severe inflammation in multiple organs (Taylor, Carballo et al. 1996). This is caused by the excessive production of inflammatory cytokines like TNF-α and IL-23

(Carballo, Lai et al. 1998, Molle, Zhang et al. 2013), which are otherwise degraded by Zfp36 after recruitment of the mRNA deadenylation complex and decapping enzymes (Fenger-Gron, Fillman et al. 2005, Lykke-Andersen and Wagner 2005). Further members of the Zfp36 family are the RBPs Zfp36l1 and Zfp36l2, which have been shown to be required for B cell development. B cells rearrange their antigen receptor genes to generate the necessary diversity for recognizing a variety of antigens. To ensure genomic stability during this process they are kept in a state of quiescence. This is controlled by the RBPs via binding and suppression of several mRNAs, whose protein products mediate entering into S phase of the cell cycle (Galloway, Saveliev et al. 2016).

The RNA-binding protein human antigen R (HuR, or Elavl1 in mouse) is an essential gene, whose deletion is embryonic lethal (Ghosh, Aguila et al. 2009). It exerts its function by binding AREs as well as U-rich sequences (UREs) and stabilizes its target mRNA (Figure 5) (Brennan and Steitz 2001, Kim, Wilce et al. 2011) and participates in regulation of a multitude of biological processes such as apoptosis, cell proliferation, tumorigenesis and angiogenesis (Kovarik, Ebner et al. 2017). Additionally, it fulfills several functions in immune cells by being involved in positive T cell selection (Papadaki, Milatos et al. 2009) and B cell development, germinal center response and production of class-switched antibodies (Diaz-Munoz, Bell et al. 2015).

Similar to Zfp36, the RBP Auf1 is responsible for destabilizing mRNAs of pro-inflammatory cytokines. *Auf1* knockout mice show increased sensitivity to LPS, which results from increased levels of IL-1β and TNF. However, Auf1 has additional functions such as promoting translation of many of its targets as well as stabilizing mRNAs involved in the maintenance of DNA integrity (Sadri and Schneider 2009, Yoon, De et al. 2014). It has been found to have a broad binding specificity by binding AREs as well as UREs and GREs (Yoon, De et al. 2014).

Other prominent examples of important RNA-binding proteins are Roquin 1 and 2. They contain RING-type and CCCH-zinc finger domains and bind and destabilize their target mRNAs via recognition of constitutive decay elements, which are RNA secondary structures consisting of a stem and a trinucleotide loop (Leppek, Schott et al. 2013). Mice carrying the *sanroque* mutation show excessive numbers of follicular T (Tfh) cells and exhibit a lupus-like autoimmune disease caused by a dominant negative mutation in Roquin 1 (Vinuesa, Cook et al. 2005). Roquin 1 and 2 are functionally redundant and maintain immune tolerance by destabilizing mRNAs of the inducible costimulator (Icos) and the Ox40 costimulator receptor (Glasmacher, Hoefig et al. 2010, Tan, Zhou et al. 2014). Also, together with the endoribonuclease Regnase-1, they inhibit Th17 cell differentiation. Roquin and Regnase-1 are cleaved and thus inactivated by the paracaspase Malt-1 after TCR stimulation. This results in stabilization of their target mRNAs such as *Il-6*, *Icos* and *c-Rel*, which in turn promote Th17 differentiation (Jeltsch, Hu et al. 2014).

The RNase Regnase-1 (Zc3h12a) contains a CCCH-type Zn-finger and a PIN-like RNase domain and is mainly expressed in immune cells as a cytoplasmic RBP (Xu, Peng et al. 2012, Uehata and Akira 2013). Target mRNA binding takes place via stem-loop structures with pyrimidine-purine-pyrimidine sequence in the loop while not being sequence specific in the

stem region (Uehata and Akira 2013, Mino, Murakawa et al. 2015). One crucial function of Regnase-1 is its anti-inflammatory effect in macrophages by targeting proinflammatory *Il-6* mRNA and therefore, mice lacking Regnase-1 develop a complex autoimmune syndrome, severe anemia and spontaneously die within 12 weeks after birth (Matsushita, Takeuchi et al. 2009). Interestingly, Regnase-1 and Roquin proteins have been shown to have an overlapping set of target mRNAs but differ in the subcellular location where they exert their function. Regnase-1 degrades translationally active mRNAs located at the endoplasmic reticulum or in polysomes and is dependent on the helicase UPF1. Roquin on the other hand, targets mRNAs located to processing-bodies and stress granules, which are translationally inactive. Regnase-1 and Roquin proteins are thus functioning in a spatiotemporally distinct manner and predominantly regulate the acute and late stage of inflammation, respectively (Matsushita, Takeuchi et al. 2009).

3.7 Aim of the study

Regulation of gene expression can take place at multiple different levels, starting from epigenetic changes over regulation of transcription and translation, as well as regulation on the post-transcriptional level of mRNA or post-translational level of protein. Over the last years, especially post-transcriptional regulation gained increasing interest from researchers and a multitude of studies have been published highlighting its crucial importance and describing mechanisms utilized by immune cells in their development and function (Newman, McHugh et al. 2016).

In this work, we investigated multiple questions concerning post-transcriptional regulation in T cells. Firstly, a recently developed technique from Landthaler and Hentze allows for the unbiased identification of all RNA-binding proteins of a cell, the so-called "mRNA interactome" or "RBPome" (Baltz, Munschauer et al. 2012, Castello, Fischer et al. 2012). Although there are a lot of studies employing this method on various different cell types, the RBPome of $CD4^+$ T cells has yet to be determined. As it is now believed that post-transcriptional regulation is especially important for lineage identity (Lichti, Gallus et al. 2018), we chose to perform this holistic approach and investigated the differences in the RBPomes as well as proteomes and expressed genes of T_{eff} compared to T_{Foxp3+} cells. We thus planned to identify and characterize important post-transcriptional regulators in $CD4^+$ T cells in general, as well as the differences between these two crucial antagonistic T helper cell subsets.

Additionally, we wanted to determine in what way the transcription factor Foxp3 is post-transcriptionally regulated in regulatory T cells. Due to its significance for development and stability of Treg cells, transcriptional and post-translational regulatory mechanisms of *Foxp3* have been intensively studied. However, it still remains unclear if and to what degree *Foxp3* is post-transcriptionally regulated. We had indications that *Foxp3* is post-transcriptionally

regulated (unpublished and confidential observation of a collaboration partner) and tried to elucidate this mechanism.

4. Materials

4.1 Antibodies

4.1.1 Cell culture antibodies

Table 1: Antibodies for cell culture

Antibody	Manufacturer
Anti-CD3 (Clone: 145-2C11)	Collaboration with E. Kremmer
Anti-CD28 (Clone: 37N)	Collaboration with E. Kremmer
Anti-IL4 (Clone: 11B11)	Collaboration with E. Kremmer
Anti-IFN-γ (Clone: Xmg-121)	Collaboration with E. Kremmer
Goat anti-hamster immunoglobulin G	MP Biomedicals
Anti-CD62L (Clone: Mel-14)	Collaboration with E. Kremmer
Proleukin S	Novartis
Anti-CTLA-4 (Clone: UC10-4B9)	BioLegend

4.1.2 Western blot antibodies

Table 2: Western Blot antibodies

Antibody	Manufacturer
Anti-GFP (Clone: 3E5-111)	Collaboration with E. Kremmer
Anti-Ptbp1	Cell Signaling
Anti-β-tubulin	Cell Signaling
Anti-rat IgG, HRP-linked	Cell Signaling
Anti-mouse IgG, HRP-linked	Cell Signaling
Anti-Roquin (Clone: Roc 3F12-111)	Collaboration with E. Kremmer

4.1.3 FACS antibodies

Table 3: FACS antibodies

Antibody	Manufacturer
Anti-Foxp3	eBioscience
Anti-CD4	eBioscience
Anti-CD8	eBioscience
Anti- CD45	eBioscience
Anti-TCRab	eBioscience
DAPI	eBioscience

4.2 Cytokines

Table 4: Cytokines

Cytokines	Manufacturer
Recombinant mouse IL-2	R&D Systems
Recombinant mouse TGF-β	R&D Systems
Recombinant mouse IL-6	R&D Systems
Recombinant mouse IL-23	R&D Systems
Recombinant mouse IL-10	R&D Systems
Recombinant mouse TNF-α	R&D Systems
Recombinant mouse IL-1β	R&D Systems
Recombinant mouse IL-21	R&D Systems
Recombinant mouse IL-7	R&D Systems
Recombinant mouse IL-15	R&D Systems
Recombinant mouse IL-12	R&D Systems
Recombinant mouse IL-33	R&D Systems

4.3 Oligonucleotides

4.3.1 Cloning Primers

Table 5: Cloning Primers

Primer name	Sequence from 5´ to 3´ end	Purpose
GFP for Tag forw	GGGGGGAGATCTGGGGGGATGG TGTCCAAG	Primer to amplify GFP from plasmid
GFP for Tag KDEL rev	CCCCTCGACCCCTCACAGCTCGT CCTTTTTGTACAGCTCGTC	Primer to add KDEL sequence to GFP
Foxp3 5´UTR forw	GGGGGGAGATCTGGGGGGAGTT TCCCACAAGCCAGGCTGA	Primer to amplify Foxp3 5´UTR
Foxp3 5´UTR rev to SspI	CCCAATATTCTCTCTTTTCGCGCG CGCCCCCCTGGGTTCT	Primer to add SspI site to 5´end end of Foxp3 5´UTR
GFP forw BglII to SspI	GGAATATTGGGGGCGCGCGCAA AAGAGAGGGGGGGATGGTGTC	Primer to exchange BglII site to SspI site at the 5´end of GFP
GFP Foxp3 5´UTR rev	CCCCCGAATTCCCCCCCTCGAGC CCCCCTCATTTGTACAGCTC	Primer to amplify Foxp3 5´UTR
Foxp3 3´UTR forw	TTCCTCAAAACCAAGAAAAGGTG GGC	Primer to amplify Foxp3 3´UTR
Foxp3 3´UTR rev (321)	TGGTGTCTGTCATCTTTCTGCTTG G	Primer to amplify short version of Foxp3 3´UTR
Foxp3 3´UTR rev FL	CGGGGTGATCACACAGGGACT	Primer to amplify full length version of Foxp3 3´UTR
HindIII KpnI Rbms1 forw	AAGCTTGGGGGTACCATGATCTT CCCCAG	Primer to clone gene from cDNA, later to be N-terminally GFP-tagged via HindIII and KpnI
HindIII KpnI Rbms1 rev	TTACTTATTGGGTGGAAAGGTAT ATGGAGAATGGTCATTAGACG	Primer to clone gene from cDNA, later to be N-terminally GFP-tagged via HindIII and KpnI
HindIII KpnI Crip1 forw	AAGCTTGGGGGTACCATGCCGAA GTGCCC	Primer to clone gene from cDNA, later to be N-terminally GFP-tagged via HindIII and KpnI
HindIII KpnI Crip1 rev	CTACTTGAAAGTGTGGCTCTCAG CTCCACCTCGCC	Primer to clone gene from cDNA, later to be N-terminally GFP-tagged via HindIII and KpnI

HindIII KpnI Ppia forw	AAGCTTGGGGGTACCATGGTCAA CCCCAC	Primer to clone gene from cDNA, later to be N-terminally GFP-tagged via HindIII and KpnI
HindIII KpnI Ppia rev	TTAGAGCTGTCCACAGTCGGAAA TGGTGATCTTCTTGC	Primer to clone gene from cDNA, later to be N-terminally GFP-tagged via HindIII and KpnI
HindIII KpnI Ldha forw	AAGCTTGGGGGTACCATGGCAAC CCTCAA	Primer to clone gene from cDNA, later to be N-terminally GFP-tagged via HindIII and KpnI
HindIII KpnI Ldha rev	TTAGAACTGCAGCTCCTTCTGGA TTCCCCAGAGG	Primer to clone gene from cDNA, later to be N-terminally GFP-tagged via HindIII and KpnI
HindIII KpnI Stat1 forw	AAGCTTGGGGGTACCATGTCACA GTGGTT	Primer to clone gene from cDNA, later to be N-terminally GFP-tagged via HindIII and KpnI
HindIII KpnI Stat1 rev	TTATACTGTGCTCATCATACTGTC AAATTCGGGGCC	Primer to clone gene from cDNA, later to be N-terminally GFP-tagged via HindIII and KpnI
HindIII KpnI Stat4 forw	AAGCTTGGGGGTACCATGTCTCA GTGGAA	Primer to clone gene from cDNA, later to be N-terminally GFP-tagged via HindIII and KpnI
HindIII KpnI Stat4 rev	TCATTCAGCAGAATATGGGGAAT TCATTGCAGTTTCA	Primer to clone gene from cDNA, later to be N-terminally GFP-tagged via HindIII and KpnI

4.3.2 qPCR Primers

Table 6: qPCR Primers

Primer name	Forward (5´ to 3´)	Reverse (5´ to 3´)
Beta actin	GGCTGTATTCCCCTCCATCG	CCAGTTGGTAACAATGCCATGT
Hprt	TCAGTCAACGGGGGACATAAA	GGGGCTGTACTGCTTAACCAG
Ox40	CTGCATTTGCTGTTCTCCTA	CCACTCCTGTAGTAATGCTC
18S rRNA	GTAACCCGTTGAACCCCATT	CCATCCAATCGGTAGTAGCG
Foxp3	CCTGACTCTGCCTTCAGACG	GGGTTGGGCATTGGGTTCTT
GFP	TGAACTTCAAGATCCGCCACA	TGCTCAGGTAGTGGTTGTCG
Foxp3 race 1	TCCCTATCTAGCTGCCCTCC	TTGGAACTAGGGGCTAGGCT
Foxp3 race 2	GAACCACGGGCACTATCACA	TATGCCTGTGTGGTTTGGGG
Foxp3 race 3	ACTGACCCCAGTTCCCTACC	AGGGGCCTTGGATCCCAAATA
Foxp3 race 4	GAAGGGCTCGGTAGTCCTCA	GCTGAAGAAGTGTGCATCCTG
Foxp3 race 5	GCTACTGGCTAGCTTCAGGTC	GCGCTGAGAGTCTTTGAAACC
Foxp3 race 6	GCAGGGCAGCTAGGTACTTG	TCTCGGAGATCCCCTTTGTCT
Foxp3 race 7	TCAGTGATAACACTCACGTGCC	TGTTCAGGCACACTCCAACA

4.3.3 Target specific biotinylated oligonucleotides

Table 7: Oligonucleotides for specific mRNA pull down

Oligonucleotide Name	Sequence (5´ to 3´)
Foxp3 20mer Biotin 1	Biotin-CTGAGATGTGACTGTCTTCC
Foxp3 20mer Biotin 2	Biotin-TGGGTGCAGTCTTCCAGCTT
Foxp3 20mer Biotin 3	Biotin-ACGGTGCCACCATGACTAGG

Foxp3 20mer Biotin 4	Biotin-TGGGTTGTCCAGTGGACGCA
Foxp3 20mer Biotin 5	Biotin-CAAAAGGTTGCTGTCTTTCC
Foxp3 20mer Biotin 6	Biotin-GCTCCAGAGACTGCACCACT
Foxp3 20mer Biotin 7	Biotin-GCAGCAAGAGCTCTTGTCCA
Foxp3 20mer Biotin 8	Biotin-TCCATGTTGTGGAAGAACTC
Foxp3 20mer Biotin 9	Biotin-CGAAACTCAAATTCATCTAC
Foxp3 20mer Biotin 10	Biotin-TCTTGGTTTTGAGGTCAAGG
Foxp3 20mer Biotin 11	Biotin-CCTCTCAGCTGTAAGGCAGA
Foxp3 20mer Biotin 12	Biotin-ATAGCTGGTTGTGAGGGCTC
Foxp3 20mer Biotin 13	Biotin-GTCATGTGTGACTGCATGAC
Foxp3 20mer Biotin 14	Biotin-TGCTGTTGCTGTGTAAGGGT
Foxp3 20mer Biotin 15	Biotin-GTGGTTTGGGGGGATGTAAT
Foxp3 20mer Biotin 16	Biotin-TGGGTAGGGAACTGGGGTCA
Foxp3 20mer Biotin 17	Biotin-AAGCCCAGTGATGGGAAGGA
Foxp3 20mer Biotin 18	Biotin-GGGATAGTTCCTTGTTTTGC
Foxp3 20mer Biotin 19	Biotin-TCTTGCTGTCTCCAGAATTG
Foxp3 20mer Biotin 20	Biotin-TGGAAAAGGGGGAATGGCTT
Foxp3 20mer 3Bio 1	GGGCATTGGGTTCTTGTCAG-Biotin
Foxp3 20mer 3Bio 2	TCGGATAAGGGTGGCATAGG-Biotin
Foxp3 20mer 3Bio 3	CGCACAAAGCACTTGTGCAG-Biotin
Foxp3 20mer 3Bio 4	CGGTTTCCATAGGTACACGT-Biotin
Foxp3 20mer 3Bio 5	TTGGAACTAGGGGCTAGGCT-Biotin
Foxp3 20mer 3Bio 6	TGTGGGTGAGTGCTTTGGGG-Biotin
Foxp3 20mer 3Bio 7	CTGACAAGCTGTGTCTGACT-Biotin
Foxp3 20mer 3Bio 8	GAACTCAGGAGATAGAGTGG-Biotin
Foxp3 20mer 3Bio 9	GCTAGCCAGTAGCCTACTCT-Biotin
Foxp3 20mer 3Bio 10	CATGAGGTGAGGGGAGCCAT-Biotin
GFP 20mer Biotin 1	Biotin-ACGCTGAACTTGTGGCCGTT
GFP 20mer Biotin 2	Biotin-TGAAGTTCACCTTGATGCCG
GFP 20mer Biotin 3	Biotin-CTGGGTGCTCAGGTAGTGGT
GFP 20mer Biotin 4	Biotin-GTAGGTCAGGGTGGTCACGA
GFP 20mer Biotin 5	Biotin-GAAGTCGTGCTGCTTCATGT
GFP 20mer Biotin 6	Biotin-GCGCTCCTGGACGTAGCCTT
GFP 20mer Biotin 7	Biotin-AGTTGTACTCCAGCTTGTGC
GFP 20mer Biotin 8	Biotin-CAGATGAACTTCAGGGTCAG
GFP 20mer Biotin 9	Biotin-GGCACGGGCAGCTTGCCGGT
GFP 20mer Biotin 10	Biotin-CTGCACGCTGCCGTCCTCGA
Ox40 20mer 3Biotin 1	GTTTTTCCTTGCAGGGTGTG-Biotin
Ox40 20mer 3Biotin 2	TTGTGACCACTGGGGTAGGT-Biotin
Ox40 20mer 3Biotin 3	AGAGTATCCCTGGTATGATC-Biotin
Ox40 20mer 3Biotin 4	GTACACTGCTTGCAGGTATC-Biotin
Ox40 20mer 3Biotin 5	TGGGTGCCTGGTCTACATCT-Biotin
Ox40 20mer 3Biotin 6	ATAAGGTACAATTGGTCCAG-Biotin
Ox40 20mer 3Biotin 7	AGCTGTCACTGGCTGGGTGG-Biotin
Ox40 20mer 3Biotin 8	GAGTCACCAAGGTGGGTGGA-Biotin
Ox40 20mer 3Biotin 9	ACAAGGCCAGCAGGACAGTC-Biotin
Ox40 20mer 3Biotin 10	TTGGGAGTGTTAGGCAATCT-Biotin

4.4 Buffers

Nuclear lysis buffer (in nuclease-free H_2O):
50 mM Tris pH 7.0
10 mM EDTA
1% SDS
Add fresh before use: 1 mM DTT, 1 mM PMSF, 1 x complete protease inhibitor (Roche)

Hybridization buffer (in nuclease-free H_2O):
500 mM NaCl
100 mM Tris pH 7.0
10 mM EDTA
1% SDS
15% Formamide
Add fresh before use: 1 mM DTT, 1 mM PMSF, 1 x complete protease inhibitor (Roche)

Wash buffer (in nuclease-free H_2O):
2 x SSC
Add fresh before use: 1 mM DTT, 1 mM PMSF, 1 x complete protease inhibitor (Roche)

2x HBS
8.0 g NaCl
6.5 g HEPES (260.29 MW)
10 ml Na_2HPO_4
stock solution (Na2HPO4 stock solution: 5.25 g Na_2HPO_4 in 500 ml of water) adjusted pH to 7.0 at room temperature;
aliquoted and stored at -20°C

SDS buffer
200 mM Tris-HCl pH 6.8
8% SDS,
0.1% bromphenol blue,
4% glycerol,
10% β-mercaptoethanol (fresh)

TBS
10 mM Tris/HCl pH 8.0,
150 mM NaCl

TBST
TBS (1x),
0.05% Tween 20

PBS
1 PBS tablet in 500 ml H_2O

Western Blot buffer
25 mM Tris-Base
192 mM glycin
20% methanol (pH 8.4) in H_2O

NP-40 lysis buffer
150 mM NaCl
1% NP-40
50 mM Tris-HCl, pH 7.4
5 mM EDTA

1 mM DTT
1 mM PMSF
Protease inhibitor mixture (Complete, Roche)

IP wash buffers 1-3
50 mM Tris-HCl, pH 7.5 in H_2O
with decreasing salt (500 mM, 350 mM, 150 mM, 50 mM NaCl) and
SDS (0.05%, 0.035%, 0.015%, 0.005%) concentrations

Elution Buffer
50 mM glycine, pH 2.2 in H_2O

Church buffer
0.36 M Na_2HPO_4
0.14 M NaH_2PO_4
1 mM EDTA
7% SDS

4.5 Mice

C57BL/6J mice were purchased from the Jackson Laboratory and Foxp3-RFP reporter mice were a kind gift of Caspar Ohnmacht. They were bred in a specific pathogen-free barrier facility. Mice were euthanized with CO_2 at 8-12 weeks of age for spleen and lymph node removal. All procedures were in accordance with the Helmholtz Zentrum München institutional, as well as the state and federal guidelines.

4.6 Chemicals, enzymes, devices and kits

Table 8: Chemicals

Chemical	Manufacturer
β-mercaptoethanol	Sigma-Aldrich
0,05% Trypsin/ 0,02% EDTA in PBS	Life Technologies
100 bp Plus Marker	Thermo Scientific
Agarose	Biozym
Agencourt RNAClean XP beads	Beckman Coulter
BSA (Albumin Fraktion V)	Merck
Chloroform	Sigma-Aldrich
DETACHaBEAD	Thermo Scientific
Dithiothreitol (DTT)	Roth
DMEM Medium	Thermo Scientific
Dynabeads Mouse CD4	Thermo Scientific
Dynabeads Protein G	Invitrogen
ECL prime western blot detection reagent	GE Healthcare Life Sciences
EDTA (UltraPure, 0.5M, pH 8.0)	Thermo Scientific
Ethanol	Merck
Fetal bovine serum (FBS)	Sigma-Aldrich

GlutaMAX	Life Technologies
Glycine	Sigma-Aldrich
GlycoBlue Coprecipitant	Thermo Scientific
HEPES buffer (1M)	Life Technologies
Isopropanol	Merck
LB Agar	Roth
LB Medium	Roth
M-450 Tosylactivated Magnetic Beads	Invitrogen
MEM vitamin solution	Life Technologies
NaCl (5M)	Sigma-Aldrich
Non-essential amino acids	Life Technologies
Nuclease-free H_2O	Sigma-Aldrich
Nuclease-free Tris HCl (1M), pH 7.4	Lonza
PBS tablet	Thermo Scientific
Penicillin-streptomycin	Life Technologies
Power SYBRgreen Master mix	Thermo Scientific
Protease Inhibitor (cOmplete, EDTA-free)	Roche
QIAzol Lysis Reagent	Qiagen
RNaseZap	Sigma
RPMI 1640	Thermo Scientific
Skimmed milk powder	Roth
Sodium pyruvate	Lonza
Tween 20	Sigma-Aldrich

Table 9: Enzymes

Enzyme	**Manufacturer**
Calf intestine phosphatase (CIP)	New England Biolabs
Gateway LR Clonase	Invitrogen
HindIII	New England Biolabs
KpnI	New England Biolabs
SspI	New England Biolabs
T4 DNA Ligase	Invitrogen
Taq DNA Polymerase	Invitrogen
Phusion® High-Fidelity DNA Polymerase	New England Biolabs
XhoI	New England Biolabs

Table 10: Kits

Kit	**Manufacturer**
µMACS mRNA isolation Kit	Miltenyi
BCA protein assay kit	Thermo Fisher
DynaMag-96 side skirted magnet	Thermo Scientific
Foxp3 fixation and staining kit	eBioscience
Gel extraction kit	Qiagen
Nucleobond®Xtra Maxi Kit	Macherey-Nagel GmbH & Co. KG
pCR™8/GW/TOPO® Kit	Invitrogen
PCR purification kit	Qiagen

QuantiTect Reverse Transcription Kit	Qiagen
SilverQuest kit	Invitrogen

Table 11: Devices

Device	**Company**
Blotting chamber	Bio-Rad
DynaMag-2 Magnet	Life Technologies
E-Gel iBase Power System	Invitrogen
FACS AriaIII Flow Cytometer	BD Bioscience
GelDoc-It TS Imaging System	UVP
HERA cell 150i CO_2 incubator	Thermo Scientific
High-speed centrifuge	Thermo Scientific
High-speed rotor	Thermo Scientific
Fluorescence Microscope	Zeiss
Nanodrop 2000	Thermo Scientific
Neubauer chamber (hemocytometer)	Carl Roth
PHERAstar microplate reader	BMG Labtech
Refrigerated table-top centrifuge	Eppendorf
Thermocycler	Eppendorf
Thermo mixer	Eppendorf
UVC 500 Crosslinker	Amersham Biosciences
ViiA 7 real-time PCR system	Thermo Fisher

Table 12: Software

Software	**Version**
Bioconductor packages for R	Various
DAVID	6.8
FlowJo	9.7.6
MaxQuant	1.5.1.6
Perseus	1.5.3.0
RStudio	Various

5. Methods

.

5.1 Bacterial culture

5.1.1 Bacterial culture

LB medium and LB agar were prepared and following antibiotics were added for selection: ampicillin (100 µg/ml), spectinomycin (50 µg/ml) or kanamycin (30 µg/ml).

5.1.2 Transformation of bacteria

Chemical competent DH5α (Invitrogen) were thawed on ice and 100 – 300 ng of plasmid was added. After 15 – 30 min of incubation on ice, cells were heat shocked at 42°C for 30 s and afterwards incubated on ice for 2 min. 250 µl of LB medium was added and the cells incubated at 37°C and 400 rpm in a thermo mixer for 1 h. Cells were then plated on LB agar and incubated over night at 37°C. For further experiments, single cell colonies were used.

5.2 Cell culture and viral transduction

5.2.1 T cell isolation and *in vitro* differentiation

Peripheral $CD4^+$ T cells were isolated from spleen and lymph nodes with CD4 Dynabeads and Detachabeads (Invitrogen). For differentiation into T_{Foxp3+} cells, they were additionally selected for CD62L with anti-CD62L coated beads (clone: Mel14). To activate and differentiate the cells into T_{eff} and T_{Foxp3+}, they were cultured on plates coated with anti-hamster antibody and soluble anti-CD3 (0,1 µg/ml, clone: 2C11H) and anti-CD28 (1 µg/ml, clone: 37N) in T cell medium (below). For T_{Foxp3+} cells, the following cytokines and blocking antibodies were added: rmIL-2 and rmTGF-β (both: 5 ng/ml, R&D Systems), anti-IL-4 (10 µg/ml, clone: 11B11) and anti-IFN-γ (10 µg/ml, clone: Xmg-121). All antibodies were obtained in collaboration with and from Elisabeth Kremmer (Helmholtz Center Munich). Cells were then differentiated for 36-48 h, collected and expanded for 2-3 days in T cell medium containing Proleukin S (200 units/ml for T_{eff} cells and 2000 units/ml for T_{Foxp3+} cells, MP Biomedicals).

T cell medium:
RPMI medium
10% (v/v) fetal bovine serum (FBS)
0.05 mM β-mercaptoethanol

100 U/ml penicillin-streptomycin
10 mM HEPES pH 7.2
1 mM sodium pyruvate
1x non-essential amino acids
1x MEM Vitamin solution
1x Glutamax

5.2.2 Cell culture conditions

The murine EL4 cell line was provided by Vigo Heissmeyer. It was originally established from a lymphoma induced in a C57BL/6N mouse (Gorer 1950). HEK293T cells were purchased from ATCC. EL-4 cells were grown in EL-4 cell medium (below) and HEK293T cells were grown in cell line medium (below).

<u>EL-4 cell medium:</u>
RPMI medium
10% (v/v) fetal bovine serum (FBS)
100 U/ml penicillin-streptomycin
10 mM HEPES pH 7.2

<u>Cell line medium:</u>
DMEM medium
10% (v/v) fetal bovine serum (FBS)
100 U/ml penicillin-streptomycin
10 mM HEPES pH 7.2

5.2.3 Storage of cells

Cells from cell lines can be stored in liquid nitrogen in a mixture of 90% FBS and 10% DMSO. For this, ~$10x10^6$ EL4 cells or ~$25x10^6$ HEK293T cells were resuspended in 1.3 ml of this solution and transferred to freezing tubes and placed into a freezing box, whose isopropanol isolation allows for slow temperature adjustment in the -80°C freezer thus minimizing the formation of ice crystals. After one day, cells were transferred to liquid nitrogen. For taking the cells back into cell culture, they were quickly thawed and transferred to pre-warmed medium.

5.2.4 Calcium Phosphate transfection

HEK293T cells were seeded at a density of $0.4x10^6$ cells/ml and transfected on the next day. In the morning chloroquine was added to the medium at a final concentration of 25 µM. Then, transfection reaction was prepared by mixing DNA with water (20 µg DNA in 450 µl H_2O for a 10 cm plate and 40 µg DNA in 1125 µl H_2O for a 15 cm plate). Ice-cold $CaCl_2$ was

added to the reaction (50 µl for a 10 cm plate and 125 µl for a 15 cm plate). The reaction was mixed and put on a vortexer at medium speed, while 2xHBS was added drop by drop (500 µl for 10 cm plate, 1250 µl for 15 cm plate). The samples were then incubated at RT for 30 to 45 minutes and then added to the cells. After 7-8 h, the medium was exchanged to remove the chloroquine.

5.2.5 Retroviral T cell transduction

For retroviral transduction of primary T cells, HEK293T cells were transfected via the Calcium-Phosphate method with the target vector as well as an ecotroph packaging vector (EcoPac). After two days the virus containing supernatant was collected, the virus concentrated over night with retro-x concentrator (Clontech) and fresh medium added to the cells. On day three the concentrated virus pellet was resuspended in cell supernatant with freshly produced virus and polybrene was added at a concentration of 10 µg/ml. On day one after transfection, naïve T cells were isolated and seeded to 48-well plates. The virus transduction experiment was performed on day three after transfection. For each 48-well, 900 µl virus supernatant was added and first centrifuged at 2000 rpm for 1 h and then incubated at 37° C for 2.5 h. The supernatant was removed and the T cells were collected and transferred to fresh T cell medium and cultured for two days to allow for the production of the protein. On day three, FACS analysis was performed, to analyze the transduction efficiency of the virus.

5.2.6 FACS analysis and sorting

For flow cytometry analysis of Foxp3 expression, cells were fixed and stained with the Foxp3 staining kit (eBioscience) according to the manufacturer´s instructions. To measure GFP expression, cells were analyzed directly in medium.
For cell sorting, the respective organs were removed, mashed through a 70 µm filter and stored in FACS buffer. They were then stained in this buffer for the surface markers CD4, CD8, CD45, TCRab and DAPI as a dead cell marker. We started by removing doublets and in the following sorted $DAPI^{-}CD4^{+}CD8^{-}CD45^{+}TCRab^{+}RFP^{+}$ cells.
Flow cytometry was performed on a FACS Aria III (BD Biosciences) or a MACSQuant (Miltenyi) and raw data were analyzed with FlowJo software (Treestar).

<u>FACS buffer</u>
PBS pH 7.4
1% FBS
0.01% sodium azide

5.3 Molecular methods for analysis of nucleic acids

5.3.1 PCR and generating target constructs

First, we created destination vectors for the reporter assays. The vector backbone for the constructs was the plasmid pMSCVpuro, which carries long terminal repeats (LTRs) for retroviral transduction as well as Gateway recombination sites (attR1 and attR2). Upstream of the Gateway cassette, we inserted two sequences. First, the 5´UTR of the *Foxp3* gene and afterwards the GFP coding sequence with an additional endoplasmic reticulum (ER) retention signal sequence (the amino acids KDEL). For GFP, we ordered a plasmid with its coding sequence from Geneart (Thermo Fisher), where the sequence was optimized for the mouse codon usage. We amplified the Foxp3 5´UTR from cDNA of T_{Foxp3+} cells and added a BglII site in front and an SspI site at the end of the sequence (see Primers). Next, we added an SspI site in front of GFP as well as KDEL sequence followed by an XhoI site at the end (see Primers) by using Taq polymerase (Invitrogen) according to the manufacturer´s instructions and the PCR program depicted in Table 13.

Table 13: Two-step PCR

Step	Cycles	Temperature	Time
1	1	95°C	3 min
2	3	95°C T_M-5°C 72°C	15 s 30 s 1 min
3	34	95°C T_M-5°C 72°C	15 s 30 s 1 min
4	1	95°C	1 min

Since the primers were not completely complementary to the original sequence, we first conducted 3 additional amplification cycles where the melting temperature was only based on the complementary part of the DNA. We then cut the 5´UTR, the GFP sequence and the vector backbone with the respective restriction enzymes, purified them with the PCR purification kit (Qiagen) and set up a three-way ligation by combining the DNA fragments and added T4 DNA ligase (see below). The result was the destination vector as depicted in . We then generated pCR™8/GW/TOPO® vector entry vectors by amplifying either a short version of the Foxp3 3´UTR (1-321 bp) or the full length 3´UTR (1-2200 bp) by using Taq polymerase and the PCR program depicted in Table 14.

Table 14: One-step PCR

Step	Cycles	Temperature	Time
1	1	95°C	3 min

2	34	95°C T_M-5°C 72°C	15 s 30 s 1 min
3	1	72°C	10 min

We checked via agarose gel electrophoresis whether there were any PCR by-products present and if not, we directly used 2 µl for the TOPO cloning reaction according to the manufacturer´s instructions. In case of unwanted by-products, the PCR was first purified via agarose gel electrophoresis and cutting of the respective band. These sequences were then inserted from the entry vector into the destination vector via lambda recombination by the gateway cloning technology according to the manufacturer´s instructions and afterwards sequenced for verification.

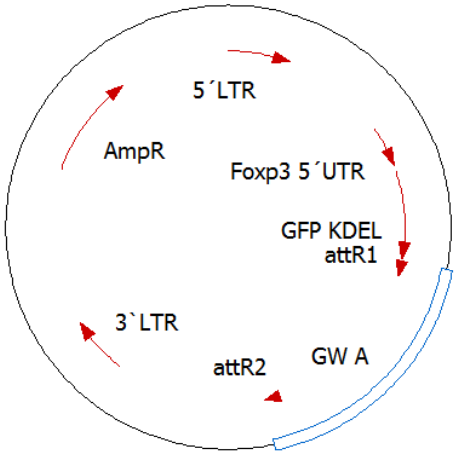

Figure 6: Vector backbone of pMSCVpuro.
LTR: long terminal repeat: identical sequences of DNA that mediate integration of the retroviral DNA into the host chromosome. AmpR: Ampicillin resistance. GW A: Gateway cassette A, containing the death-gene ccdB, which kills cells unless they are ccdB-resistant. attR1 and attR2: Gateway recombination sites for recognition of lambda recombinase for LR reaction to insert sequence of interest.

To generate the N-terminally GFP-tagged constructs for verification of RNA binding, we first amplified the respective genes from cDNA of either T_{eff} or T_{Foxp3+} cells. The forward primer additionally contained a HindIII and a KpnI site. Since these primers were not fully complementary to the gene sequence, we again used the PCR program from Table 13. They were also inserted into pCR™8/GW/TOPO® vector according to the manufacturer´s instructions. We then used HindIII and KpnI to insert the GFP sequence after we removed the bases for the stop codon via PCR (see Primers). The respective sequences were subsequently transferred to the expression vector pMSCV via lambda recombination. Only GFP-Roquin-1 (a kind gift of Vigo Heissmeyer) was expressed from the vector pDEST12.2.

5.3.2 Plasmid purification

For plasmid purification, bacteria were inoculated in 3.5 ml LB medium (Miniprep) or 400 ml medium (Maxiprep) and grown over night at 37°C. On the next day, plasmids were isolated with Kits form Qiagen (Miniprep) or Macherey and Nagel (Maxiprep) according to the manufactuer´s instructions.

5.3.3 Ligation of DNA fragments

Plasmids were digested with restriction enzymes (New England Biolabs) and their respective buffers over night at 37°C. They were then loaded on an agarose gel and the respective bands cut and purified with the gel extraction kit (Qiagen). For ligation of a fragment into a vector, we always used three times molar excess of insert compared to vector and T4 DNA ligase (New England Biolabs) according to the manufacturer´s instructions.

5.3.4 Total RNA isolation

For RNA isolation, cell pellets were lysed with QIAzol lysis reagent by mixing and incubation for 5 min at RT. Next, chloroform was added (200 µl / ml Qiazol lysis reagent), samples shaken vigorously by hand and incubated for 2 min at RT. After centrifugation for 15 min at 4°C and 12.000 g, the upper aqueous phase was taken and transferred to a new tube. 500 µl of isopropanol were added together with 1 µl GlycoBlue and vigorously shaken for precipitation. The samples were again centrifuged for 10 min at 4°C and 12.000 g and the supernatant removed. Pellets were then washed with 1 ml 75% (v/v) ethanol by centrifugation for 5 min at 4°C and 7.600 g. The supernatant was removed and the pellet dried for 10 min. The RNA was then resuspended in 30 µl of nuclease-free H_2O.

5.3.5 RNA purification from cell lysates

Total RNA of input from cell lysates was purified with Agencourt RNAClean XP Beads (Beckman Coulter) according to the manufacturer´s instructions and eluted in nuclease-free H_2O.

5.3.6 cDNA synthesis and Real-Time PCR

cDNA was synthesized from RNA with the QuantiTect Reverse Transcription Kit (Qiagen) according to the manufacturer´s instructions. All qRT-PCRs were performed with the SYBR green method and run on a Viia 7 real-time PCR system. For Primer sequences see Table 6.

5.3.7 RNA sequencing

For RNA sequencing total RNA was isolated using QIAzol reagent. Library preparation and rRNA depletion was performed using the TruSeq Stranded Total RNA Library Prep Kit (Illumina) starting with 400 ng RNA as input for each sample. 12 cycles were used for PCR amplification to minimize PCR bias. Amplified cDNA libraries were further purified using Agencourt RNAClean XP Beads (Beckman Coulter) and quality control was performed using Agilent Bioanalyzer with High Sensitivity DNA Reagents (Agilent Technologies, 5067-4626). Barcoded libraries were sequenced on a HiSeq 4000 (Illumina) with paired-end, 100 bp reads. Sequencing reads were mapped against the mouse genome (GRCm38) and rRNA sequences using ContextMap v2.7.9 (Bonfert, Kirner et al. 2015) (using BWA as short read aligner (Li and Durbin 2009) and allowing a maximum indel size of 3 and at most 5 mismatches). Quantification of gene expression and transcription read-through. Number of read fragments per gene were determined in a strand-specific manner using featureCounts (Liao, Smyth et al. 2014) and gene annotations from Ensembl (version 88 for GRCm38). All read pairs (=fragments) overlapping exonic regions on the corresponding strand by ≥25bp were counted for the corresponding gene. Gene expression was quantified in terms of fragments per kilobase of exons per million mapped reads (FPKM) and averaged between replicates.

5.4 Total and specific mRNA pull down

5.4.1 Total mRNA pull down/RBPome capture

For each RBPome capture experiment for mass spectrometry, $20x10^6$ T_{eff} or T_{Foxp3+} cells were used. They were either lysed directly (nonirradiated, control) in 1 ml lysis buffer from the µMACS mRNA isolation Kit or suspended in 1 ml PBS and dispensed on a 10 cm dish and UV irradiated at 0.2 J/cm^2 at 254 nm for 1 min, washed with PBS, pelleted and subsequently lysed (UV irradiated) and mRNA was isolated from both samples with the µMACS mRNA isolation Kit according to the manufacturer's instructions. RNAs and cross-linked proteins were eluted with 70°C RNase-free H_2O and frozen in liquid nitrogen. A schematic of the workflow is shown in Figure 7.

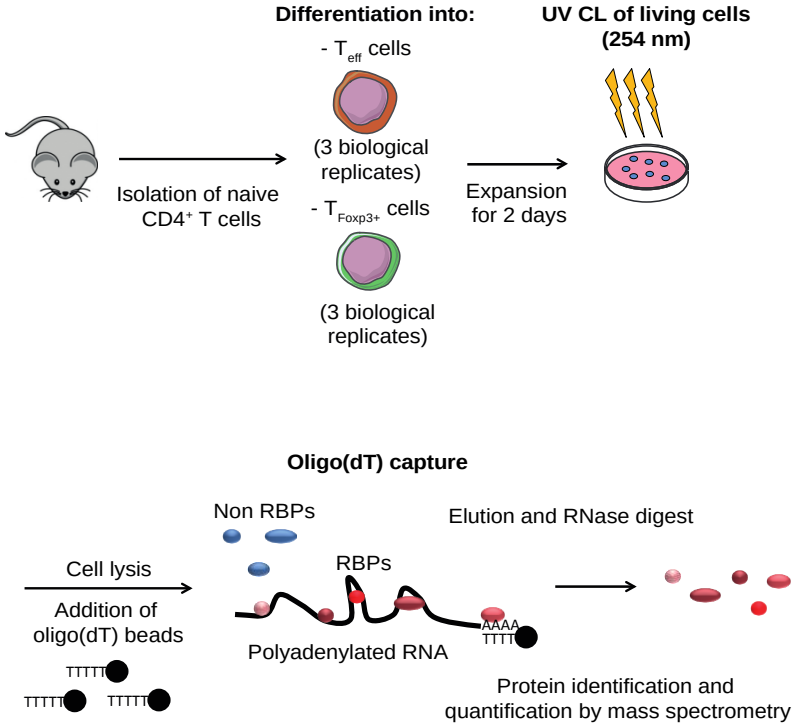

Figure 7: Experimental setup for total mRNA pull down
Primary naïve CD4$^+$ T cells were isolated and differentiated. After UV cross-link, polyadenylated RNA and bound proteins were captured via oligo(dT) beads. After elution and RNase digest, the proteins were identified via mass spectrometry.

For RBPome analysis via western blot, 400x10^6 EL-4 T cells were either lysed directly in 8 ml lysis buffer (nonirradiated, control) or suspended in 16 ml PBS and dispensed on sixteen 10 cm dishes and UV irradiated as before, washed with PBS, pelleted and lysed in 8 ml lysis buffer (UV irradiated) and then mRNA was isolated from both samples with the µMACS mRNA isolation Kit using 500 µl oligo(dT) beads per sample. Each sample was split and run over two M columns and each column was eluted with two times 100 µl RNase-free H_2O. The eluate was concentrated in Amicon centrifugal filter units to a final volume of ~25 µl. 8 µl Lämmli buffer (4x) with 10% (v/v) β-mercaptoethanol was added and the samples boiled for 5 min at 95°C.

5.4.2 Generation of antisense oligonucleotides

To pull down one specific mRNA we generated antisense oligonucleotides for several mRNAs, e.g. *Hprt1*, *Ox40*, *Icos* and *Foxp3*. Here we used the online tool "Sfold" (Ding, Chan et al. 2004) and the respective mRNA sequence including their 5´ and 3´UTRs as input. Sfold predicts the mRNA´s secondary structure and is thus able to locate regions that are more likely to be single-stranded. If possible, probes complementary to these regions were used, since their lack of secondary structure makes binding most probable. Next, probes were

checked via BLAST to see if they bind other unspecific target genes and if this was the case whether these genes are expressed in T cells. Only very few probes complementary to unstructured regions showed no unspecific binding, therefore several probes complementary to structured regions had to be included and were manually analyzed and selected for no or least number of unspecific targets. Probes were ordered from Eurofins Genomics, labeled with an additional 5´ or 3´ Biotin. For Oligonucleotide sequences see Table 7.

5.4.3 Specific mRNA pull down

The specific pull down was either performed on endogenous mRNA in primary T cells or on mRNA of a transfected target construct in HEK 293T cells. For the endogenous pull down, between $5x10^6$ and $120x10^6$ primary T cells were either lysed directly in lysis buffer (~1 ml / $10x10^6$ cells) as non-cross-link control or resuspended in PBS and dispensed on 10 cm dishes and UV irradiated at 0.2 J/cm^2 at 254 nm for 1 min and subsequently lysed in lysis buffer as cross-linked sample.
For pull down of the target construct, HEK293T cells were transfected (as in 5.2.4). After 2 days they were either directly lysed or cross-linked as above and subsequently lysed in lysis buffer (~1 ml / $15x10^6$ cells). The lysate was then pressed through a 20G syringe several times until it became less viscous and clear. The sample was centrifuged at 15.000 g for 10 min and the supernatant transferred to a new tube. Hybridization buffer was added to the sample at a ratio of 2:1 as well as each of the ten oligonucleotide probes (0.3 µl of 10 pmol / µl for $10x10^6$ cells). The annealing temperature of the probes and the mRNA depends on the oligonucleotides themselves as well as the buffer conditions and can be calculated by the following formula:

$$T_A = 67 + 16.6log_{10}\left(\frac{\{Na^+\}}{1.0 + 0.7\{Na^+\}}\right) + 0.8\big(\%(GC)\big) - 500/n$$

Equation 1: Calculation of annealing temperature T_A of DNA oligonucleotides

with:
Na^+ being the concentration of Na^+ ions in mol/l
(%GC) being the percentage of CG in the probe
n being the length of oligonucleotide

After addition of oligonucleotides, the sample was mixed by end-to-end rotation for 4 h at an annealing temperature of 60°C. Then, Pierce Streptavidin magnetic beads (30 µl / $10x10^6$ cells) were added and also incubated at annealing temperature for 30 min. After that, beads were captured with a magnet, supernatant removed and the beads washed twice by resuspending in 1 ml of wash buffer. Beads were taken up in 1 ml of wash buffer and transferred to a new tube, the supernatant was removed again and the sample washed once more with 1 ml wash buffer. Supernatant was removed again and the beads were resuspended

in the respective amount of nuclease-free H_2O, transferred to a new tube and RNA eluted at 95°C at 1100 rpm for 15 min. Beads were captured with a magnet and the RNA/protein containing supernatant was transferred to a new tube. Samples for MS were frozen in liquid nitrogen and samples for western blot were concentrated in Amicon centrifugation tubes if necessary and 4x Lämmli buffer was added. To determine mRNA pull down recovery rate R we first performed cDNA synthesis of the recovered mRNA and then conducted qPCR using the following formula:

$$R = 2^{-(Ct\ Eluate - Ct\ Input)}/d$$

Equation 2: Calculation of pull down efficiency R of mRNA

with:
d being the dilution factor.

5.5 Molecular methods for analysis of proteins

5.5.1 SDS-PAGE and western blot for analysis of pull downs

For protein analysis, samples were prepared as described in sections 5.4.1 and 5.4.3. Lämmli buffer (4x) with 10% (v/v) β-mercaptoethanol was added to samples and after boiling for 5 min at 95°C they were either immediately used or frozen at -20°C. They were loaded on a 9% SDS polyacrylamide gel and run for 80 min at 120 V to separate proteins according to their molecular weight. They were then blotted onto a polyvinylidenfluoride (PVDF) membrane at 30 V for 2 h at RT or at 20 V at 4°C over night in blotting buffer. The membrane was blocked with 5% (w/v) BSA in TBST for 1 h with agitation. Afterwards, the membrane was incubated with the primary antibody either for 2 h at RT or over night at 4°C. Primary antibodies anti-GFP (1:10, clone: 3E5-111, in house), anti-Ptbp (1:1000, Cell Signaling) and anti-β-tubulin (1:1000, Cell Signaling) were diluted in 5% (w/v) BSA in TBS and 0.01% sodium azide. Then the membrane was washed twice for 5 min with TBST and incubated for 1 h with secondary antibody anti-rat (1:3000, Cell Signaling) or anti-mouse (1:3000, Cell Signaling) conjugated to HRP, which was diluted in 1% BSA (w/v) TBST. The membrane was again washed for 5 min with TBST, TBS and Milli-Q water. For detection, the membrane was incubated with ECL prime western blotting detection reagent and chemiluminescence was measured by a Licor detector.

5.5.2 Silver staining

For silver staining, we performed an RBPome capture experiment as described in 5.4.1 using $50x10^6$ primary T_{eff} cells. For the SDS-PAGE, 1/3 of the eluate was loaded on a 9% SDS gel

and it was later stained using the SilverQuest kit (Invitrogen) according to the manufacturer´s instructions.

5.6 Mass spectrometry and analysis

5.6.1 Sample preparation for mass spectrometry

Eluates from the RBPome capture were incubated with 10 µg/ml RNase A in 100 mM Tris, 50 mM NaCl, 1 mM EDTA at 37°C for 30 min. RNase-treated eluates were acetone precipitated and resuspended in denaturation buffer (6 M urea, 2 M thiourea, 10 mM Hepes, pH 8), reduced with 1 mM DTT and alkylated with 5.5 mM IAA. Samples were diluted 1:5 with 62.5 mM Tris, pH 8.1 and proteins digested with 0.5 µg Lys-C and 0.5 µg Trypsin at room temperature over night. The resulting peptides were desalted using stage-tips containing C18 material (3M, St. Paul).

5.6.2 LC-MS/MS analysis

Peptides were separated on a reverse phase column (50 cm length, 75 µm inner diameter) packed in-house with ReproSil-Pur C18-AQ 1.9 µm resin (Dr. Maisch GmbH). Reverse-phase chromatography was performed with an EASY-nLC 1000 ultra-high pressure system, coupled to a Q-Exactive HF Mass Spectrometer (Thermo Scientific). Peptides were loaded with buffer A (0.1% (v/v) formic acid) and eluted with a nonlinear 120-min gradient of 5–60% buffer B (0.1% (v/v) formic acid, 80% (v/v) acetonitrile) at a flow rate of 250 nl/min. After each gradient, the column was washed with 95% buffer B and re-equilibrated with buffer A. Column temperature was kept at 50°C by an in-house designed oven with a Peltier element and operational parameters were monitored in real time by the SprayQc software. MS data were acquired with a top8 shotgun proteomics method, where in each cycle a full scan is followed by up to 15 data-dependent MS/MS scans. Target value for the full scan MS spectra was 3×10^6 charges in the 300−1.650 m/z range with a maximum injection time of 20 ms and a resolution of 60.000. Isolation of precursors was performed with the quadrupole at window of 1.4 m/z. Precursors were fragmented by higher-energy collisional dissociation (HCD) with normalized collision energy (NCE) / stepped NCE of 27. MS/MS scans were acquired at a resolution of 15.000 with an ion target value of 1×10^5, a maximum injection time of 120 ms, and an underfill ratio of 2%. Repeated sequencing of peptides was minimized by a dynamic exclusion time of 20 s.

5.6.3 Computational MS-data analysis

MS raw files were analyzed by the MaxQuant software (version 1.5.1.6) and peak lists were searched against the mouse Uniprot FASTA database, and a common contaminants database

(247 entries) by the Andromeda search engine. Cysteine carbamidomethylation was set as fixed modification, methionine oxidation and N-terminal protein acetylation as variable modifications. False discovery rate was 1% for proteins and peptides (minimum length of 7 amino acids) and was determined by searching a reverse database. Peptides specificity was set to trypsin requiring C-terminal arginine or lysine with a maximum of two missed cleavages. Maximal allowed precursor mass deviation for peptide identification was 4.5 ppm after time-dependent mass calibration and maximal fragment mass deviation was 20 ppm. "Match between runs" was activated with a retention time alignment window of 20 min, a match time window of 0.5 min, and a minimum ratio setting of 2.

5.6.4 Statistical analyses of MS-data

Statistical analysis of MS data was done with Perseus (vers. 1.5.3.0). To determine which RBPs were bound to mRNA, we used two quantification approaches. First, it was calculated which proteins were significantly enriched over the non-cross-link control using label-free quantification intensities (false discovery rate (FDR) < 0.05, red dots Figure 9). However, this was not feasible for all proteins, as a significant number of them had only very low intensity values in the cross-link samples, while not being detected in the non-cross-link controls. For enrichment analysis it is necessary to allocate artificial intensity values to undetected peptides, which are usually similar to the intensities of weakly measured peptides. Therefore, a reliable assessment of their enrichment was prevented. To circumvent this problem we took a semi-quantitative approach as employed previously (Sysoev, Fischer et al. 2016), where the number of peptide occurrences in the cross-link samples and non-cross-link controls are used to calculate the expected frequency of false-positives and to estimate the false discovery rate. For this analysis we only considered proteins if they were measured with at least two unique peptides in a sample. According to this we could allocate all peptides to 16 groups as shown in Figure 10. The FDRs were then estimated as ratios resulting from division of the transposed matrix by itself. For example, there were 79 peptides that were identified in two cross-link replicates and in no non-cross-link replicate and two peptides that were identified in two non-cross-link replicates and in no cross-link replicate in T_{eff} cells. FDR for those 79 peptides is estimated as 2/79=0.0253. We considered all peptides high confidence hits, which had a FDR $\leq$ 0.05 (colored cells Figure 10). Proteins that were confidently identified via this method were also added to the RBPome dataset.

5.6.5 Whole proteome analysis

For the total proteome of T_{eff} and T_{Foxp3+}, ~3-5x10^6 cells were pelleted, frozen in liquid nitrogen and analyzed via mass spectrometry. Each cell type was measured in duplicate. For the total proteome of T_{eff} and T_{Foxp3+} cells we only considered proteins part of the respective proteome if they were present in both measurements.

5.7 Validation of RNA binding ability

For the validation of the RNA binding ability of the identified proteins after RBPome analysis, HEK293T cells were transfected by calcium phosphate transfection with plasmids expressing the respective proteins with an N-terminal GFP-tag or GFP alone. After 3 days, cells were washed with PBS on plates, UV cross-linked as before or directly scraped from the plates. Cell lysates were generated by flash-freezing pellets in liquid nitrogen and subsequently incubating them in NP-40 lysis buffer. After lysis, extracts were cleared by centrifugation at 17000 g for 15 min at 4°C. We then determined protein concentration via the BCA method and used 2-10 mg of protein for the subsequent GFP immunoprecipitation, depending on transfection efficiency and expected RNA-binding capacity. We pre-coupled 200 µl Protein-G beads (Invitrogen) with 20 µg antibody (anti-GFP, clone: 3E5-111, in house) in PBS (1 h, RT), washed beads in lysis buffer, added them to cell lysates and incubated with rotation for 4 h at 4°C. Beads were then washed 3 times with IP wash buffers 1 to 3 with decreasing salt concentrations. Proteins and cross-linked RNAs were eluted with 50 mM glycine, pH 2.2 at 70°C for 5 min. Lämmli buffer (4x) was added and samples were divided for mRNA and protein detection and separated via SDS gel electrophoresis (6% SDS gels for detection of mRNA samples and 9% gels to verify immunoprecipitation efficiency). For RNA detection we blotted onto nitrocellulose membranes and for protein detection onto PVDF membranes. After transfer, the nitrocellulose membrane was prehybridized with church buffer for 30 min and then incubated for 4 h with church buffer containing 40 nM 3´- and 5´-Biotin labeled oligo$(dT)_{20}$ probe to anneal to the poly(A) tail of the bound mRNA. The membrane was washed twice with 1 x SSC, 0.5% SDS and twice with 0.5 x SSC, 0.5% SDS. Bound mRNA was detected with the Chemiluminescent Nucleic Acid Detection Kit Module (Thermo Fisher) according to the manufacturer´s instructions.

5.8 Bioinformatics and statistical analysis

GO and Pfam annotation for proteins was obtained from Ensembl release 91 via the Biomart R package. Proteins were classified as RNA binding using the GO-term “RNA binding” and its child terms.

For GO, Reactome and KEGG enrichment analysis, the DAVID database (version 6.8) was used (Huang da, Sherman et al. 2009, Huang da, Sherman et al. 2009). As a background, we used the total $CD4^+$ proteome.

We used the webtool from ExPASy (Gasteiger, Gattiker et al. 2003) to compute the isoelectric point of all reviewed Uniprot sequences. The amount of disordered regions in proteins are based on published data (Vincent and Schnell 2016). For low complexity regions we referred another recent publication (Kirmitzoglou and Promponas 2015). In both cases we again first filtered for and only used reviewed Uniprot protein sequences.

Classical and non-classical RBDs were selected from all Pfam domains as described previously (Kwon, Yi et al. 2013). Classical RBDs were tested for enrichment in the $CD4^+$

RBPome compared to the $CD4^+$ proteome by Fisher´s exact test. Proteins not containing a classical RBD were tested for enrichment of non-classical RBDs. Finally, proteins not containing either a classical or a non-classical RBD were tested for unknown RBDs present in at least 2 proteins in the $CD4^+$ RBPome. *P* values were corrected for multiple testing by the method of Benjamini-Hochberg.

5.9 Human orthologs

Human orthologous genes were downloaded from Ensembl release 91. A mouse gene is considered present (as ortholog) in the human RBPome if at least one of its orthologous human genes is contained in the human RBPome.

6. Results

6.1 Establishment of total mRNA pull down in CD4$^+$ T cells

We decided to determine the difference of all RBPs bound to mRNA in proinflammatory T effector versus anti-inflammatory regulatory T cells. For this, a technique developed in 2012 by the laboratories of Matthias Hentze and Markus Landthaler (Baltz, Munschauer et al. 2012, Castello, Fischer et al. 2012) was applied, termed "mRNA interactome capture". The mRNA interactome or RBPome of a cell comprises all RBPs bound to the total amount of mRNA. After generation of *in vitro* differentiated T_{eff} and T_{Foxp3+} cells, they were UV cross-linked and the mRNA and cross-linked proteins were captured via magnetic oligo(dT) beads. The proteins were digested and identified via mass spectrometry. A schematic of the workflow is shown in Figure 7. To validate this technique, capture of mRNA as well as the cross-linked proteins was confirmed. By performing qPCR on input and eluate we determined the pull down efficiency of known housekeeping gene mRNAs such as *Hprt1* and *β-actin* as seen in Figure 8a. Notably, there was no recovery of non-polyadenylated 18S rRNA. To verify capture of proteins cross-linked to the mRNA, silver staining of an SDS gel was performed. Figure 8b shows that UV cross-linking indeed leads to a strong enrichment of proteins compared to the non-cross-linked control.

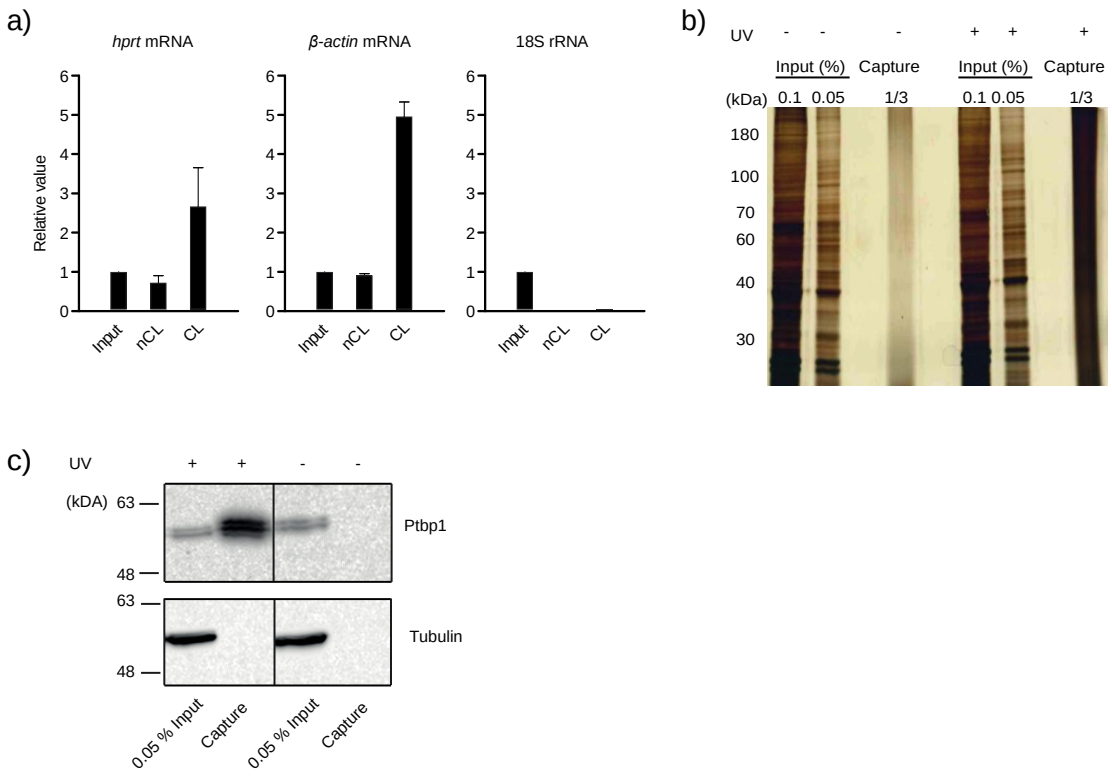

Figure 8: Verification experiments for total mRNA pull down
(a) Quantitative RT-PCR to determine RNA pull-down efficiency with (CL) and without cross-link (nCL). Error bars show the standard deviation around the means of three independent experiments. (b) Silver staining analysis of oligo(dT) captured samples with and without UV cross-link. (c) Western blotting of UV irradiated and nonirradiated samples of EL-4 T cells. Membranes were probed with antibodies for β-tubulin and the known mRNA-binding protein polypyrimidine tract binding protein 1 (Ptbp1). kDa, kilo dalton

Additionally, a pull down experiment was conducted on EL-4 T cells, a T cell line. Here, it was shown via western blot that the known mRNA-binding protein Ptbp1 was enriched in the cross-linked sample compared to the non-cross-linked control, while no recovery of the non RNA-binding protein β-Tubulin was observed (Figure 8c).

Next, the pull down experiment was conducted on primary T_{eff} and T_{Foxp3+} cells and the captured proteins subsequently analyzed via MS. For this analysis two quantification methods were employed (see Methods sections for details). The quantitative analysis showed 264 proteins in T_{eff} and 227 proteins in T_{Foxp3+} cells to be significantly enriched compared to the non-cross-link control (Figure 9).

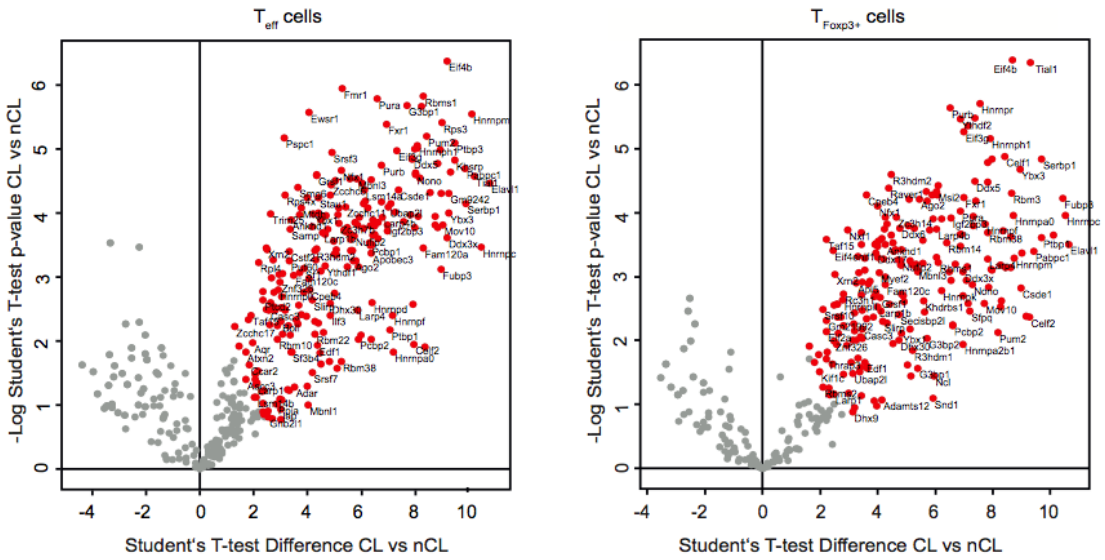

Figure 9: Quantitative analysis of T_{eff} and T_{Foxp3+} RBPome
Volcano plots with the –log p-value of the Student´s t-test (y-axis) and the Student´s t-test difference (x-axis) of UV cross-linked (CL) versus non-cross-linked (nCL) samples. Proteins, which are significantly different in CL compared to nCL are indicated (red, $p < 0.05$). Selective examples are labeled.

Furthermore, the semi-quantitative method showed significant enrichment of additional 33 proteins in T_{eff} cells and 19 proteins in T_{Foxp3+} cells (Figure 10). Combination of the two lists of RBPs for both cell types for their respective RBPome resulted in 297 proteins for T_{eff} cells and 246 proteins for T_{Foxp3+} cells.

T_{eff} cells

	nCL 0	nCL 1	nCL 2	nCL 3
CL 0	20	7	2	0
CL 1	7	1	4	0
CL 2	79 0.025	8	9	12
CL 3	159 0.000	28 0.000	23	65

T_{Foxp3+} cells

	nCL 0	nCL 1	nCL 2	nCL 3
CL 0	25	4	1	0
CL 1	52	6	1	2
CL 2	27 0.037	19	12	6
CL 3	139 0.000	40 0.05	32	58

Figure 10: Semi-quantitative analysis of T_{eff} and T_{Foxp3+} RBPome
Semi-quantitative identification method for RBPs was performed as previously (Sysoev, Fischer et al. 2016). Numbers of proteins, which are identified by at least two unique peptides in irradiated and nonirradiated samples. Colored cells exhibit a false discovery rate ≤ 0.05 (shown below the protein number) and are considered significant. CL, cross-link; nCL, non-cross-link

6.2 Validation of mRNA binders

Next, the mRNA binding capability of the identified proteins was further validated via a second experimental approach. Here, for several of the identified proteins (Stat1, Stat4, Ppia, Rbms1, Crip1 and Ldha) N-terminally GFP-tagged fusion constructs were generated. These fusion proteins were then overexpressed in HEK293T cells and captured via GFP immunoprecipitation after applying UV cross-link or no UV cross-link as control. It was first verified that equal amounts of protein were recovered after IP in cross-linked and non-cross-linked samples (Figure 11, left). Figure 11 (right) shows the detected polyadenylated RNA in the cross-linked sample, whereas there was little to none polyadenylated RNA in the non-cross-linked sample. Overexpressed GFP, which does not bind mRNA was used as negative control, while overexpressed known RBP Roquin was used as positive control and showed strong mRNA-binding.

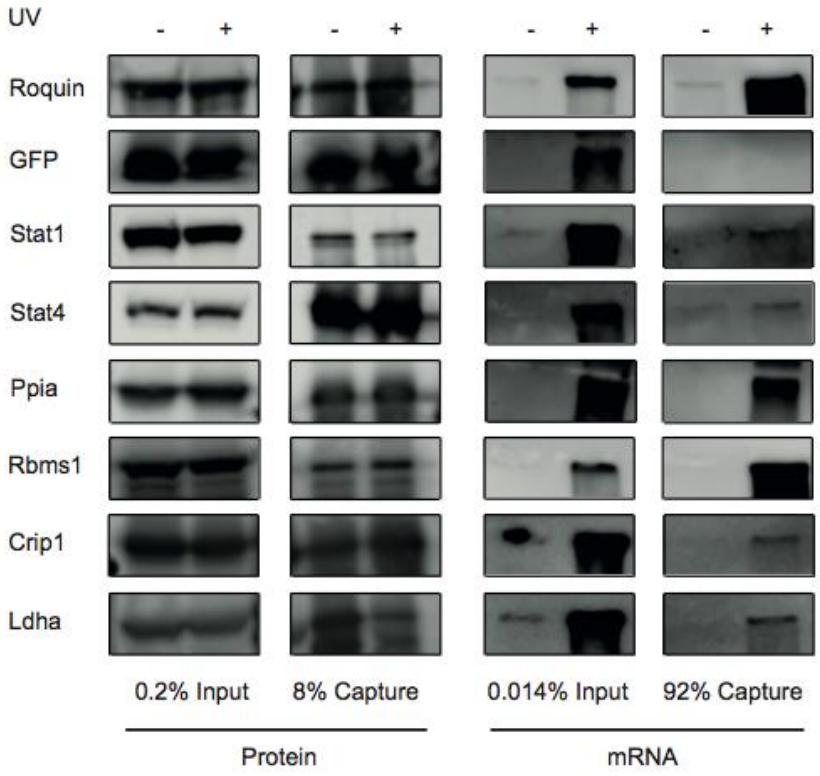

Figure 11: Validation of mRNA binding of selected proteins identified in the RBPome dataset
Overexpressed protein constructs are immunoprecipitated after UV cross-link and IP efficiency is verified (left) as well as mRNA binding via a biotinylated oligo(dT) probe (right). Roquin and GFP were used as positive and negative control respectively.

6.3 Analysis of identified RNA-binding proteins

6.3.1 Functional and biophysical analysis of RBPome

To conduct a more thorough and detailed interpretation of the data, the analysis was not confine to the respective RBPome and additional datasets were generated by determining the entirety of expressed genes using RNA sequencing and the entire proteome via mass spectrometry for the two cell types. First, the commonality between T_{eff} and T_{Foxp3+} cells was determined for all datasets (RBPome, RNA sequencing and proteome) and termed 'CD4$^+$ RBPome' (Supplementary Table 1), 'CD4$^+$ expressed genes' and 'CD4$^+$ proteome', respectively. All datasets were then analyzed for the percentage of genes/proteins that carry the gene ontology (GO) term "RNA-binding" or one of its child terms. As shown in Figure 12, RBPome capture strongly enriches for RNA-binding proteins as there are only 11.9% and 29.5% of annotated RBPs in CD4$^+$ expressed genes and the CD4$^+$ proteome respectively, compared to more than 98% of proteins being annotated as RBPs in the CD4$^+$ RBPome.

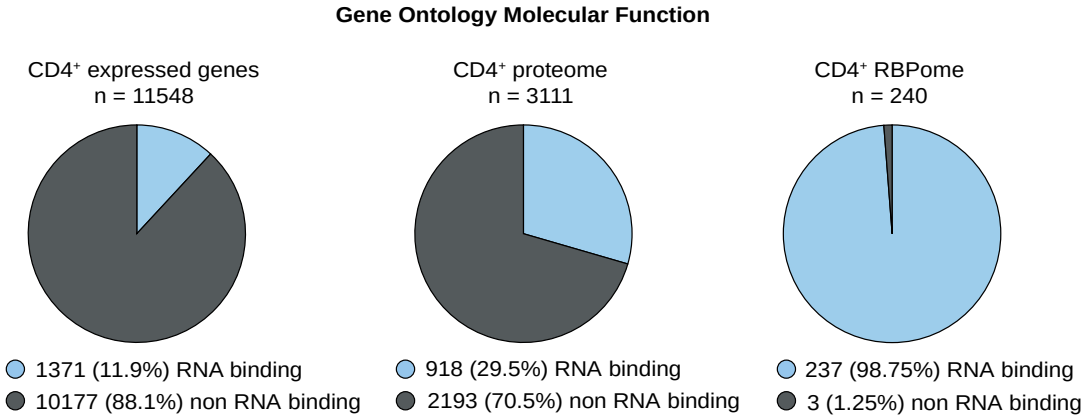

Figure 12: Classification of CD4$^+$ expressed genes, CD4$^+$ proteome and CD4$^+$ RBPome datasets into known and previously unknown RBPs
Genes and proteins were classified according to the GO term "RNA binding" and its child terms. Genes with a median FPKM ≥ 1 of three technical replicates where considered expressed in T_{eff} and T_{Foxp3+} cells respectively. Proteins were considered part of the proteome if they were measured in two of two technical replicates. Proteins were considered part of the RBPome as described above. The commonality between T_{eff} and T_{Foxp3+} expressed genes was termed 'CD4$^+$ expressed genes' and the proteome and RBPome were named accordingly.

This is also seen in various enrichment analyses for example for "GO Molecular Function", "GO Biological Process", "GO Cellular Component" as well as pathway enrichment analysis of KEGG and Reactome pathways (Figure 13a-e).

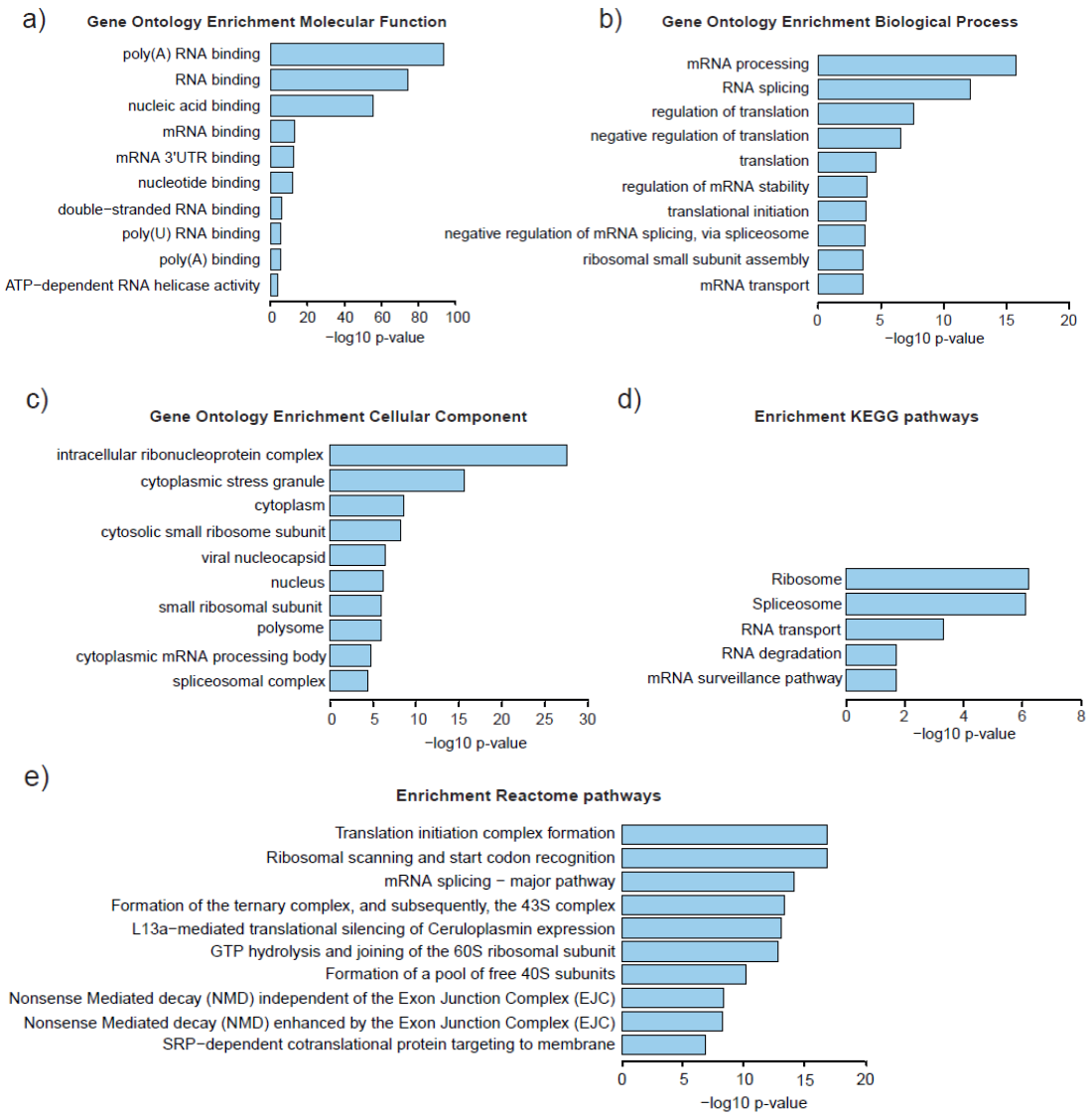

Figure 13: Functional characterization of CD4⁺ RBPome
(a-c) Top 10 most enriched gene ontology terms for molecular function (a), biological process (b) and cellular component (c) of the CD4⁺ RBPome. (d) 5 significantly enriched KEGG pathways of the CD4⁺ RBPome. (e) Top 10 most enriched pathways associated with the CD4⁺ RBPome according to the Reactome database.

Only three proteins (Crip1, Cnot2 and Ldha) of the 240 proteins found in the CD4⁺ RBPome are not annotated as RNA binding. We therefore took a closer look at their structure (Figure 14) and found that none of them had a known RNA binding domain. Solely Cnot2 exhibits a long stretch of low complexity and disordered amino acids, which is thought to facilitate RNA binding.

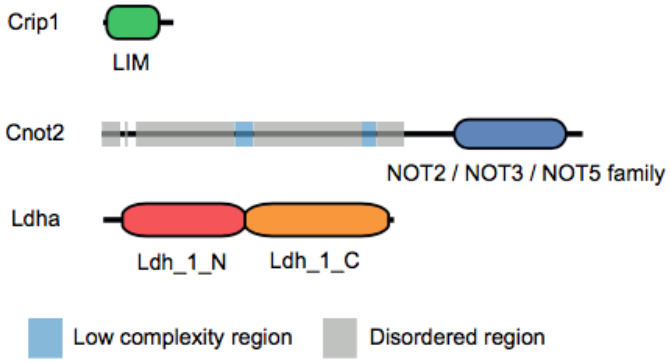

Figure 14: Overview of proteins and their domains and regions that are not classified as RNA binding by GO
Known protein domains according to the Pfam database as well as low complexity and disordered regions in the three proteins not classified as "RNA-binding" in the $CD4^+$ RBPome.

An analysis of all domains of the identified proteins was conducted by comparing the $CD4^+$ RBPome with the $CD4^+$ proteome and dividing the domains into classical, non-classical and unknown RNA-binding domains (Figure 15) as has been suggested before (Castello, Fischer et al. 2012). Most of the proteins possess either a classical or non-classical RBD with some of them being statistically overrepresented (Figure 15b-c). Additionally, there were a number of proteins that only exhibited domains, which are unknown to be involved in RNA-binding (Figure 15d).

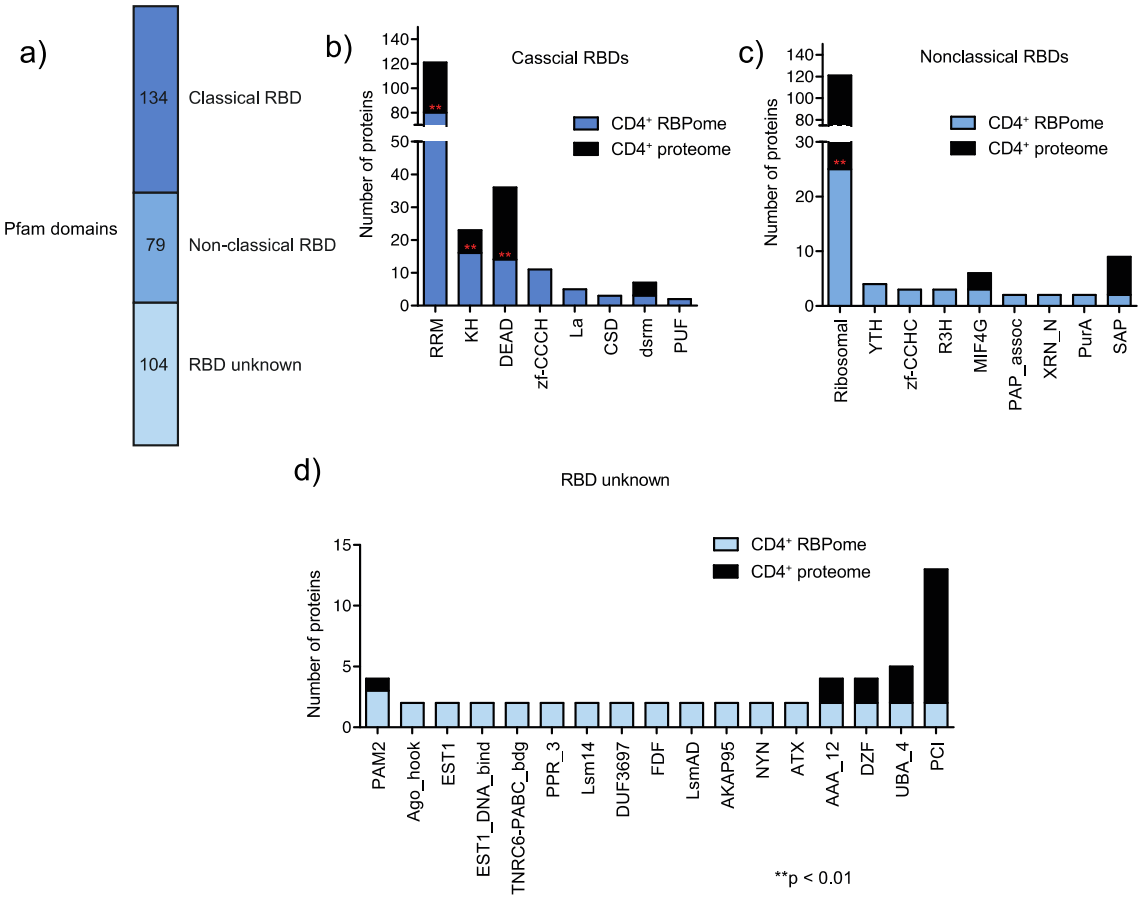

Figure 15: Number of proteins containing classical, non-classical, or unknown RNA binding domains in the CD4⁺ RBPome
Domain classification as previously described (Castello, Fischer et al. 2012). (a) Distribution of Pfam domains according to classical, non-classical und unknown RBD (b-d) Number of proteins annotated with the respective classical (b), non-classical (c) or unknown RNA binding domain (d) in the CD4⁺ RBPome (blue) or CD4⁺ proteome (black).

RNA-binding proteins are characterized by some specific biochemical properties compared to non RNA-binding proteins. They are thought to have a more basic isoelectric point (Castello, Fischer et al. 2016), and exhibit a greater portion of low complexity and disordered regions (Jarvelin, Noerenberg et al. 2016). This is in line with data for the RBPs identified in T cells. As seen in Figure 16 there is indeed a shift of the isoelectric point to a more basic value for proteins of the CD4⁺ RBPome compared to the CD4⁺ proteome as well as the increased presence of low complexity and disordered regions.

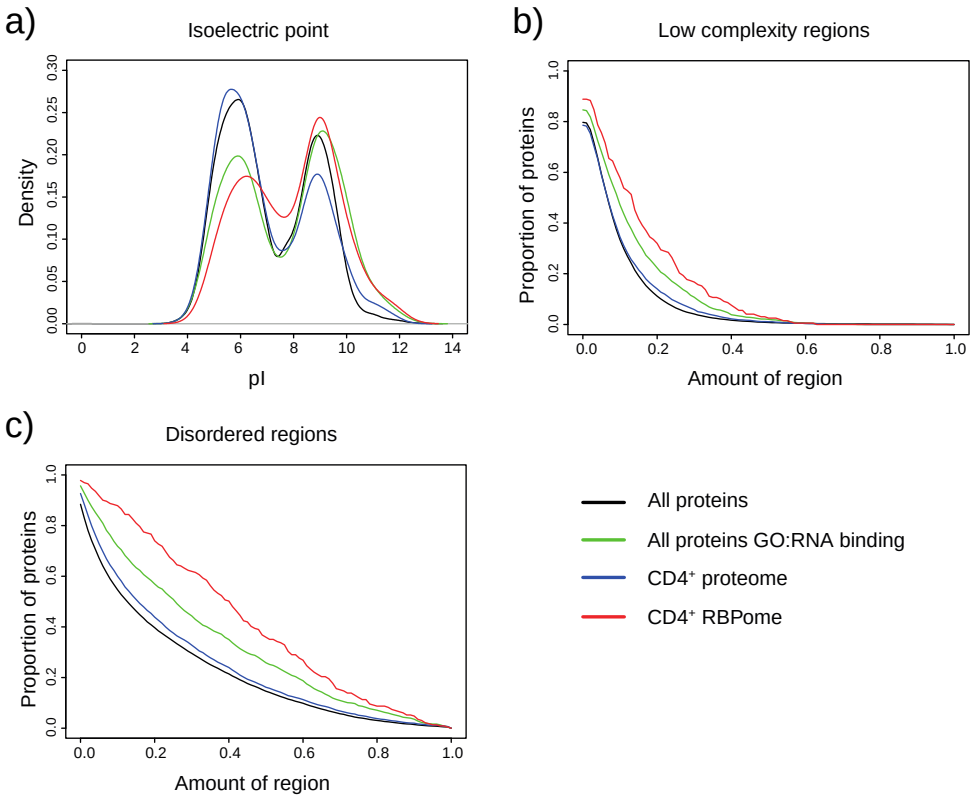

Figure 16: Biophysical features of CD4$^+$ RBPome
(a) Density of isoelectric point (pI). Displayed are all annotated and reviewed mouse proteins from Uniprot (black), all of those proteins which are known to bind RNA according to GO (green), all proteins in the CD4$^+$ proteome (blue) and the CD4$^+$ RBPome (red). (b-c) Distribution of low complexity (b) and disordered regions (c) in protein datasets. The significance of difference between the CD4$^+$ RBPome and the CD4$^+$ proteome was tested via Kolmogorov-Smirnov test and is significant for low complexity regions ($p = 4.90 \times 10^{-11}$) and disordered regions ($p = 2.2 \times 10^{-16}$).

6.3.2 CD4$^+$ RBPome in context to published datasets

To put these results into a broader biological perspective, a variety of analyses of the RBPome were added and integrated with the generated RNA sequencing and proteome datasets as well as other published RBPomes from different mouse and human cells. For comparison with other RBPomes, different datasets of human cells (HeLa (Castello, Fischer et al. 2012, Castello, Fischer et al. 2016), HEK293T (Baltz, Munschauer et al. 2012), HuH-7 (Beckmann, Horos et al. 2015) and K562 nucleus (Conrad, Albrecht et al. 2016)) as well as murine cells (embryonic stem cells (Kwon, Yi et al. 2013), cardiomyocytes (Liao, Castello et al. 2016), embryonic fibroblasts (Boucas, Fritz et al. 2015) and RAW264.7 (Liepelt, Naarmann-de Vries et al. 2016)) were compared with the combined CD4$^+$ RBPome (all RBPs identified in either T_{eff} or T_{Foxp3+} cells). First, all mouse proteins were divided according to whether they have a human orthologous protein or not. In total, 1239 mouse RBPs have been identified so far with 1156 of them having a human ortholog while 83 do not. Of the 303 proteins of the combined CD4$^+$ RBPome, 289 have and 14 do not have an ortholog. Figure 17

shows a venn diagrams of the overlap between a) total mouse and combined CD4⁺ RBPome proteins with a human orhtolog and b) total mouse and combined CD4⁺ RBPome proteins without a human ortholog. This analysis reveals several newly identified RBPs. In total 22 new RBPs were found in mouse cells. 8 of them have been identified in human cells before. Of these 22 proteins, 11 are unique for CD4⁺ T cells, while additional 3 are previously unidentified for mouse cells but are without a human ortholog (Figure 17 and Supplementary Table 2).

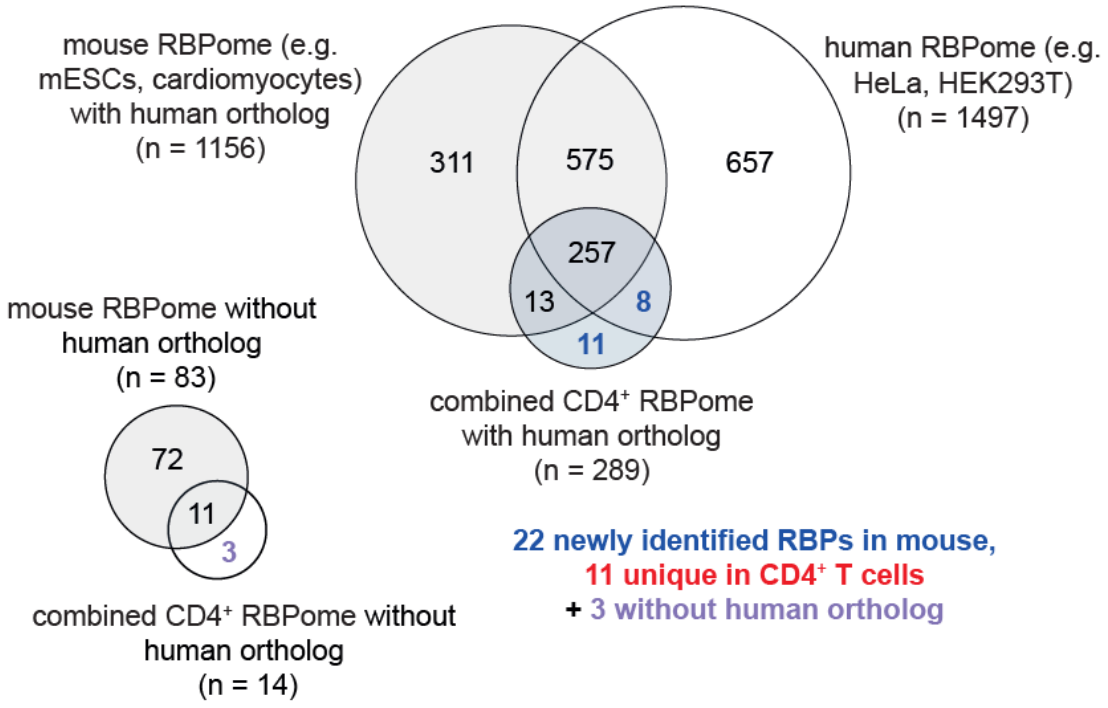

Figure 17: Overlap of the combined CD4⁺ RBPome (proteins detected in either T_{eff} or T_{Foxp3+} cells) with other previously identified mammalian RBPome datasets.
Human (HeLa (Castello, Fischer et al. 2012, Castello, Fischer et al. 2016), HEK293T (Baltz, Munschauer et al. 2012), K562 nucleus (Conrad, Albrecht et al. 2016), HuH-7 (Beckmann, Horos et al. 2015)) and mouse (mESCs (Kwon, Yi et al. 2013), MEFs (Boucas, Fritz et al. 2015), cardiomyocytes (Liao, Castello et al. 2016), RAW264.7 (Liepelt, Naarmann-de Vries et al. 2016)) published datasets. 22 proteins were newly identified in mouse cells, and 14 of them are unique for CD4⁺ T cells (with 3 proteins lacking a human ortholog).

Next it was investigated whether the RBPs identified in CD4⁺ T cells already have a known association with functions in the immune system by a manual search of the pubmed database for respective publications. We discovered that ~42% of the proteins have a described function, which connects them to the immune system (Figure 18).

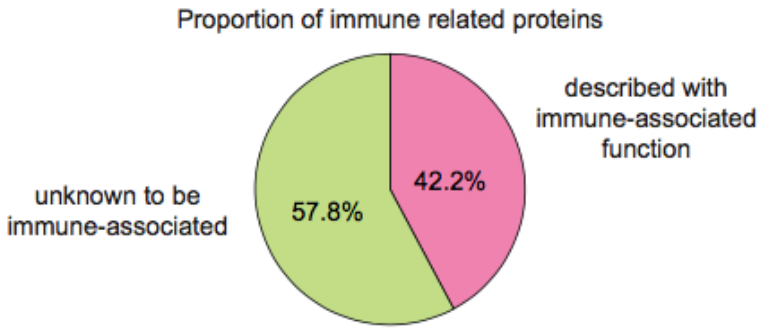

Figure 18: Percentage of proteins of the CD4⁺ RBPome that are known to be associated to an immune function
It was assessed whether proteins of the CD4⁺ RBPome are known to be immune-associated by a manual search of the pubmed database for respective publications.

On the other hand, for ~58% of analyzed proteins no connection was indicated.
To directly compare T_{eff} with T_{Foxp3+} cells, we focused on the RBPs, which have only been preferentially detected in one of the two cell types. These are 57 proteins for T_{eff} cells and 6 proteins for T_{Foxp3+} cells, respectively (Figure 19, Supplementary Table 3 and Supplementary Table 4).

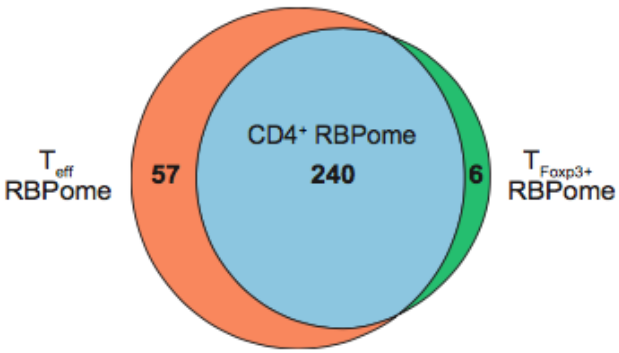

Figure 19: Overlap of the T_{eff} and T_{Foxp3+} RBPome
The 240 proteins present in both datasets are referred to as the CD4⁺ RBPome. 57 and 6 proteins are preferentially identified in the T_{eff} and T_{Foxp3+} RBPome, respectively.

Interestingly, the T_{eff} RBPome displayed a higher enrichment for previously not annotated RBPs (21 not annotated) compared to the T_{Foxp3+} RBPome (6 not annotated) (Figure 20).

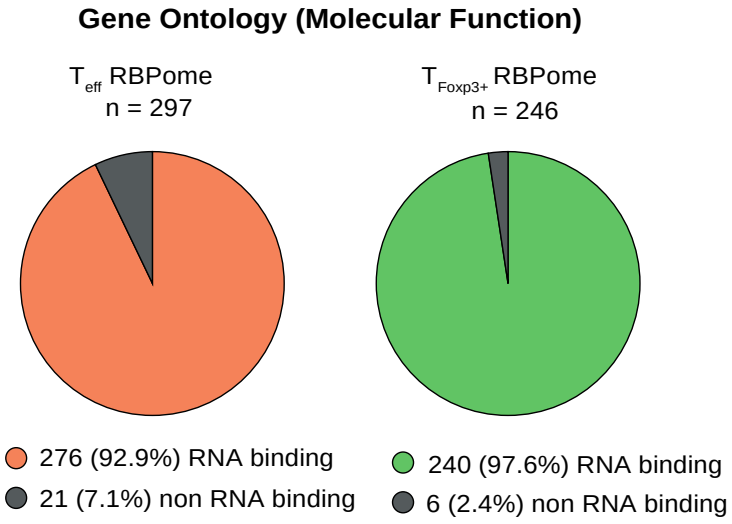

Figure 20: Classification of T_{eff} and T_{Foxp3+} RBPome datasets into known and previously unknown RBPs
Proteins of the two datasets were classified according to the GO term "RNA binding" and its child terms as before**.**

Finally, to estimate the binding strength of RNA binding of the identified RBPs, the FPKM (Fragments per kilobase of transcript per million mapped reads) values of the RNA sequencing data for all identified RBPs were plotted in T_{Foxp3+} versus T_{eff} cells (Figure 21).

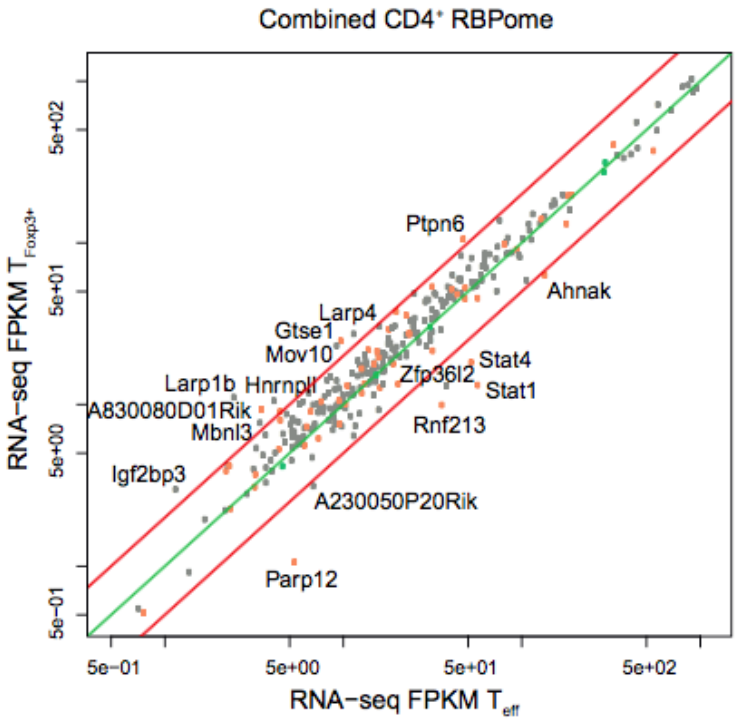

Figure 21: Scatterplot of RNA sequencing FPKM values in T_{Foxp3+} versus T_{eff} cells of proteins, which were identified in the combined CD4⁺ RBPome
Labeled proteins exhibit a more than twofold difference in expression levels (indicated by red lines) between cell types. A pseudocount of 0.5 was added to FPKM values to enable fold change calculation on genes whose expression was close to zero in one sample. Preferential binders in T_{eff} and T_{Foxp3+} cells are indicated as orange and as green dots respectively. FPKM, Fragments per kilobase of transcript per million mapped reads

This analysis of the data suggests that proteins, which are significantly lower expressed, e.g. Igf2bp3 with FPKM values around 3-4 but are nonetheless detected in the RBPome, have a stronger RNA binding capacity than for example Ldha with FPKM values of around 300. Of note, this quantification method is not absolute as there are differences in measured peptide intensities in the RBPome, however it does allow for a general estimation of binding strength. Especially interesting are the 23 proteins, which were only detected in one or both of the RBPome datasets, but in neither of the proteome sets (Supplementary Table 5). Furthermore, 16 of the identified proteins showed a more than twofold difference in FPKM values between T_{eff} and T_{Foxp3+} cells. It was also observed that some proteins (A830080D01Rik, Gtse1 and Ptpn6) showed more than twofold higher FPKM values in T_{Foxp3+} cells compared to T_{eff} cells, even though they were only detected as RNA binding proteins in T_{eff} cells.
Ultimately, all the above datasets and analyses were integrated specifically in relation to the 22 newly identified proteins in mouse cells and summarized in form of a comprehensive table (Figure 22).

	Gene name	Protein ID	Immune related	PMID
●	Adamts12	Q811B3	ADAMTS-12 metalloprotease is necessary for normal inflammatory response	23019333
▲	Aven	Q9D9K3	Fox1 factor 1 affects the apoptosis of natural regulatory T cells by controlling Aven expression.	28283017
*	Boll	Q924M5-2	no	-
▲	Capzb	P47757-2	no	-
▲	Chtf8	P0CG14	no	-
▲	Cnn2	Q08093	Deletion of calponin 2 in macrophages attenuates the severity of inflammatory arthritis in mice	27488671
▲	Cnot9	Q9JKY0	no	-
▲	Coro1a	O89053	Coronin 1A, a novel player in integrin biology, controls neutrophil trafficking in innate immunity	28615221
*	Crip1	P63254	Overexpression of CRIP in transgenic mice alters cytokine patterns and the immune response.	12006348
▲	Dap	Q91XC8	Mediator of the gamma interferon-induced cell death	7828849
▲	Gtse1	Q8R080	no	-
▲	Iap	P03975	no	-
*	Larp1b	Q8R3F0	no	-
*	Myh9	Q8VDD5	neutrophil non-muscle myosin heavy chain-IIA localization for efficient genetic diagnosis of MYH9 disorders.	2919935728
▲	Ptpn6	P29351	Protein Tyrosine Phosphatase 6 as Checkpoint Regulator in Immunity.	929190
▲	Rbm15b	Q6PHZ5	no	-
▲	Rpl37	Q9D823	no	-
▲	Rps27	Q6ZWU9	no	-
▲	Snw1	Q9CSN1	no	-
▲	Stat1	P42225	Signal transducer and transcription activator mediating cellular responses to interferons (IFNs) and cytokines	12797537
▲	Stat4	P42228	Mediating responses to IL12 in lymphocytes, and regulating the differentiation of T helper cells	10851056
▲	Vav1	P27870	Important in hematopoiesis, playing a role in T-cell and B-cell development and activation	7700358

* CD4+ RBPome
▲ preferentially in T_{eff} cells
● preferentially in T_{Foxp3+} cells

T cell unique RBP
Not detected in either proteome
Without human ortholog, previously unidentified in mouse

Figure 22: Integration of the analyses of Figures 17-19 and Figure 21 with a more detailed analysis of the known immune related function of a protein and the PubMed identifier of the respective publication
Depicted are the 22 newly identified RBPs in mouse cells with their gene name, protein ID, immune relation if present and the pubmed ID of the respective publication describing their immune association.

6.4 Pull down of one specific mRNA

In 2011 Howard Chang and colleagues developed a method named Chromatin Isolation by RNA Purification (ChIRP) to investigate which proteins and DNA sequences are bound to one specific long noncoding RNA. Within this study, tiling oligonucleotides complementary to the lncRNA were designed, biotinylated and incubated with the cell lysate after cross-linking RNAs and proteins with formaldehyde. The resulting complexes were then captured using magnetic streptavidin beads and the proteins were analyzed via mass spectrometry (Chu, Quinn et al. 2012). Since the aim of this thesis was to determine which RBPs are bound to a specific mRNA, we tried to develop a method for an mRNA pull down on the basis of ChIRP. In contrast to ChIRP, ultraviolet light with 254 nm wavelength was used to cross-link RBPs to RNA. It has been shown that UV light activates nucleotide bases, which then form covalent bonds especially with nucleophilic and aromatic amino acid residues at "zero distance", thus avoiding protein-protein cross-links (Saito and Matsuura 1985). Biotinylated complementary oligonucleotides were designed for the target mRNAs (for details of designing see the method section), namely *Hprt1*, *Ox40*, *Foxp3* and *GFP*. *Hprt1* is an abundantly expressed housekeeping gene and was therefore supposed to serve as a control for the background of nonspecific mRNA-binding proteins. *GFP* served as an additional negative

control, since it is not expressed in the investigated cells. *Ox40* was chosen as positive control, since it has been shown that its 3´ UTR is bound by the RBP Roquin in $CD4^+$ T cells (Janowski, Heinz et al. 2016). The detection of Roquin after *Ox40* pull down was therefore intended to confirm the efficacy of the method. To recover sufficient amounts of mRNA, at least 10 probes were designed for every oligonucleotide set for one mRNA. Different sets of oligonucleotides displayed higher recovery rates than others and the average annealing temperature for the probe sets ranges from 70° to 80°C as calculated via Equation 1. The hybridization buffer contained formamide, which is known to reduce the annealing temperature by ~0.7°C / % formamide (Landre, Gelfand et al. 1995). Additionally, the annealing temperature was kept as low as possible to prevent damage to mRNA or protein, therefore differences in recovery rates were investigated with temperatures between 55° and 65°C. Here, best recovery efficiency was achieved with an annealing temperature of 60°C.
For *Hprt1*, recovery rate R calculated via Equation 2 lies at around 0.219, meaning that ~ 22% of input *Hprt1* mRNA was recovered after pull down (Figure 23). Recovery rate of *Ox40* showed differences between T helper cell subsets. In T_{Foxp3+} cells a recovery rate of ~ 1.6 was determined and thus an apparent enrichment of 1.6-fold after pull down (Figure 23). On the other hand, in T effector cells R was calculated to be ~ 0.75, recovering 75% of mRNA (Figure 23). This shows, that pull down recovery is strongly dependent on cell types and varies between diverse mRNAs. To achieve optimal recovery rate for *Foxp3*, several different probe sets were tested. First, 20 probes with a 5´ biotinylation (Foxp3 20mer Biotin 1-20) were generated and validated in different combinations regarding their pull down efficiency. The combination of probes 2, 4, 6, 8, 10, 12, 14, 16, 18 and 20 (Foxp3 Set1) had the highest recovery rate with about 20% (Figure 23). For further optimization, one additional probe set was designed (Foxp3 Set2), this time with a 3´ biotinylation (Foxp3 20mer 3Bio 1-10). This set had a recovery rate of around 50% (Figure 23).

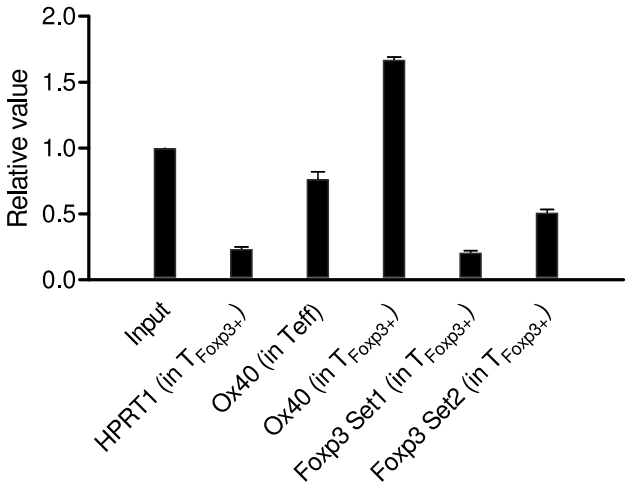

Figure 23: Efficiency of specific mRNA pull down
Shown is the relative value of mRNA recovery after pull down compared to the input for different biotinylated oligonucleotide sets. Error bars show the standard deviation around the means of at least two independent experiments.

To verify the specificity of the mRNA pull down, recovery rates of non-targeted mRNAs were assessed in pull down eluates. For example, a pull down was performed on *Ox40* mRNA and mRNA levels of *β-actin* and *Hprt1* were measured in the eluate. Here, a very high specificity was observed, as recovery rates for unspecific mRNAs were in the range of $1.0x10^{-5}$ to $1.2x10^{-6}$. Since only a few select mRNAs were tested as unspecific controls, it cannot be ruled out that other unspecific targets were recovered. However, due to the aforementioned results and the high stringency during probe design, this seems to be rather unlikely.

The next step was to identify the proteins bound to the respective mRNA. To this end, pull down experiments were performed on endogenous as well as transgenically overexpressed mRNAs in different cell types and the samples analyzed via western blot and mass spectrometry. As recovery rates for *Foxp3* and *Ox40* mRNA were within a reasonable range, endogenous pull downs were performed with $20x10^6$ T_{Foxp3+} cells and subsequently analyzed via mass spectrometry. However, we were not able to detect any proteins above the unspecific background. This did not change, even after increasing cell numbers by six-fold to $120x10^6$ T_{Foxp3+} cells. Since it was not possible to further scale up the cell number, the aim was to optimize other experimental conditions. Therefore, HEK293T cells were transfected with constructs of target mRNAs known to be bound by Roquin such as the *Icos* 3´UTR or *Ox40* 3´UTR followed by a GFP sequence. Additionally, Roquin itself was cotransfected. This resulted in a significant increase of the amount of target mRNA and corresponding RBP in the cell. It became apparent, that capture of overexpressed mRNA via GFP probes was very inefficient with a recovery rate of only 4 to 6%, depending on the construct. However, because of the aforementioned increase in amount of mRNA and RBP in the cell, we nonetheless continued with this approach. Since this approach was not reliant on primary cells, it was possible to test a broader spectrum of experimental variables in a shorter timeframe, including the change of annealing temperature, probe concentration, type of detergent in lysis and wash buffers and ratio of probe concentration to bead volume for example. After pull down, it was examined whether bound Roquin could be detected via western blot. Here, the results were very inconsistent and eventually recovery of Roquin could not be verified reproducibly.

6.5 Reporter assays for Foxp3 regulation

As an approach to investigate in what way *Foxp3* is regulated, a reporter system was employed, which was aimed at determining if there are external signals by stimuli or cytokines that are necessary for induction of regulation. We tried to establish this system in parallel to the specific mRNA pull down, as it was planned to use these two methodologies in combination. After identification of a signal involved in *Foxp3* regulation, we planned to perform the specific pull down before and after this treatment. It would thus be possible to

directly compare the bound state, in which the putative RBP exerts its regulatory effect on *Foxp3* mRNA, with the unbound state.

For this assay, reporter constructs for *Foxp3* were designed on the basis of the vector displayed in Figure 6, where *GFP* mRNA is expressed with the respective UTR sequences and subsequently translated. The general idea behind these constructs was that they either contain a very short part of the *Foxp3* 3´UTR or the complete 3´UTR. Since we hypothesized that post-transcriptional regulation is taking place by binding of an RBP to the rear end of the 3´UTR and thus causing for example stabilization or destabilization or differences in translation of the mRNA, this would only take place in the construct with the complete 3´UTR. Therefore, a difference in GFP fluorescence intensity should be observed between the two constructs if the respective external conditions induce this regulation.

However, when the experiments with those vectors were conducted, transfection as well as transduction efficiency/virus titer for the construct carrying the full length 3´UTR were very low. To circumvent this problem, the number of virus producing cells for the experimental setup was greatly increased and retroviral concentration reagents (Clontech) used to concentrate virus supernatants. Nonetheless, it was not possible to reproducibly achieve sufficient transduction efficiencies into primary T cells.

Therefore, as a first step only endogenous Foxp3 protein levels were measured via flow cytometry after culturing T_{Foxp3+} cells in different conditions for 24 and 48 h. This more general approach was employed to identify a setup, where *Foxp3* mRNA is regulated with an effect on Foxp3 translation to subsequently test whether this is mediated via the *Foxp3* 3´UTR. On the one hand this approach is thus independent of inefficient primary cell transduction, on the other hand it is only possible to see effects on Foxp3 protein levels. This means that a regulatory effect, e.g. a change in mRNA stability, is only visible if it manifests in a difference in translation. As we assumed that changes in protein levels could be rather minute and thus difficult to detect on a logarithmic scale, Foxp3 protein was measured in flow cytometry via the linear scale. T_{Foxp3+} cells were cultured under the following conditions for 24 and 48 h:

1) Control
2) IL-6 (40 ng/ml), IL-23 (20 ng/ml), TGF-β (5 ng/ml)
3) IL-10 (20 ng/ml), anti-CTLA-4 (1 µg/ml)
4) TNF-α (20 ng/ml), IL-1β (20 ng/ml)
5) IL-2 (10 ng/ml)
6) IL-21 (20 ng/ml)
7) IL-7 (20 ng/ml)
8) IL-15 (20 ng/ml)
9) IL-12 (20 ng/ml)
10) IL-33 (20 ng/ml)
11) anti-CD3/CD28 (0.1/1 µg/ml)
12) anti-CD3/CD28 (0.2/2 µg/ml)

The rationale behind the application of various cytokines and antibodies was to mimic a variety of different *in vivo* conditions, thus potentially inducing regulatory effects on *Foxp3*. To simulate a pro-inflammatory milieu IL-6, IL-23, TNF-α, IL-1β, IL-12 or a combination of these were employed. On the other hand, IL-10 is a cytokine secreted by Treg cells and CTLA-4 a receptor on the Treg surface (Verhagen, Gabrysova et al. 2014), which characterize this condition as more anti-inflammatory. IL-2 is essential for T cell survival and growth (Kelly, Won et al. 2002). Interleukin-33 is a member of the IL-1 superfamily of cytokines. It is expressed in epithelial cells at barrier sites such as the intestine and has been shown to enhance Treg cell function (Schiering, Krausgruber et al. 2014). IL-21 is known to inhibit the production of IL-2 by other T cells, thus impairing Treg cell homeostasis (Attridge, Wang et al. 2012). IL-7 has been shown to be critical for T cell development (Hong, Luckey et al. 2012) as well as T cell homeostasis (Surh and Sprent 2008). Similar to IL-2 and IL-7, IL-15 is also involved in T cell survival and homeostasis and has a crucial role for T cell activation and effector function (Kanegane and Tosato 1996, Read, Powell et al. 2016). Lastly, the cells were restimulated with two different concentrations of CD3/CD28, as it was shown that continuous TCR signaling is required for *Foxp3* expression (Vahl, Drees et al. 2014). Figure 24 shows Foxp3 protein levels on a linear scale in T_{Foxp3+} cells under these various conditions after 24 and 48 h. Only the combination of IL-6, IL-23 and TGF-β results in a slight increase in Foxp3 protein levels after 24 h, and even more so after 48 h. In all other conditions, there is no observable effect on Foxp3 levels.

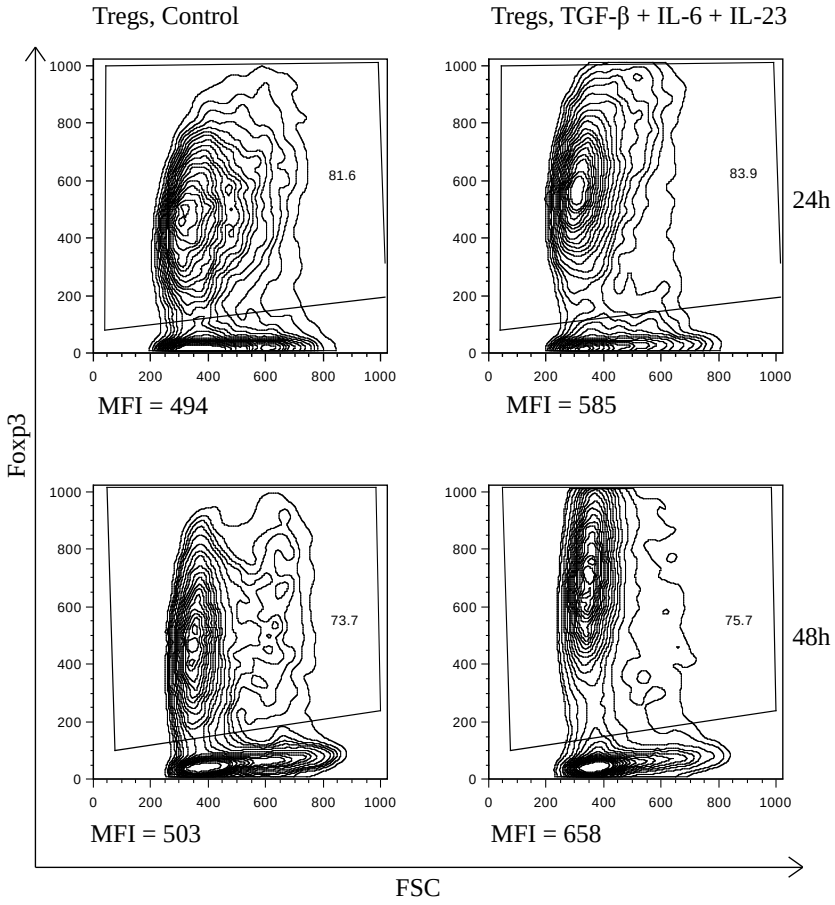

Figure 24: Foxp3 upregulation in response to cytokines
Effect of a combination of cytokines on Foxp3 protein levels after incubation for 24 and 48 h. MFI, Mean fluorescence intensity; FSC, Forward scatter

T_{Foxp3+} cells were then separately cultured with IL-6, IL-23 and TGF-β to delineate which of the factors is responsible for the upregulation. IL-6 did not show an effect, while IL-23 and TGF-β on their own seem to result in a slight upregulation, which is even increased when combining both factors (Figure 25).

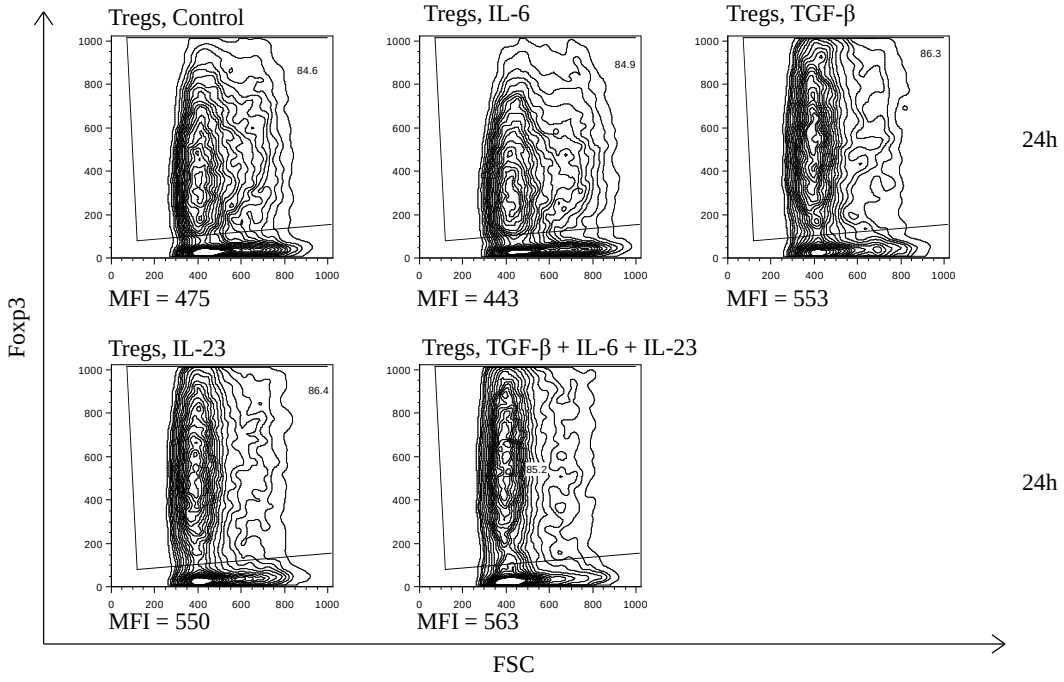

Figure 25: Effects of different cytokines on Foxp3
Effect of IL-6, IL-23 and TGF-β on Foxp3 protein levels after incubation for 24 h. MFI, Mean fluorescence intensity; FSC, Forward scatter

Since it is known that TGF-β is upregulating *Foxp3* on a transcriptional level (Horwitz, Zheng et al. 2008), the cells were additionally treated with actinomycin D (actD), a transcriptional blocking agent, to determine whether there is also a post-transcriptional regulation taking place in this setup. However, it was not possible to incubate the cells 48 and not even 24 h with actD, as its strong cytostatic effects resulted in greatly increased cell death after these extended time periods. Thus, it cannot be excluded that the increase in Foxp3 protein levels in this setup is solely caused by a transcriptional upregulation.

6.6 Different isoforms of *Foxp3* mRNA

Analysis of the *Foxp3* 3´UTR, revealed one poly(A) signal sequence at position 785-790 bp (of 2200 bp total). In principle, it is not surprising for an mRNA to have more than one poly(A) signal, as alternative polyadenylation is a common post-transcriptional regulatory mechanism (Gupta, Clauder-Munster et al. 2014). For *Foxp3* however, we were not able to identify the distal poly(A) signal sequence, although we used more than 10 of the most commonly utilized sequences as reference (Neve, Burger et al. 2016). Even though this is uncommon, it has been shown before that cleavage and polyadenylation can also take place

without a specific signal sequence (Beaudoing, Freier et al. 2000, Neve, Burger et al. 2016). Additionally, the proximal poly(A) signal has the sequence AAUAAA, which is the most widely utilized form. Therefore, it seems likely that the mRNA isoform ending at this position is the predominant form compared to the isoform carrying the complete 3´UTR. To verify this hypothesis, 6 qPCR primer sets (race1-6) were generated, which bind at different positions along the 3´UTR (Figure 26). First, primer efficiency was verified by using a plasmid carrying the complete *Foxp3* 3´UTR as reference.

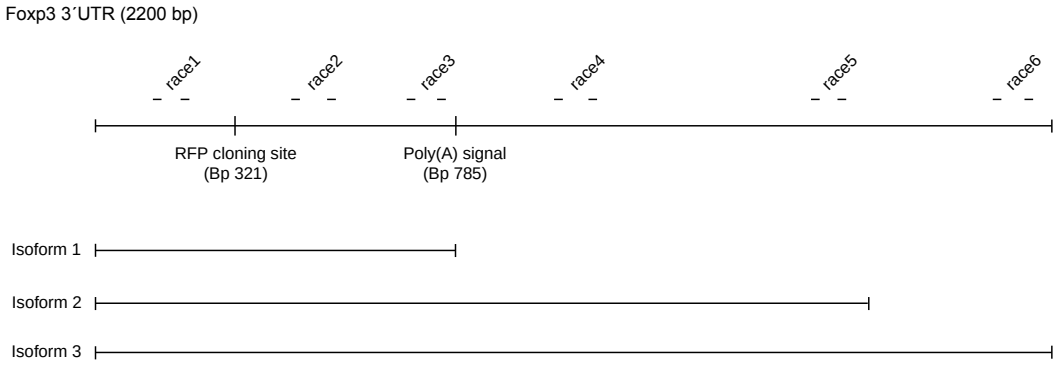

Figure 26: Foxp3 qPCR race primers and mRNA isoforms
Sections in the Foxp3 3´UTR where race primers 1-6 bind as well as location of RFP cloning site in Foxp3-RFP reporter mice and the endogenous poly(A) signal. Analyses with these primers point at the presence of the three depicted Foxp3 mRNA isoforms.

Subsequently, race qPCRs were conducted using cDNA from *in vitro* generated T_{Foxp3+} cells, Treg cells isolated via the $CD4^+$ $CD25^+$ regulatory T cell isolation kit from miltenyi (*in vivo* Tregs) as well as cells from a Foxp3-RFP reporter mouse line (RFP^+ *in vivo* Tregs). For the latter, we sorted $CD4^+CD8^-TCRab^+RFP^+$ cells from different organs such as spleen and mesenteric lymph nodes directly into QIAzol lysis reagent, isolated RNA, synthesized cDNA and performed qPCRs. The resulting data indicated that there are at least 3 different isoforms of *Foxp3* mRNA present in various types of cells and their relative distribution is depicted in Table 15.

Table 15: Distribution of isoforms of *Foxp3* mRNA in different cell types.
Depicted are the means of at least two independent experiments with their standard deviation.

	T_{Foxp3+} cells	***In vivo* Tregs**	**RFP^+ *in vivo* Tregs**
Isoform 1	73.2%±2.5	75.5%±1.8	69.3%±2.3
Isoform 2	7.1%±1.1	8.8%±1.2	5.6%±1.5
Isoform 3	19.8%±1.4	15.7%±0.9	25.3%±0.5

As expected, isoform 1, which ends with the most widely used polyadenylation signal is also the most predominant isoform with ~75% abundance. Furthermore, the isoform with the full length 3´UTR (isoform 3) was only slightly more abundant in T_{Foxp3+} cells compared to *in vivo* isolated Treg cells with 15.7% to 19.8%. In RFP^+ *in vivo* Treg cells, this isoform was again more abundant at 25.3%. Altogether, we were able to identify and quantify the distribution of 3 different mRNA isoforms of *Foxp3* mRNA in different types of regulatory T cells.

7. Discussion

Identification and characterization of mRNA-binding proteins in CD4$^+$ T cells

In this thesis, we aimed to identify and characterize proteins bound to the mRNA of *Foxp3* as well as all RBPs bound to the total mRNA in two subsets of CD4$^+$ T helper cells, namely T_{eff} and T_{Foxp3+} cells. In the following section we will first discuss the technical achievements as well as limitations of the conducted experiments and subsequently analyze the results with regard to their biological relevance.

7.1 Discussion of experimental aspects: RBPome capture in CD4$^+$ T cells

To determine the RBPome of T_{eff} and T_{Foxp3+} cells, all proteins bound to the total mRNA were captured and identified via mass spectrometry. The specificity of this method was verified with regard to capture of mRNA as well as mRNA-binding proteins via qPCR and western blot, respectively (Figure 8). This has been similarly shown in recent publications (Kwon, Yi et al. 2013, Sysoev, Fischer et al. 2016). Mass spectrometry data was analyzed using a quantitative method based on label-free quantification intensities with a false discovery rate (FDR) of ≤ 0.5 (Figure 9) as well as a semi-quantitative method based on identified peptide counts (Figure 10) as was recently proposed (Sysoev, Fischer et al. 2016). To further substantiate the validity of the identified proteins, additional verification experiments were performed to show mRNA-binding of a select group of proteins from the RBPome (Figure 11). Here, some of them were found to bind noticeably more mRNA as observed in western blot analysis. This correlates well with the amount of detected peptides in mass spectrometry data for the respective proteins after endogenous pull down, as for example Rbms1 was detected by ~10 peptides and showed a very strong signal in pull down experiments. Conversely, only 2 peptides were detected for Stat1, Stat4 and Crip1, respectively, in MS data. These proteins also displayed a considerably lower signal in pull down experiments. Altogether, we expect the RBPome datasets of these two cell types to be highly reliable, as we employed stringent statistical as well as biochemical methods for their identification.

7.2 Discussion of experimental aspects: Attempt to identify and characterize *Foxp3* mRNA binding factors and their regulatory role for *Foxp3*

7.2.1 Specific pull down of one mRNA and identification of bound RBPs

The methodological approach to establish a pull down of one specific mRNA in $CD4^+$ T cells was based on ChIRP, a technique established by Howard Chang´s laboratory (Chu, Quinn et al. 2012). We were able to recover around 20-30% of *Hprt1* mRNA and 30-50% of *Foxp3* mRNA. Additionally, *Ox40* mRNA was successfully enriched up to 1.6-fold after pull down, depending on the specific set of oligonucleotides used and the cell type with which the pull down was performed (Figure 23). The differences in recovery efficiency between oligonucleotide sets were probably due to the fact that different regions of the mRNA are folded into secondary structures and/or covered by RBPs and thus less available for binding of certain probes. As described in the methods section, we tried to avoid probe binding to regions predicted to be folded by using the software "Sfold". Nonetheless, because of the complex situation of an *in vivo* environment, folding of mRNA can deviate strongly from its predicted form. Therefore, only experimental evaluation can finally determine recovery efficiency for a specific set of probes. For *Foxp3*, Set2 had a significantly higher recovery rate than Set1. We can only speculate whether this is caused by the aforementioned differences in folding or RBP coverage of the mRNA or due to the used 3´ biotinylation and thus possible steric differences in binding.

Unlike as for the mRNA, we were unable to reproducibly show in western blot or via mass spectrometry the simultaneous recovery of bound RNA-binding proteins. There are a variety of possible explanations for this lack of detection. For example, a significant increase in recovery rate might be necessary. To achieve this, several experimental variables which are crucial for pull down efficiency were varied, for example annealing temperature of probes, probe concentration, duration of probe annealing, salt and detergent concentration and type of detergent in lysis and wash buffers as well as type and concentration of magnetic beads for recovery. The annealing temperature is generally calculated via Equation 1. As noted before, it seems to be optimal at 60°C and a minimum of 4 h incubation with the probes is necessary. Additionally, a wide variety of detergents with different concentrations in the washing buffer, such as sodium deoxycholate or lithium dodecylsulfate as well as different concentrations of sodium chloride (500 mM, 350 mM or 150 mM) were used and compared to generic wash buffers on the basis of saline-sodium citrate (SSC). However, none of these changes resulted in a strong improvement of pull down efficiency or allowed detection of Roquin after *Ox40* pull down. We thus hypothesize, that the amount of recovered protein is very low and therefore below the detection limit of a western blot or mass spectrometry analysis. Especially in comparison to ChIRP, this seems to be a likely scenario. Here, the authors use Xist lncRNA (Chu, Zhang et al. 2015) with a length of 17 kbp or U1 snRNA with an estimated copy number of ~$1x10^6$ per cell as their target RNAs (Gesteland, Cech et al. 1999). As we

were interested in various mRNAs, we chose the transcripts of *Foxp3* (~3,8 kbp), *Hprt1* (~1,3 kbp) and *Tnfrsf4* (Ox40) (~1,2 kbp) as targets. Copy numbers of protein coding RNAs in mammalian cells can differ according to the specific cell type, type of RNA or state of cell development but they generally range from ~100 – 500 per cell for transcription factors and secretory proteins, such as *Nanog*, *Oct4* and *Chgb* (Bengtsson, Hemberg et al. 2008, Albayrak, Jordi et al. 2016, Skinner, Xu et al. 2016), 1000-3000 per cell for *Gapdh*, essential for glycolysis and often used as a housekeeping gene (Marinov, Williams et al. 2014) up to ~10.000 for transcripts of the ribosomal protein Rps29 (Bengtsson, Hemberg et al. 2008). These numbers clearly show, that it is much more challenging to detect RBPs bound to the mRNA targets we chose, as these transcripts are both smaller in size as well as less frequently present in the cell. Furthermore, in ChIRP the authors use formaldehyde as their means of cross-linking, which induces RNA-protein as well as protein-protein cross-links (Engreitz, Sirokman et al. 2014). Since many RBPs exert their function in ribonucleoprotein complexes which are based on both types of interactions (Mitchell and Parker 2014), this results in the capture of entire protein complexes bound perhaps solely through one RBP to the RNA. However, we sought to exclusively identify RBPs directly binding to the mRNA. Accordingly, we chose UV light as cross-linking method to only induce RNA-protein cross-links, which as a negative side effect will additionally reduce the absolute number of captured proteins.

As scaling up cell numbers significantly to ~$70x10^6$ HEK and ~$120x10^6$ primary T cells per condition to increase the amount of captured protein and examination of a wide variety of experimental conditions for the pull down turned out to be unsuccessful as well, we chose to discontinue this approach. We believe that the amount of protein, which is bound to one specific mRNA, is too low to be detected at least with reasonable cell numbers in this experimental setting.

In conclusion, the pull down of one specific mRNA was successfully established, but presumably the small sizes and low abundances of selected target mRNAs prevented identification of bound RNA-binding proteins.

7.2.2 Analysis of Foxp3 regulation by retroviral reporter assays

To investigate post-transcriptional processes related to *Foxp3* regulation in primary Treg cells, we tried to establish a reporter system to determine under which conditions *Foxp3* mRNA is regulated via its 3´UTR. For this, two retroviral reporter constructs were generated, which contained the *Foxp3* 5´UTR followed by the GFP coding sequence. We then inserted either a short section of the 3´UTR (~300 bp) or the complete 3´UTR (~2200 bp) C-terminally to the GFP. The *Foxp3* 5´UTR was added to mimic the endogenous circumstances in T_{Foxp3+} cells as close as possible. Also, it has recently been shown, that post-transcriptional regulation of the mRNA by the 3´UTR can be influenced by its respective 5´UTR (Theil, Herzog et al. 2018). Additionally, the ER retention signal sequence KDEL was added C-

terminally to the GFP sequence. This seems to be beneficial for reporter constructs designed to measure post-transcriptional regulation, as mRNAs carrying an ER retention signal are retained longer at the ER, and thus are potentially subject to more post-transcriptional regulatory events (Vigo Heissmeyer, personal communication).
In the assays, it was technically extremely challenging to achieve a sufficient virus titer for the construct carrying the complete 3´UTR. We assume this resulted from the considerable size of the inserted UTR as sufficient virus titers for various other reporter constructs with smaller inserts (e.g. the short section of the *Foxp3* 3´UTR with ~320 bp or the *Ox40* 3´UTR with ~120 bp) were consistently achieved and T cells efficiently transduced. We thus tried to concentrate the virus via retrovirus concentration reagents (Clontech). Even though we increased the initial volume of supernatant fivefold, virus titers and transduction efficiencies were close to detection limit and prone to high experimental variability. Therefore, we decided to change our approach and monitored endogenous Foxp3 protein levels via flow cytometry. We found that only the combination of IL-6, TGF-β and IL-23 induced changes in Foxp3 protein levels. This can be explained, as it has been shown before that TGF-β signaling transcriptionally upregulates *Foxp3* in the beginning of Treg cell differentiation as well as in later stages (Horwitz, Zheng et al. 2008). IL-6 is generally crucial for immune homeostasis by mediating the Th17/Treg balance and together with TGF-β it induces Th17 differentiation from naïve T cells while inhibiting TGF-β induced Treg cell differentiation (Kimura and Kishimoto 2010). Additionally, in human Treg cells the synergy of IL-6 and TGF-β is able to promote post-translational FOXP3 protein degradation (Gao, Gao et al. 2012). However it is unexpected that the addition of IL-23 seems to further increase *Foxp3* upregulation as in general, IL-23 has been shown to transcriptionally down regulate *FOXP3* expression (Tarique, Saini et al. 2017), or restrain regulatory T cell activity (Izcue, Hue et al. 2008).
We tried to exclude transcriptional regulation as a cause by additionally treating the cells with actinomycin D, a transcriptional inhibitor. Since we assumed that post-transcriptional regulation, especially with an influence on translation, an extended period of time to be detectable compared to fast acting transcriptional regulation, we had to treat the cells for 24 h with the respective cytokines. However, this time span resulted in strongly increased cell death. We therefore had to conclude, that although we were able to detect changes in Foxp3 protein levels after treatment with TGF-β, especially in combination with IL-6 and IL-23, our experimental setting does not allow us to distinguish between transcriptional and post-transcriptional regulation of *Foxp3*.

7.3 Discussion of biological results: RBPome capture of primary mouse T helper cells

By using RBPome capture, we were able to identify all RBPs bound to the total mRNA in T_{eff} and T_{Foxp3+} cells. As described in Figure 13, the $CD4^+$ RBPome shows a strong overrepresententation of various RNA associated terms of GO Molecular Function,

Biological Process and Cellular Component as well as RNA associated pathways. The two most predominant associated functions and pathways are splicing and translation. This can be easily explained, as we identified large groups of splicing factors such as Srsf1, Srsf2, Srsf3 etc. This in turn results in an overrepresententation of biological processes like mRNA processing or RNA splicing (Figure 13b), overrepresententation of cellular components like intracellular ribonucleoprotein complex or spliceosomal complex (Figure 13c) and overrepresententation of pathways such as Spliceosome or mRNA splicing (Figure 13d and e). Additionally, ribosomal proteins such as Rps10, Rps11, Rps12 etc. are very abundant, which results in processes like translation or regulation of translation (Figure 13b), cellular components like intracellular ribonucleoprotein complex or cytosolic small ribosome subunit (Figure 13c) and pathways like Ribosome or translation initiation complex formation to be overrepresented (Figure 13d and e). Both splicing and translation are prevalent post-transcriptional regulatory processes and consequently the respective protein groups have been extensively identified in various published RBPome datasets before (Castello, Fischer et al. 2012, Kwon, Yi et al. 2013).

Next, we analyzed the different protein domains of proteins in the RBPome and found that they show a significant overrepresentation of classical RNA binding domains (RBDs). These include the RNA recognition motif (RRM), the most abundant RBD in vertebrates (Cléry and Allain 2011) and other common RBDs like the KH domain or DEAD box helicase domain (Figure 15). Considering the great number of ribosomal proteins, it is not surprising that we also identified a very high number of different ribosomal RBDs (Figure 15c) that are categorized as non-classical RBDs. Additionally, there was also a number of proteins containing solely domains, that are unknown to be associated with RNA binding (Figure 15d). As all of those domains occurred at a very low frequency (between two and three times), they were not considered significantly enriched. However, some of them have also been found in other RBPome datasets, for example the Ataxin-2 C-terminal region (PAM2) in HeLa cells (Castello, Fischer et al. 2012), or the pentatricopeptide repeat (PPR_3) in mouse cardiomyocytes (Liao, Castello et al. 2016). This further substantiates that these domains are indeed actively involved in mRNA binding.

Even though RBDs play an important role in RNA binding there are also other mechanisms employed. It has already been shown, that additionally to RBDs, the presence of intrinsically disordered regions without a stable tertiary structure in proteins can mediate their RNA binding. These regions are often found to be rich in serine and arginine (S/R) or arginine and glycine (R/G) (Jarvelin, Noerenberg et al. 2016). They form RG- and RS-rich repeats and in concert with other amino acids compose a variety of motifs that can appear multiple times in a protein. The recurrence of those motifs therefore results in a lower complexity of amino acids compared to non RNA-binding proteins in the proteome. This enrichment of RS-rich, RG-rich and other basic regions also generally results in a shift of the isoelectric point of these proteins towards more basic values (Castello, Fischer et al. 2016). All of the above characteristics are reflected in published RBPome datasets (Castello, Fischer et al. 2012, Kwon, Yi et al. 2013, Sysoev, Fischer et al. 2016) and correlate with our analyses of the $CD4^+$ RBPome (Figure 16). Interestingly, we found that the proteins Crip1, Ldha and Cnot2

were not annotated by GO as RNA-binding and do not carry RBDs. However, Ldha has been shown to be an ARE-binding protein which interacts with RNA via its NAD^+-binding region (Rossman fold) (Pioli, Hamilton et al. 2002). Cnot2 exhibits a long region of low complexity and disordered amino acids, through which RNA-binding could be mediated. However, this is not the case for Crip1 and since its structure is dominated by its respective protein domain (Figure 14), it seems likely, that this LIM domain is responsible for the protein's RNA binding capability and thus a promising candidate as new RBD.

Altogether we were able to identify 303 RBPs in the combined $CD4^+$ RBPome, with 57 and 6 differentially discovered in T_{eff} and T_{Foxp3} cells respectively, as well as an overlap of 240 common proteins. We identified fewer proteins than in many other capture experiments (e.g. ~400 and ~500 RBPs have been identified for the fly embryo and in mouse embryonic stem cells (Kwon, Yi et al. 2013, Wessels, Imami et al. 2016)). This could have been caused by the small size and low cytoplasm content of T helper cells, where mRNA is contained. Specifically, it is known that lymphocytes in general have a high nucleus-to-cytoplasm ratio (N/C ratio) of ~4:1 (Turgeon 2012) compared to other cell types such as mouse embryonic stem cells (~1:1, (Zhou, Basu et al. 2016)) or HeLa cells (~1:2, (Eida, Van Cauteren et al. 2016)). Additionally, we cannot exclude that T cells have a relatively limited RBPome that is highly specialized, which would be in line with the highly specific functions of these cells.

In general, the great overlap of ~80% of RBPs between the two cell types as well as the strong enrichment of proteins associated with RNA-binding support the robustness of the employed experimental procedure.

It has recently been shown, that many metabolic enzymes can "moonlight" as RNA binding proteins (Castello, Hentze et al. 2015), and are also able to bind and regulate RNAs in addition to their function in metabolic pathways. Especially in the RBPome of HeLa cells many of these moonlighting enzymes have been found (Castello, Fischer et al. 2012). We therefore analyzed the $CD4^+$ RBPome in this regard but could only identify one metabolic protein, lactate dehydrogenase A (Ldha), which is responsible for interconversion of L-lactate and NAD to pyruvate and NADH in anaerobic glycolysis. This could possibly also be attributed to the lack of depth of the dataset. The very high expression levels in combination with low to moderate detection in the RBPome suggest that Ldha in this setup indeed primarily functions as a metabolic enzyme.

7.4 Discussion of biological results: Expanding the knowledge on primary mouse RNA-binding proteins

We identified a number of new as well as already known RBPs for the first time in primary $CD4^+$ T helper cells. The majority of them has already been described to bind to mRNA in other cellular contexts, however we additionally expanded the analysis by adding proteome and RNA sequencing data and integrated those with the RBPome sets. From this integration we can deduce three interesting observations:

1) There are 23 proteins which we identified in the RBPome dataset, which were not detected in the proteome sets (Supplementary Table 5). It seems likely, that these proteins are only expressed at a low level and require RBPome capture to enrich them above the necessary threshold to be detected by MS. This makes them very interesting and potentially important regulators as some of those are already known RBPs that play a vital role in T cells, e.g. Roquin 1 (Cui, Mino et al. 2017) or Zfp36l2 (Galloway, Saveliev et al. 2016). It will thus be worth investigating all of them.
2) There are three proteins (Gtse1, Ptpn6 and A830080D01Rik) which show a more than twofold higher FPKM value in T_{Foxp3+} cells but are only detected in the T_{eff} RBPome. This could hint towards cell subtype specific mRNA binding and makes them promising mRNA regulator candidates that are dependent on or involved in establishing cellular identity. Ptpn6 has been shown to be an important regulator of not only $CD4^+$ T cell homeostasis in general by inhibiting IL-4 signaling (Johnson, Pao et al. 2013) but also Treg cells specifically, where a loss of Ptpn6 results in a skewing of Treg cells towards a Th2 cell phenotype, thus impairing oral tolerance (Noval Rivas, Burton et al. 2015). One could thus speculate that in T_{eff} cells, the function of Ptpn6 is separated into its phosphatase function as well as its mRNA binding with unknown effects, whereas in Treg cells the protein primarily functions as a phosphatase that is essential for cell function with little or no mRNA-binding function. This would explain the higher RNA sequencing values and presumably higher protein levels without a concomitant detection in the RBPome of T_{Foxp3+} cells. Gtse1 and A830080D01Rik are so far unknown to have a specific function in immune cells, although generally, Gtse1 is thought to be p53 dependent and upregulated as response to DNA damage (Utrera, Collavin et al. 1998). Nonetheless, our results also indicate that these proteins primarily exert their mRNA binding function in T_{eff} cells while in T_{Foxp3+} cells their other molecular functions seem to be predominant.
3) In general, we can compare and evaluate the mRNA binding strengths of proteins in relation to their expression levels. Here, proteins, which are significantly lower expressed than others (for example Igf2bp3 with ~5 FPKM compared to Ldha and Cfl1 with ~200-300 FPKM) and are either measured with comparable peptide numbers in the RBPome or in this case Igf2bp3 with even more peptides, strongly suggests either an increased binding affinity of Igf2bp3 for one specific or several different mRNAs compared to Ldha and Cfl1. The distinction between these two alternatives of binding is not possible with our methodology.

Especially interesting are the 11 and 3 newly identified proteins that have not been detected in any other RBPome dataset before (Supplementary Table 2) with and without human orthologs, respectively. Some of the identified proteins such as Crip1 already have a known association with the immune system ((Lanningham-Foster, Green et al. 2002), while others like Rps27 do not. Both cases are equally interesting. In general, for immune-associated proteins, their function is known (Crip1, (Khoo, Blanchard et al. 1997)) or thought (Adamts12, (Moncada-Pazos, Obaya et al. 2018)) to be unrelated to mRNA binding. On the

other hand, there are two possible explanations why proteins we identified do not have a known immune association. Either their mRNA binding function is not immune cell specific (which is likely for ribosomal protein Rsp27 or the CCR4-NOT transcription complex subunit Cnot9 for example), or additionally to their known function, they exert an unknown secondary function in immune cells which is mediated by mRNA binding.

From the three newly identified proteins without a human ortholog (Cnn2, Iap and Rps27), mRNA binding of Iap (Intracisternal particle A) is not easy to interpret. It is a retrovirus-like mobile genetic element in the mouse genome (Jiao, Jin et al. 2009), which is why there are no RNA sequencing values for correlation. It is very possible that earlier studies excluded this protein because of its ambiguous nature. However, one explanation for its detection in our RBPome dataset is an auto-regulatory translational feedback loop of Iap binding to its own mRNA and thus ensuring translation and propagation in the genome.

The analysis of the differences between the identified RBPs in both cell types is depicted in Figure 19 and here, 57 and 6 proteins are identified as preferentially bound in T_{eff} and T_{Foxp3+} cells, respectively. The small number for T_{Foxp3+} cells is likely due to generally fewer identified proteins in this subtype. We speculate that the preferential binding of these proteins is especially dynamic and context-dependent and find it very likely that they also exert their function in other cell types under the appropriate conditions. We chose the steady state as experimental setup, i.e. without any kind of cell stimulation, since it has been shown that here miRNA regulating networks, the action framework of some known RBPs, primarily exert their function (Lichti, Gallus et al. 2018). Of note, it seems as if the T_{eff} RBPome features slightly more proteins without RNA binding annotation compared to the T_{Foxp3+} RBPome (Figure 20). In general, this occurrence of a preferential RBPome for a particular cell type is in line with the fact that translational control programs, which are greatly influenced by RBPs, are known to differ between immune subtypes (Bjur, Larsson et al. 2013).

Interestingly, we identified three transcription factors (Stat1, Stat4 and Vav1) that have been shown to have numerous important functions in T cell development, differentiation and activation (Nishibori, Tanabe et al. 2004, Wei, Vahedi et al. 2010, Helou, Petrashen et al. 2015) but are so far unknown to bind mRNA. In general, the notion of DNA-binding transcription factors also being able to bind RNA is long standing in the field (Cassiday and Maher 2002). Even though both being nucleic acid molecules, this is not a trivial observation, as the structure of DNA and RNA differs substantially. DNA is mostly double stranded, adopting a B-form helix, while RNA is predominantly single stranded and in case of double helix formation adopts the more compact A-form. Therefore, even identical sequences of DNA and RNA are expected to fold into very distinct secondary structures (Cassiday and Maher 2002). However, researchers identified especially zinc finger (ZF) domains to be capable of binding both DNA and RNA, as exemplified in the TFs transcription factor IIIA (TFIIIA) (Pelham and Brown 1980), wilms´ tumor protein 1 (WT1) (Zhai, Iskandar et al. 2001) and the RNA pol II transcription factor TRA-1 (Graves, Segal et al. 1999). Furthermore, the tumor suppressor protein p53 has been shown to bind RNA via a phosphoserine at position 389 (Fontoura, Sorokina et al. 1992). The transcription factor Stat1 was identified to be able to bind noncoding RNA (ncRNA) (Peyman 1999, Peyman 2001),

however in this case it is thought that this RNA binding regulates Stat1 protein function, the RNA thus being the regulator. This concept of RNA as a regulator of protein activity is not uncommon and especially found in innate immunity for example in Toll-like receptors (TLRs), which are pattern recognition receptors and activated by binding of double-stranded RNA (TLR-3), single-stranded RNA (TLR-7/8) or bacterial rRNA (TLR-13) (Kawai and Akira 2010, Yu and Levine 2011, Oldenburg, Kruger et al. 2012) among others. In this study, we now additionally showed Stat1 binding to mRNA along with Stat4 and Vav1, which suggests an unknown regulatory function for these proteins by binding one or potentially several mRNA targets. This hypothesis is not entirely new, as for example also the transcription factor Stat6 was shown to bind mRNA in mouse cardiomyocytes (Liao, Castello et al. 2016). With our results we therefore not only second the observation of different TFs being capable of binding mRNA but also expand their catalogue.

7.5 Discussion of biological results: Attempt to identify and characterize Foxp3 mRNA binding factors and their regulatory role for *Foxp3*

When we examined the *Foxp3* 3´ UTR in more detail, we found the poly(A) signal sequences with the very common sequence AAUAAA (Neve, Burger et al. 2016), but were not able to detect a distal poly(A) sequence at the 3´ end of the mRNA. Nonetheless, the fact that there is a proximal poly(A) sequence present suggests that there are probably at least two mRNA isoforms differing in 3´UTR length, while the shorter isoform is likely to be more abundant because of the abundant poly(A) sequence. As expected, when we analyzed Treg cells from wild type mice (*in vitro* generated as well as freshly isolated), we found that this short isoform is present at ~73% of total *Foxp3* mRNA, while the longer isoform only appears at ~15% (Table 15). It is known that binding sites for RBPs and miRNAs are common in 3´UTRs (Mu, Lu et al. 2011, Lu and Clark 2012), therefore it is possible, that the longer isoform is differentially regulated compared to the shorter one. This could be mediated by RBPs but also via binding of other factors such as miRNAs. Since we aimed to identify the proteins bound to the target mRNA via mass spectrometry, we would not be able to directly identify bound miRNAs. However, in this case we expected to measure increased amounts of proteins associated with miRNA regulation such as Ago2. To further analyze miRNAs as regulatory factors, a Dicer-deficient mouse line could be used, as these mice are unable to generate miRNAs. Since miRNAs have been shown to be crucial for T cell differentiation (Muljo, Ansel et al. 2005), it would be necessary to use inducible knockout mice, for example via tamoxifen treatment of Cre-ERT2, to ablate Dicer after complete differentiation of T cells. Additionally, it would also be possible to perform RNA sequencing on the samples after a successful pull down and thus identify the miRNAs bound to *Foxp3* mRNA.

In general, a differential regulation of mRNA isoforms depending on 3´UTR length potentially caused by APA is a known mechanism in immune cells, e.g. in *NLRP3* expression. The NLRP3 inflammasome recognizes pathogens and is viewed as the most clinically

implicated inflammasome (Abderrazak, Syrovets et al. 2015). The longer isoform of *NLRP3* mRNA harbors binding sites for the RBP ZFP36 and this binding results in increased mRNA decay (Haneklaus, O'Neil et al. 2017), thus greatly affecting the progress of autoinflammatory and autoimmune disorders.

Interestingly, we found isoform 3 slightly more abundant in *in vivo* RFP^+ Treg cells compared to the other cell types. Many RBPs rely on the three-dimensional structure of the RNA for their binding. This structure is probably altered to a certain degree by the insertion of the RFP sequence and results in a slightly different folding of the mRNA. It is thus possible that one or more RBPs change their binding to the mRNA and thus the process of cleavage and polyadenylation experiences a decrease or increase, which results in these altered isoform levels. Additionally, we also detected an isoform of intermediate length (isoform 2), which seems to be around 200 bp shorter than isoform 3. We can only speculate whether this has a biological relevance, but because of its low abundance and the rather marginal difference in length this appears unlikely.

8. Outlook and future directions

8.1 Extending the analyses of mRNA-binding proteins and their function in CD4$^+$ T cells

In this thesis, we were able to generate several different datasets of RBPome, RNA sequencing and proteome, which can serve as starting point for a wide variety of follow-up studies and analyses.

The integration of these datasets results in several groups of RBPs, which should be considered prime candidates for subsequent analyses. These include proteins with an assumed very strong mRNA binding affinity for one or multiple targets (e.g. proteins detected in the RBPome but not the proteome), proteins preferentially bound in one of the two T cell subsets, proteins previously unknown to bind mRNA or proteins exhibiting comparable mRNA binding while being differentially expressed between the two subsets.

Another valuable aspect of RBPs is their binding specificity, which could be further investigated by performing PAR-CLIP or similar experimental approaches, where specific target mRNAs of RNA-binding proteins as well as their binding sequences within the mRNA are determined.

It will be especially interesting to investigate the specific resulting molecular and cellular effects of mRNA binding of Stat1, Stat4 and Vav1 as they are of pivotal importance in many cellular contexts. Their role as TFs suggests a possible crosstalk with a variety of different signal transduction pathways within the cell and thus possibly wide implications with a variety of cellular processes.

In general, many of the identified RBPs have known functions in post-transcriptional regulation. However, we assume to have captured the most relevant RBPs in the cell. Therefore, global approaches such as a systematic knock down of these RBPs would very likely result in a great expansion of knowledge considering their so far unexplored mechanisms of post-transcriptional regulation putatively encompassing all mechanisms depicted in Figure 4 with probable implications for a variety of cellular functions.

Additionally, we are already in the process of identifying the RBPome of human T_{Fxop3+} and T_{eff} cells, which will very likely furthermore expand the general catalogue of RBPs and specifically RBPs in CD4$^+$ T cells.

8.2 Post-transcriptional regulation of *Foxp3*

Due to technical limitations, we were unable to identify RBPs bound to *Foxp3* mRNA or specific conditions for its post-transcriptional regulation. However, unpublished observations as well as the fact that we were able to identify several different isoforms of *Foxp3* mRNA *in vivo*, strongly suggest the action of post-transcriptional regulatory mechanisms. It is thus

tempting to speculate who these regulators are and what their exact function might be.
These candidate proteins are likely to exhibit certain criteria, such as having a stable expression in Treg cells and being classified as RNA-binding or at least as nucleic acid binding, since even transcription factors which are mostly thought of as DNA-binding proteins (e.g. Stat1 or Vav1) can additionally bind mRNA, as shown in this thesis and elsewhere (Liao, Castello et al. 2016). Obviously, there are many RBPs in Treg cells fitting these criteria. However, some of them seem to be more promising candidates than others. We therefore composed a list of genes fulfilling aforementioned conditions in T cells and analyzed it also with respect to known gene functions. One interesting potential candidate we identified is the RNA uridlytransferase Zcchc11, which is necessary to maintain the poly(A) tail length and stability of cytokine mRNAs, e.g. *Il-6*. These mRNAs are targeted and repressed by binding of certain miRNAs. Terminal uridylation of cytokine mRNAs by Zcchc11 is able to prevent this binding, thus abolishing repression (Jones, Quinton et al. 2009). Another interesting candidate would be Y box protein 3 (Ybx3), which has been shown to function as translational repressor of different mRNAs (Giorgini, Davies et al. 2002) and intriguingly is able to bind the RNA consensus sequence UCCAUCA, also found in the *Foxp3* 3´UTR. The RBP Paip2, whose human homologue has been shown to mediate translational repression via binding to PABPC1 (Yoshida, Yoshida et al. 2006) is involved in the TGF-β signaling pathways according to pathcards, and could thus potentially provide a link to the development and/or stability of Treg cells.
Furthermore, in one of the many studies published concerning *Foxp3* and its function in Treg cells, the authors define a set of genes termed the "Treg signature", which is specifically characteristic for regulatory T cells (Hill, Feuerer et al. 2007). It contains Mbnl3, which is a known RNA-binding protein with different functions that has been implicated in regulation of alternative polyadenylation (Batra, Charizanis et al. 2014) and alternative splicing (Lee, Lewis et al. 2011). In general, *Foxp3* regulation could very well involve factors known to regulate APA, since we believe the different *Foxp3* mRNA isoforms are generated via this mechanism. Another Treg signature gene is the RNase Regnase-3 (Zc3h12c), which is part of the same protein family as Regnase-1. As Regnase-1 has been shown to be essential for many regulatory functions in immune cells (Matsushita, Takeuchi et al. 2009, Cui, Mino et al. 2017) it seems possible for Regnase-3 to expand the regulatory spectrum of this protein family towards Treg cells.
All in all, there is a multitude of RBPs which are possibly involved in the post-transcriptional regulation of *Foxp3* and can thus be considered interesting targets for further studies concerning this topic.

9. Conclusion

We set out to identify and characterize RNA-binding proteins as post-transcriptional regulators and thus performed RBPome capture in $CD4^+$ T_{eff} and T_{Foxp3+} cells and integrated these datasets with RNA sequencing as well as proteome analyses. We were able to identify an overlapping set of 240 direct mRNA binding proteins, detected in both T cell subsets and showed in a multitude of analyses that the biophysical properties of the identified proteins are in line with several published RBPome datasets. Moreover, we found 14 previously unidentified proteins binding to mRNA, helping to expand the catalogue of mammalian RNA-binding proteins. Importantly, many of the identified proteins do not have a known function and few of them are previously described as being relevant for T_{eff} and/or T_{Foxp3+} cells. In combination with the conducted RNA sequencing and proteome data, the presented thesis provides a sophisticated overview over mRNA-binding proteins as well as a starting point for future analyses considering post-transcriptional regulation mediated by RBPs in primary mouse $CD4^+$ T cells.

To further extend our analysis of post-transcriptional regulators, we aimed to identify RBPs specifically bound to one mRNA. Here, we successfully established an mRNA pull down but technical limitations and high experimental variability prevented the identification of RBPs bound to *Foxp3* mRNA. Furthermore, it also turned out to be very challenging to set up a retroviral reporter system to investigate potential inducers of post-transcriptional *Foxp3* regulation. We were nonetheless able to identify different isoforms of *Foxp3* mRNA, which do not differ in distribution between *in vitro* generated and *in vivo* isolated Treg cells, but still suggest the possibility of post-transcriptional regulatory processes being relevant for this ‘lineage defining’ transcription factor.

10. Contributions and Acknowledgements

First and foremost, I would like to thank Dr. Elke Glasmacher for her dedicated supervision and engagement in this project. Her scientific enthusiasm and guidance were of great help. She always provided a great amount of support, also outside of the lab.

Dr. Michael Wierer performed the mass spectrometry experiments and helped with interpreting their results as well as assisting in creating Figure 9. I would like to thank him for his help with experiments and scientific discussions.

Prof. Dr. Caroline Friedel performed mapping of all sequencing data, calculated FPKM values, helped in analyzing the results and assisted in creating Figure 21.

Annalisa Schaub helped in generating expression constructs for RNA-binding verification experiments, creating Figure 7 and performed the silver stain for Figure 8b.

Maria Fedoseeva helped with isolation of organs from Foxp3-RFP^{+} reporter mice and cell sorting.

Also, thanks to Hannah Busen for her help with bioinformatics, statistical analyses and assistance in creating Figure 16.

Thanks to all members of the AG Glasmacher. They were always a source of great support, scientific advice and discussions as well as help for any kind of experiment.

Andrew Flatley and Elisabeth Kremmer provided GFP, Roquin and T cell antibodies.

Vigo Heissmeyer provided Roquin 1-GFP in pDEST 12.2.

Caspar Ohnmacht provided Foxp3-RFP reporter mice.

I would also like to thank Prof. Dr. Matthias Tschöp and Prof. Dr. Michael Sattler for their support and scientific discussions.

Finally, I would like to thank my family for their support during the time of the thesis.

11. Literature

Aarts-Riemens, T., M. E. Emmelot, L. F. Verdonck and T. Mutis (2008). "Forced overexpression of either of the two common human Foxp3 isoforms can induce regulatory T cells from CD4(+)CD25(-) cells." Eur J Immunol **38**(5): 1381-1390.
Abderrazak, A., T. Syrovets, D. Couchie, K. El Hadri, B. Friguet, T. Simmet and M. Rouis (2015). "NLRP3 inflammasome: from a danger signal sensor to a regulatory node of oxidative stress and inflammatory diseases." Redox Biol **4**: 296-307.
Afroz, T., L. Skrisovska, E. Belloc, J. Guillen-Boixet, R. Mendez and F. H. Allain (2014). "A fly trap mechanism provides sequence-specific RNA recognition by CPEB proteins." Genes Dev **28**(13): 1498-1514.
Albayrak, C., C. A. Jordi, C. Zechner, J. Lin, C. A. Bichsel, M. Khammash and S. Tay (2016). "Digital Quantification of Proteins and mRNA in Single Mammalian Cells." Mol Cell **61**(6): 914-924.
Allan, S. E., S. Q. Crome, N. K. Crellin, L. Passerini, T. S. Steiner, R. Bacchetta, M. G. Roncarolo and M. K. Levings (2007). "Activation-induced FOXP3 in human T effector cells does not suppress proliferation or cytokine production." Int Immunol **19**(4): 345-354.
Allan, S. E., L. Passerini, R. Bacchetta, N. Crellin, M. Dai, P. C. Orban, S. F. Ziegler, M. G. Roncarolo and M. K. Levings (2005). "The role of 2 FOXP3 isoforms in the generation of human CD4+ Tregs." J Clin Invest **115**(11): 3276-3284.
Annacker, O., C. Asseman, S. Read and F. Powrie (2003). "Interleukin-10 in the regulation of T cell-induced colitis." J Autoimmun **20**(4): 277-279.
Arstila, T. P., A. Casrouge, V. Baron, J. Even, J. Kanellopoulos and P. Kourilsky (1999). "A direct estimate of the human alphabeta T cell receptor diversity." Science **286**(5441): 958-961.
Asseman, C., S. Mauze, M. W. Leach, R. L. Coffman and F. Powrie (1999). "An essential role for interleukin 10 in the function of regulatory T cells that inhibit intestinal inflammation." J Exp Med **190**(7): 995-1004.
Attridge, K., C. J. Wang, L. Wardzinski, R. Kenefeck, J. L. Chamberlain, C. Manzotti, M. Kopf and L. S. Walker (2012). "IL-21 inhibits T cell IL-2 production and impairs Treg homeostasis." Blood **119**(20): 4656-4664.
Baltz, A. G., M. Munschauer, B. Schwanhausser, A. Vasile, Y. Murakawa, M. Schueler, N. Youngs, D. Penfold-Brown, K. Drew, M. Milek, E. Wyler, R. Bonneau, M. Selbach, C. Dieterich and M. Landthaler (2012). "The mRNA-bound proteome and its global occupancy profile on protein-coding transcripts." Mol Cell **46**(5): 674-690.
Batra, R., K. Charizanis, M. Manchanda, A. Mohan, M. Li, D. J. Finn, M. Goodwin, C. Zhang, K. Sobczak, C. A. Thornton and M. S. Swanson (2014). "Loss of MBNL leads to disruption of developmentally regulated alternative polyadenylation in RNA-mediated disease." Mol Cell **56**(2): 311-322.
Beaudoing, E., S. Freier, J. R. Wyatt, J. M. Claverie and D. Gautheret (2000). "Patterns of variant polyadenylation signal usage in human genes." Genome Res **10**(7): 1001-1010.
Beckmann, B. M., R. Horos, B. Fischer, A. Castello, K. Eichelbaum, A. M. Alleaume, T. Schwarzl, T. Curk, S. Foehr, W. Huber, J. Krijgsveld and M. W. Hentze (2015). "The RNA-binding proteomes from yeast to man harbour conserved enigmRBPs." Nat Commun **6**: 10127.
Beier, U. H., L. Wang, T. R. Bhatti, Y. Liu, R. Han, G. Ge and W. W. Hancock (2011). "Sirtuin-1 targeting promotes Foxp3+ T-regulatory cell function and prolongs allograft survival." Mol Cell Biol **31**(5): 1022-1029.
Belkaid, Y. (2007). "Regulatory T cells and infection: a dangerous necessity." Nat Rev Immunol **7**(11): 875-888.
Bengtsson, M., M. Hemberg, P. Rorsman and A. Stahlberg (2008). "Quantification of mRNA in single cells and modelling of RT-qPCR induced noise." BMC Mol Biol **9**: 63.

Bennett, C. L., J. Christie, F. Ramsdell, M. E. Brunkow, P. J. Ferguson, L. Whitesell, T. E. Kelly, F. T. Saulsbury, P. F. Chance and H. D. Ochs (2001). "The immune dysregulation, polyendocrinopathy, enteropathy, X-linked syndrome (IPEX) is caused by mutations of FOXP3." Nat Genet **27**(1): 20-21.
Bin, G., Z. Jiarong, W. Shihao, S. Xiuli, X. Cheng, C. Liangbiao and Z. Ming (2012). "Aire promotes the self-renewal of embryonic stem cells through Lin28." Stem Cells Dev **21**(15): 2878-2890.
Bjur, E., O. Larsson, E. Yurchenko, L. Zheng, V. Gandin, I. Topisirovic, S. Li, C. R. Wagner, N. Sonenberg and C. A. Piccirillo (2013). "Distinct translational control in CD4+ T cell subsets." PLoS Genet **9**(5): e1003494.
Blackshear, P. J., W. S. Lai, E. A. Kennington, G. Brewer, G. M. Wilson, X. Guan and P. Zhou (2003). "Characteristics of the interaction of a synthetic human tristetraprolin tandem zinc finger peptide with AU-rich element-containing RNA substrates." J Biol Chem **278**(22): 19947-19955.
Bonfert, T., E. Kirner, G. Csaba, R. Zimmer and C. C. Friedel (2015). "ContextMap 2: fast and accurate context-based RNA-seq mapping." BMC Bioinformatics **16**: 122.
Bopp, T., C. Becker, M. Klein, S. Klein-Hessling, A. Palmetshofer, E. Serfling, V. Heib, M. Becker, J. Kubach, S. Schmitt, S. Stoll, H. Schild, M. S. Staege, M. Stassen, H. Jonuleit and E. Schmitt (2007). "Cyclic adenosine monophosphate is a key component of regulatory T cell-mediated suppression." J Exp Med **204**(6): 1303-1310.
Borbolis, F. and P. Syntichaki (2015). "Cytoplasmic mRNA turnover and ageing." Mech Ageing Dev **152**: 32-42.
Boucas, J., C. Fritz, A. Schmitt, A. Riabinska, L. Thelen, M. Peifer, U. Leeser, P. Nuernberg, J. Altmueller, M. Gaestel, C. Dieterich and H. C. Reinhardt (2015). "Label-Free Protein-RNA Interactome Analysis Identifies Khsrp Signaling Downstream of the p38/Mk2 Kinase Complex as a Critical Modulator of Cell Cycle Progression." PLoS One **10**(5): e0125745.
Brennan, C. M. and J. A. Steitz (2001). "HuR and mRNA stability." Cell Mol Life Sci **58**(2): 266-277.
Buchan, J. R., D. Muhlrad and R. Parker (2008). "P bodies promote stress granule assembly in Saccharomyces cerevisiae." J Cell Biol **183**(3): 441-455.
Buchan, J. R. and R. Parker (2009). "Eukaryotic stress granules: the ins and outs of translation." Mol Cell **36**(6): 932-941.
Burd, C. G. and G. Dreyfuss (1994). "Conserved structures and diversity of functions of RNA-binding proteins." Science **265**(5172): 615-621.
Carballo, E., W. S. Lai and P. J. Blackshear (1998). "Feedback inhibition of macrophage tumor necrosis factor-alpha production by tristetraprolin." Science **281**(5379): 1001-1005.
Cassiday, L. A. and L. J. Maher, 3rd (2002). "Having it both ways: transcription factors that bind DNA and RNA." Nucleic Acids Res **30**(19): 4118-4126.
Castello, A., B. Fischer, K. Eichelbaum, R. Horos, B. M. Beckmann, C. Strein, N. E. Davey, D. T. Humphreys, T. Preiss, L. M. Steinmetz, J. Krijgsveld and M. W. Hentze (2012). "Insights into RNA biology from an atlas of mammalian mRNA-binding proteins." Cell **149**(6): 1393-1406.
Castello, A., B. Fischer, C. K. Frese, R. Horos, A. M. Alleaume, S. Foehr, T. Curk, J. Krijgsveld and M. W. Hentze (2016). "Comprehensive Identification of RNA-Binding Domains in Human Cells." Mol Cell **63**(4): 696-710.
Castello, A., M. W. Hentze and T. Preiss (2015). "Metabolic Enzymes Enjoying New Partnerships as RNA-Binding Proteins." Trends Endocrinol Metab **26**(12): 746-757.
Chang, C. H., J. D. Curtis, L. B. Maggi, Jr., B. Faubert, A. V. Villarino, D. O'Sullivan, S. C. Huang, G. J. van der Windt, J. Blagih, J. Qiu, J. D. Weber, E. J. Pearce, R. G. Jones and E. L. Pearce (2013). "Posttranscriptional control of T cell effector function by aerobic glycolysis." Cell **153**(6): 1239-1251.
Chaplin, D. D. (2010). "Overview of the immune response." J Allergy Clin Immunol **125**(2 Suppl 2): S3-23.
Chu, C., J. Quinn and H. Y. Chang (2012). "Chromatin isolation by RNA purification (ChIRP)." J Vis Exp(61).

Chu, C., Q. C. Zhang, S. T. da Rocha, R. A. Flynn, M. Bharadwaj, J. M. Calabrese, T. Magnuson, E. Heard and H. Y. Chang (2015). "Systematic discovery of Xist RNA binding proteins." Cell **161**(2): 404-416.
Cléry, A. and F. H. Allain (2011). From Structure to Function of RNA binding domains, Madame Curie Bioscience Database.
Collison, L. W., C. J. Workman, T. T. Kuo, K. Boyd, Y. Wang, K. M. Vignali, R. Cross, D. Sehy, R. S. Blumberg and D. A. Vignali (2007). "The inhibitory cytokine IL-35 contributes to regulatory T-cell function." Nature **450**(7169): 566-569.
Conrad, T., A. S. Albrecht, V. R. de Melo Costa, S. Sauer, D. Meierhofer and U. A. Orom (2016). "Serial interactome capture of the human cell nucleus." Nat Commun **7**: 11212.
Cougot, N., S. Babajko and B. Seraphin (2004). "Cytoplasmic foci are sites of mRNA decay in human cells." J Cell Biol **165**(1): 31-40.
Cui, X., T. Mino, M. Yoshinaga, Y. Nakatsuka, F. Hia, D. Yamasoba, T. Tsujimura, K. Tomonaga, Y. Suzuki, T. Uehata and O. Takeuchi (2017). "Regnase-1 and Roquin Nonredundantly Regulate Th1 Differentiation Causing Cardiac Inflammation and Fibrosis." J Immunol **199**(12): 4066-4077.
de Zoeten, E. F., L. Wang, H. Sai, W. H. Dillmann and W. W. Hancock (2010). "Inhibition of HDAC9 increases T regulatory cell function and prevents colitis in mice." Gastroenterology **138**(2): 583-594.
Decker, C. J. and R. Parker (2012). "P-bodies and stress granules: possible roles in the control of translation and mRNA degradation." Cold Spring Harb Perspect Biol **4**(9): a012286.
Derti, A., P. Garrett-Engele, K. D. Macisaac, R. C. Stevens, S. Sriram, R. Chen, C. A. Rohl, J. M. Johnson and T. Babak (2012). "A quantitative atlas of polyadenylation in five mammals." Genome Res **22**(6): 1173-1183.
Diaz-Munoz, M. D., S. E. Bell, K. Fairfax, E. Monzon-Casanova, A. F. Cunningham, M. Gonzalez-Porta, S. R. Andrews, V. I. Bunik, K. Zarnack, T. Curk, W. A. Heggermont, S. Heymans, G. E. Gibson, D. L. Kontoyiannis, J. Ule and M. Turner (2015). "The RNA-binding protein HuR is essential for the B cell antibody response." Nat Immunol **16**(4): 415-425.
Dieckmann, D., H. Plottner, S. Berchtold, T. Berger and G. Schuler (2001). "Ex vivo isolation and characterization of CD4(+)CD25(+) T cells with regulatory properties from human blood." J Exp Med **193**(11): 1303-1310.
Ding, Y., C. Y. Chan and C. E. Lawrence (2004). "Sfold web server for statistical folding and rational design of nucleic acids." Nucleic Acids Res **32**(Web Server issue): W135-141.
Dranoff, G. (2004). "Cytokines in cancer pathogenesis and cancer therapy." Nat Rev Cancer **4**(1): 11-22.
Eida, S., M. Van Cauteren, Y. Hotokezaka, I. Katayama, M. Sasaki, M. Obara, T. Okuaki, M. Sumi and T. Nakamura (2016). "Length of intact plasma membrane determines the diffusion properties of cellular water." Sci Rep **6**: 19051.
El Gazzar, M. and C. E. McCall (2010). "MicroRNAs distinguish translational from transcriptional silencing during endotoxin tolerance." J Biol Chem **285**(27): 20940-20951.
Engreitz, J. M., K. Sirokman, P. McDonel, A. A. Shishkin, C. Surka, P. Russell, S. R. Grossman, A. Y. Chow, M. Guttman and E. S. Lander (2014). "RNA-RNA interactions enable specific targeting of noncoding RNAs to nascent Pre-mRNAs and chromatin sites." Cell **159**(1): 188-199.
Esposito, M., F. Ruffini, A. Bergami, L. Garzetti, G. Borsellino, L. Battistini, G. Martino and R. Furlan (2010). "IL-17- and IFN-gamma-secreting Foxp3+ T cells infiltrate the target tissue in experimental autoimmunity." J Immunol **185**(12): 7467-7473.
Fast, L. D. (2013). Non-Hodgkin Lymphoma: Prognostic Factors and Targets, Springer.
Fenger-Gron, M., C. Fillman, B. Norrild and J. Lykke-Andersen (2005). "Multiple processing body factors and the ARE binding protein TTP activate mRNA decapping." Mol Cell **20**(6): 905-915.
Feuerer, M., J. A. Hill, D. Mathis and C. Benoist (2009). "Foxp3+ regulatory T cells: differentiation, specification, subphenotypes." Nat Immunol **10**(7): 689-695.

Fontenot, J. D., M. A. Gavin and A. Y. Rudensky (2003). "Foxp3 programs the development and function of CD4+CD25+ regulatory T cells." Nat Immunol **4**(4): 330-336.
Fontoura, B. M., E. A. Sorokina, E. David and R. B. Carroll (1992). "p53 is covalently linked to 5.8S rRNA." Mol Cell Biol **12**(11): 5145-5151.
Fu, X. D. and M. Ares, Jr. (2014). "Context-dependent control of alternative splicing by RNA-binding proteins." Nat Rev Genet **15**(10): 689-701.
Galloway, A., A. Saveliev, S. Lukasiak, D. J. Hodson, D. Bolland, K. Balmanno, H. Ahlfors, E. Monzon-Casanova, S. C. Mannurita, L. S. Bell, S. Andrews, M. D. Diaz-Munoz, S. J. Cook, A. Corcoran and M. Turner (2016). "RNA-binding proteins ZFP36L1 and ZFP36L2 promote cell quiescence." Science **352**(6284): 453-459.
Gao, Y., F. Lin, J. Su, Z. Gao, Y. Li, J. Yang, Z. Deng, B. Liu, A. Tsun and B. Li (2012). "Molecular mechanisms underlying the regulation and functional plasticity of FOXP3(+) regulatory T cells." Genes Immun **13**(1): 1-13.
Gao, Z., Y. Gao, Z. Li, Z. Chen, D. Lu, A. Tsun and B. Li (2012). "Synergy between IL-6 and TGF-beta signaling promotes FOXP3 degradation." Int J Clin Exp Pathol **5**(7): 626-633.
Garneau, N. L., J. Wilusz and C. J. Wilusz (2007). "The highways and byways of mRNA decay." Nat Rev Mol Cell Biol **8**(2): 113-126.
Gasteiger, E., A. Gattiker, C. Hoogland, I. Ivanyi, R. D. Appel and A. Bairoch (2003). "ExPASy: The proteomics server for in-depth protein knowledge and analysis." Nucleic Acids Res **31**(13): 3784-3788.
Gavin, M. A., J. P. Rasmussen, J. D. Fontenot, V. Vasta, V. C. Manganiello, J. A. Beavo and A. Y. Rudensky (2007). "Foxp3-dependent programme of regulatory T-cell differentiation." Nature **445**(7129): 771-775.
Gesteland, R. F., T. Cech and J. F. Atkins (1999). The RNA World: The Nature of modern RNA suggests a Prebiotic RNA, Cold Spring Harbor Laboratory Press.
Ghosh, M., H. L. Aguila, J. Michaud, Y. Ai, M. T. Wu, A. Hemmes, A. Ristimaki, C. Guo, H. Furneaux and T. Hla (2009). "Essential role of the RNA-binding protein HuR in progenitor cell survival in mice." J Clin Invest **119**(12): 3530-3543.
Giorgini, F., H. G. Davies and R. E. Braun (2002). "Translational repression by MSY4 inhibits spermatid differentiation in mice." Development **129**(15): 3669-3679.
Glasmacher, E., K. P. Hoefig, K. U. Vogel, N. Rath, L. Du, C. Wolf, E. Kremmer, X. Wang and V. Heissmeyer (2010). "Roquin binds inducible costimulator mRNA and effectors of mRNA decay to induce microRNA-independent post-transcriptional repression." Nat Immunol **11**(8): 725-733.
Gondek, D. C., L. F. Lu, S. A. Quezada, S. Sakaguchi and R. J. Noelle (2005). "Cutting edge: contact-mediated suppression by CD4+CD25+ regulatory cells involves a granzyme B-dependent, perforin-independent mechanism." J Immunol **174**(4): 1783-1786.
Gorer, P. A. (1950). "Studies in antibody response of mice to tumour inoculation." Br J Cancer **4**(4): 372-379.
Graves, L. E., S. Segal and E. B. Goodwin (1999). "TRA-1 regulates the cellular distribution of the tra-2 mRNA in C. elegans." Nature **399**(6738): 802-805.
Gupta, I., S. Clauder-Munster, B. Klaus, A. I. Jarvelin, R. S. Aiyar, V. Benes, S. Wilkening, W. Huber, V. Pelechano and L. M. Steinmetz (2014). "Alternative polyadenylation diversifies post-transcriptional regulation by selective RNA-protein interactions." Mol Syst Biol **10**: 719.
Hall, A. O., D. P. Beiting, C. Tato, B. John, G. Oldenhove, C. G. Lombana, G. H. Pritchard, J. S. Silver, N. Bouladoux, J. S. Stumhofer, T. H. Harris, J. Grainger, E. D. Wojno, S. Wagage, D. S. Roos, P. Scott, L. A. Turka, S. Cherry, S. L. Reiner, D. Cua, Y. Belkaid, M. M. Elloso and C. A. Hunter (2012). "The cytokines interleukin 27 and interferon-gamma promote distinct Treg cell populations required to limit infection-induced pathology." Immunity **37**(3): 511-523.
Haneklaus, M., J. D. O'Neil, A. R. Clark, S. L. Masters and L. A. J. O'Neill (2017). "The RNA-binding protein Tristetraprolin (TTP) is a critical negative regulator of the NLRP3 inflammasome." J Biol Chem **292**(17): 6869-6881.
Hawrylowicz, C. M. and A. O'Garra (2005). "Potential role of interleukin-10-secreting regulatory T cells in allergy and asthma." Nat Rev Immunol **5**(4): 271-283.

Helou, Y. A., A. P. Petrashen and A. R. Salomon (2015). "Vav1 Regulates T-Cell Activation through a Feedback Mechanism and Crosstalk between the T-Cell Receptor and CD28." J Proteome Res **14**(7): 2963-2975.
Hentze, M. W., A. Castello, T. Schwarzl and T. Preiss (2018). "A brave new world of RNA-binding proteins." Nat Rev Mol Cell Biol **19**(5): 327-341.
Hill, J. A., M. Feuerer, K. Tash, S. Haxhinasto, J. Perez, R. Melamed, D. Mathis and C. Benoist (2007). "Foxp3 transcription-factor-dependent and -independent regulation of the regulatory T cell transcriptional signature." Immunity **27**(5): 786-800.
Hong, C., M. A. Luckey and J. H. Park (2012). "Intrathymic IL-7: the where, when, and why of IL-7 signaling during T cell development." Semin Immunol **24**(3): 151-158.
Hong, S., M. A. Freeberg, T. Han, A. Kamath, Y. Yao, T. Fukuda, T. Suzuki, J. K. Kim and K. Inoki (2017). "LARP1 functions as a molecular switch for mTORC1-mediated translation of an essential class of mRNAs." Elife **6**.
Horwitz, D. A., S. G. Zheng and J. D. Gray (2008). "Natural and TGF-beta-induced Foxp3(+)CD4(+) CD25(+) regulatory T cells are not mirror images of each other." Trends Immunol **29**(9): 429-435.
Huang da, W., B. T. Sherman and R. A. Lempicki (2009). "Bioinformatics enrichment tools: paths toward the comprehensive functional analysis of large gene lists." Nucleic Acids Res **37**(1): 1-13.
Huang da, W., B. T. Sherman and R. A. Lempicki (2009). "Systematic and integrative analysis of large gene lists using DAVID bioinformatics resources." Nat Protoc **4**(1): 44-57.
Ingolia, N. T. (2014). "Ribosome profiling: new views of translation, from single codons to genome scale." Nat Rev Genet **15**(3): 205-213.
Izcue, A., S. Hue, S. Buonocore, C. V. Arancibia-Carcamo, P. P. Ahern, Y. Iwakura, K. J. Maloy and F. Powrie (2008). "Interleukin-23 restrains regulatory T cell activity to drive T cell-dependent colitis." Immunity **28**(4): 559-570.
Janowski, R., G. A. Heinz, A. Schlundt, N. Wommelsdorf, S. Brenner, A. R. Gruber, M. Blank, T. Buch, R. Buhmann, M. Zavolan, D. Niessing, V. Heissmeyer and M. Sattler (2016). "Roquin recognizes a non-canonical hexaloop structure in the 3'-UTR of Ox40." Nat Commun **7**: 11032.
Jarvelin, A. I., M. Noerenberg, I. Davis and A. Castello (2016). "The new (dis)order in RNA regulation." Cell Commun Signal **14**: 9.
Jeltsch, K. M., D. Hu, S. Brenner, J. Zoller, G. A. Heinz, D. Nagel, K. U. Vogel, N. Rehage, S. C. Warth, S. L. Edelmann, R. Gloury, N. Martin, C. Lohs, M. Lech, J. E. Stehklein, A. Geerlof, E. Kremmer, A. Weber, H. J. Anders, I. Schmitz, M. Schmidt-Supprian, M. Fu, H. Holtmann, D. Krappmann, J. Ruland, A. Kallies, M. Heikenwalder and V. Heissmeyer (2014). "Cleavage of roquin and regnase-1 by the paracaspase MALT1 releases their cooperatively repressed targets to promote T(H)17 differentiation." Nat Immunol **15**(11): 1079-1089.
Jiao, Y., X. Jin, J. Yan, F. Jiao, X. Li, B. A. Roe, H. W. Jarrett and W. Gu (2009). "An insertion of intracisternal A-particle retrotransposon in a novel member of the phosphoglycerate mutase family in the lew allele of mutant mice." Genes Genet Syst **84**(5): 327-334.
Jing, Q., S. Huang, S. Guth, T. Zarubin, A. Motoyama, J. Chen, F. Di Padova, S. C. Lin, H. Gram and J. Han (2005). "Involvement of microRNA in AU-rich element-mediated mRNA instability." Cell **120**(5): 623-634.
Johnson, D. J., L. I. Pao, S. Dhanji, K. Murakami, P. S. Ohashi and B. G. Neel (2013). "Shp1 regulates T cell homeostasis by limiting IL-4 signals." J Exp Med **210**(7): 1419-1431.
Jonas, S. and E. Izaurralde (2015). "Towards a molecular understanding of microRNA-mediated gene silencing." Nat Rev Genet **16**(7): 421-433.
Jones, M. R., L. J. Quinton, M. T. Blahna, J. R. Neilson, S. Fu, A. R. Ivanov, D. A. Wolf and J. P. Mizgerd (2009). "Zcchc11-dependent uridylation of microRNA directs cytokine expression." Nat Cell Biol **11**(9): 1157-1163.

Jonuleit, H., E. Schmitt, M. Stassen, A. Tuettenberg, J. Knop and A. H. Enk (2001). "Identification and functional characterization of human CD4(+)CD25(+) T cells with regulatory properties isolated from peripheral blood." J Exp Med **193**(11): 1285-1294.
Kafasla, P., A. Skliris and D. L. Kontoyiannis (2014). "Post-transcriptional coordination of immunological responses by RNA-binding proteins." Nat Immunol **15**(6): 492-502.
Kanegane, H. and G. Tosato (1996). "Activation of naive and memory T cells by interleukin-15." Blood **88**(1): 230-235.
Kawai, T. and S. Akira (2010). "The role of pattern-recognition receptors in innate immunity: update on Toll-like receptors." Nat Immunol **11**(5): 373-384.
Kedde, M., M. van Kouwenhove, W. Zwart, J. A. Oude Vrielink, R. Elkon and R. Agami (2010). "A Pumilio-induced RNA structure switch in p27-3' UTR controls miR-221 and miR-222 accessibility." Nat Cell Biol **12**(10): 1014-1020.
Kedersha, N., G. Stoecklin, M. Ayodele, P. Yacono, J. Lykke-Andersen, M. J. Fritzler, D. Scheuner, R. J. Kaufman, D. E. Golan and P. Anderson (2005). "Stress granules and processing bodies are dynamically linked sites of mRNP remodeling." J Cell Biol **169**(6): 871-884.
Kelley, D. R., D. G. Hendrickson, D. Tenen and J. L. Rinn (2014). "Transposable elements modulate human RNA abundance and splicing via specific RNA-protein interactions." Genome Biol **15**(12): 537.
Kelly, E., A. Won, Y. Refaeli and L. Van Parijs (2002). "IL-2 and related cytokines can promote T cell survival by activating AKT." J Immunol **168**(2): 597-603.
Khoo, C., R. K. Blanchard, V. K. Sullivan and R. J. Cousins (1997). "Human cysteine-rich intestinal protein: cDNA cloning and expression of recombinant protein and identification in human peripheral blood mononuclear cells." Protein Expr Purif **9**(3): 379-387.
Kim, H. S., M. C. Wilce, Y. M. Yoga, N. R. Pendini, M. J. Gunzburg, N. P. Cowieson, G. M. Wilson, B. R. Williams, M. Gorospe and J. A. Wilce (2011). "Different modes of interaction by TIAR and HuR with target RNA and DNA." Nucleic Acids Res **39**(3): 1117-1130.
Kimball, S. R., R. L. Horetsky, D. Ron, L. S. Jefferson and H. P. Harding (2003). "Mammalian stress granules represent sites of accumulation of stalled translation initiation complexes." Am J Physiol Cell Physiol **284**(2): C273-284.
Kimura, A. and T. Kishimoto (2010). "IL-6: regulator of Treg/Th17 balance." Eur J Immunol **40**(7): 1830-1835.
Kirmitzoglou, I. and V. J. Promponas (2015). "LCR-eXXXplorer: a web platform to search, visualize and share data for low complexity regions in protein sequences." Bioinformatics **31**(13): 2208-2210.
Kitagawa, Y., N. Ohkura, Y. Kidani, A. Vandenbon, K. Hirota, R. Kawakami, K. Yasuda, D. Motooka, S. Nakamura, M. Kondo, I. Taniuchi, T. Kohwi-Shigematsu and S. Sakaguchi (2017). "Guidance of regulatory T cell development by Satb1-dependent super-enhancer establishment." Nat Immunol **18**(2): 173-183.
Kobie, J. J., P. R. Shah, L. Yang, J. A. Rebhahn, D. J. Fowell and T. R. Mosmann (2006). "T regulatory and primed uncommitted CD4 T cells express CD73, which suppresses effector CD4 T cells by converting 5'-adenosine monophosphate to adenosine." J Immunol **177**(10): 6780-6786.
Koch, M. A., G. Tucker-Heard, N. R. Perdue, J. R. Killebrew, K. B. Urdahl and D. J. Campbell (2009). "The transcription factor T-bet controls regulatory T cell homeostasis and function during type 1 inflammation." Nat Immunol **10**(6): 595-602.
Kojima, S., D. L. Shingle and C. B. Green (2011). "Post-transcriptional control of circadian rhythms." J Cell Sci **124**(Pt 3): 311-320.
Konig, J., K. Zarnack, G. Rot, T. Curk, M. Kayikci, B. Zupan, D. J. Turner, N. M. Luscombe and J. Ule (2010). "iCLIP reveals the function of hnRNP particles in splicing at individual nucleotide resolution." Nat Struct Mol Biol **17**(7): 909-915.
Kontoyiannis, D., M. Pasparakis, T. T. Pizarro, F. Cominelli and G. Kollias (1999). "Impaired on/off regulation of TNF biosynthesis in mice lacking TNF AU-rich elements: implications for joint and gut-associated immunopathologies." Immunity **10**(3): 387-398.

Koralov, S. B., S. A. Muljo, G. R. Galler, A. Krek, T. Chakraborty, C. Kanellopoulou, K. Jensen, B. S. Cobb, M. Merkenschlager, N. Rajewsky and K. Rajewsky (2008). "Dicer ablation affects antibody diversity and cell survival in the B lymphocyte lineage." Cell **132**(5): 860-874.
Kovarik, P., F. Ebner and V. Sedlyarov (2017). "Posttranscriptional regulation of cytokine expression." Cytokine **89**: 21-26.
Kwon, S. C., H. Yi, K. Eichelbaum, S. Fohr, B. Fischer, K. T. You, A. Castello, J. Krijgsveld, M. W. Hentze and V. N. Kim (2013). "The RNA-binding protein repertoire of embryonic stem cells." Nat Struct Mol Biol **20**(9): 1122-1130.
Lahr, R. M., B. D. Fonseca, G. E. Ciotti, H. A. Al-Ashtal, J. J. Jia, M. R. Niklaus, S. P. Blagden, T. Alain and A. J. Berman (2017). "La-related protein 1 (LARP1) binds the mRNA cap, blocking eIF4F assembly on TOP mRNAs." Elife **6**.
Landre, P. A., D. H. Gelfand and R. M. Watson (1995). The use of cosolvents to enhance amplification by the polymerase chain reaction.
Lanningham-Foster, L., C. L. Green, B. Langkamp-Henken, B. A. Davis, K. T. Nguyen, B. S. Bender and R. J. Cousins (2002). "Overexpression of CRIP in transgenic mice alters cytokine patterns and the immune response." Am J Physiol Endocrinol Metab **282**(6): E1197-1203.
Lee, K. S., K. A. Lewis, S. Tom, E. A. Wayner and E. H. Wang (2011). "Monoclonal antibodies against Muscleblind-like 3, a protein with punctate nuclear localization." Hybridoma (Larchmt) **30**(2): 181-188.
Lee, W. and G. R. Lee (2018). "Transcriptional regulation and development of regulatory T cells." Exp Mol Med **50**(3): e456.
Leppek, K., J. Schott, S. Reitter, F. Poetz, M. C. Hammond and G. Stoecklin (2013). "Roquin promotes constitutive mRNA decay via a conserved class of stem-loop recognition motifs." Cell **153**(4): 869-881.
Li, H. and R. Durbin (2009). "Fast and accurate short read alignment with Burrows-Wheeler transform." Bioinformatics **25**(14): 1754-1760.
Li, M. O. and A. Y. Rudensky (2016). "T cell receptor signalling in the control of regulatory T cell differentiation and function." Nat Rev Immunol **16**(4): 220-233.
Li, Z., D. Li, A. Tsun and B. Li (2015). "FOXP3+ regulatory T cells and their functional regulation." Cell Mol Immunol **12**(5): 558-565.
Liao, Y., A. Castello, B. Fischer, S. Leicht, S. Foehr, C. K. Frese, C. Ragan, S. Kurscheid, E. Pagler, H. Yang, J. Krijgsveld, M. W. Hentze and T. Preiss (2016). "The Cardiomyocyte RNA-Binding Proteome: Links to Intermediary Metabolism and Heart Disease." Cell Rep **16**(5): 1456-1469.
Liao, Y., G. K. Smyth and W. Shi (2014). "featureCounts: an efficient general purpose program for assigning sequence reads to genomic features." Bioinformatics **30**(7): 923-930.
Lichti, J., C. Gallus and E. Glasmacher (2018). "Immune Responses - Transcriptional and Post-Transcriptional Networks Pass the Baton." Trends Biochem Sci **43**(1): 1-4.
Liepelt, A., I. S. Naarmann-de Vries, N. Simons, K. Eichelbaum, S. Fohr, S. K. Archer, A. Castello, B. Usadel, J. Krijgsveld, T. Preiss, G. Marx, M. W. Hentze, D. H. Ostareck and A. Ostareck-Lederer (2016). "Identification of RNA-binding Proteins in Macrophages by Interactome Capture." Mol Cell Proteomics **15**(8): 2699-2714.
Lin, W., D. Haribhai, L. M. Relland, N. Truong, M. R. Carlson, C. B. Williams and T. A. Chatila (2007). "Regulatory T cell development in the absence of functional Foxp3." Nat Immunol **8**(4): 359-368.
Liu, Y., L. Wang, J. Predina, R. Han, U. H. Beier, L. C. Wang, V. Kapoor, T. R. Bhatti, T. Akimova, S. Singhal, P. K. Brindle, P. A. Cole, S. M. Albelda and W. W. Hancock (2013). "Inhibition of p300 impairs Foxp3(+) T regulatory cell function and promotes antitumor immunity." Nat Med **19**(9): 1173-1177.
Lu, J. and A. G. Clark (2012). "Impact of microRNA regulation on variation in human gene expression." Genome Res **22**(7): 1243-1254.
Lu, Y. C., S. H. Chang, M. Hafner, X. Li, T. Tuschl, O. Elemento and T. Hla (2014). "ELAVL1 modulates transcriptome-wide miRNA binding in murine macrophages." Cell Rep **9**(6): 2330-2343.

Lueong, S., C. Merce, B. Fischer, J. D. Hoheisel and E. D. Erben (2016). "Gene expression regulatory networks in Trypanosoma brucei: insights into the role of the mRNA-binding proteome." Mol Microbiol **100**(3): 457-471.
Lunde, B. M., C. Moore and G. Varani (2007). "RNA-binding proteins: modular design for efficient function." Nat Rev Mol Cell Biol **8**(6): 479-490.
Lykke-Andersen, J. and E. Wagner (2005). "Recruitment and activation of mRNA decay enzymes by two ARE-mediated decay activation domains in the proteins TTP and BRF-1." Genes Dev **19**(3): 351-361.
Lykke-Andersen, S. and T. H. Jensen (2015). "Nonsense-mediated mRNA decay: an intricate machinery that shapes transcriptomes." Nat Rev Mol Cell Biol **16**(11): 665-677.
Mailer, R. K., K. Falk and O. Rotzschke (2009). "Absence of leucine zipper in the natural FOXP3Delta2Delta7 isoform does not affect dimerization but abrogates suppressive capacity." PLoS One **4**(7): e6104.
Mailer, R. K., A. L. Joly, S. Liu, S. Elias, J. Tegner and J. Andersson (2015). "IL-1beta promotes Th17 differentiation by inducing alternative splicing of FOXP3." Sci Rep **5**: 14674.
Manning, K. S. and T. A. Cooper (2017). "The roles of RNA processing in translating genotype to phenotype." Nat Rev Mol Cell Biol **18**(2): 102-114.
Marinov, G. K., B. A. Williams, K. McCue, G. P. Schroth, J. Gertz, R. M. Myers and B. J. Wold (2014). "From single-cell to cell-pool transcriptomes: stochasticity in gene expression and RNA splicing." Genome Res **24**(3): 496-510.
Matsushita, K., O. Takeuchi, D. M. Standley, Y. Kumagai, T. Kawagoe, T. Miyake, T. Satoh, H. Kato, T. Tsujimura, H. Nakamura and S. Akira (2009). "Zc3h12a is an RNase essential for controlling immune responses by regulating mRNA decay." Nature **458**(7242): 1185-1190.
McHugh, R. S., M. J. Whitters, C. A. Piccirillo, D. A. Young, E. M. Shevach, M. Collins and M. C. Byrne (2002). "CD4(+)CD25(+) immunoregulatory T cells: gene expression analysis reveals a functional role for the glucocorticoid-induced TNF receptor." Immunity **16**(2): 311-323.
Mellor, A. L. and D. H. Munn (2004). "IDO expression by dendritic cells: tolerance and tryptophan catabolism." Nat Rev Immunol **4**(10): 762-774.
Mino, T., Y. Murakawa, A. Fukao, A. Vandenbon, H. H. Wessels, D. Ori, T. Uehata, S. Tartey, S. Akira, Y. Suzuki, C. G. Vinuesa, U. Ohler, D. M. Standley, M. Landthaler, T. Fujiwara and O. Takeuchi (2015). "Regnase-1 and Roquin Regulate a Common Element in Inflammatory mRNAs by Spatiotemporally Distinct Mechanisms." Cell **161**(5): 1058-1073.
Mitchell, S. F. and R. Parker (2014). "Principles and properties of eukaryotic mRNPs." Mol Cell **54**(4): 547-558.
Molle, C., T. Zhang, L. Ysebrant de Lendonck, C. Gueydan, M. Andrianne, F. Sherer, G. Van Simaeys, P. J. Blackshear, O. Leo and S. Goriely (2013). "Tristetraprolin regulation of interleukin 23 mRNA stability prevents a spontaneous inflammatory disease." J Exp Med **210**(9): 1675-1684.
Moncada-Pazos, A., A. J. Obaya, M. Llamazares, R. Heljasvaara, M. F. Suarez, E. Colado, A. Noel, S. Cal and C. Lopez-Otin (2018). "ADAMTS-12 metalloprotease is necessary for normal inflammatory response." J Biol Chem **293**(29): 11648.
Mu, X. J., Z. J. Lu, Y. Kong, H. Y. Lam and M. B. Gerstein (2011). "Analysis of genomic variation in non-coding elements using population-scale sequencing data from the 1000 Genomes Project." Nucleic Acids Res **39**(16): 7058-7076.
Mukherjee, N., N. C. Jacobs, M. Hafner, E. A. Kennington, J. D. Nusbaum, T. Tuschl, P. J. Blackshear and U. Ohler (2014). "Global target mRNA specification and regulation by the RNA-binding protein ZFP36." Genome Biol **15**(1): R12.
Muljo, S. A., K. M. Ansel, C. Kanellopoulou, D. M. Livingston, A. Rao and K. Rajewsky (2005). "Aberrant T cell differentiation in the absence of Dicer." J Exp Med **202**(2): 261-269.
Muller-McNicoll, M. and K. M. Neugebauer (2013). "How cells get the message: dynamic assembly and function of mRNA-protein complexes." Nat Rev Genet **14**(4): 275-287.
Nakamura, K., A. Kitani and W. Strober (2001). "Cell contact-dependent immunosuppression by CD4(+)CD25(+) regulatory T cells is mediated by cell surface-bound transforming growth factor beta." J Exp Med **194**(5): 629-644.

Neve, J., K. Burger, W. Li, M. Hoque, R. Patel, B. Tian, M. Gullerova and A. Furger (2016). "Subcellular RNA profiling links splicing and nuclear DICER1 to alternative cleavage and polyadenylation." Genome Res **26**(1): 24-35.
Newman, R., J. McHugh and M. Turner (2016). "RNA binding proteins as regulators of immune cell biology." Clin Exp Immunol **183**(1): 37-49.
Nishibori, T., Y. Tanabe, L. Su and M. David (2004). "Impaired development of CD4+ CD25+ regulatory T cells in the absence of STAT1: increased susceptibility to autoimmune disease." J Exp Med **199**(1): 25-34.
Noval Rivas, M., O. T. Burton, P. Wise, L. M. Charbonnier, P. Georgiev, H. C. Oettgen, R. Rachid and T. A. Chatila (2015). "Regulatory T cell reprogramming toward a Th2-cell-like lineage impairs oral tolerance and promotes food allergy." Immunity **42**(3): 512-523.
Oberle, N., N. Eberhardt, C. S. Falk, P. H. Krammer and E. Suri-Payer (2007). "Rapid suppression of cytokine transcription in human CD4+CD25 T cells by CD4+Foxp3+ regulatory T cells: independence of IL-2 consumption, TGF-beta, and various inhibitors of TCR signaling." J Immunol **179**(6): 3578-3587.
Ohkura, N., M. Hamaguchi, H. Morikawa, K. Sugimura, A. Tanaka, Y. Ito, M. Osaki, Y. Tanaka, R. Yamashita, N. Nakano, J. Huehn, H. J. Fehling, T. Sparwasser, K. Nakai and S. Sakaguchi (2012). "T cell receptor stimulation-induced epigenetic changes and Foxp3 expression are independent and complementary events required for Treg cell development." Immunity **37**(5): 785-799.
Ohkura, N., Y. Kitagawa and S. Sakaguchi (2013). "Development and maintenance of regulatory T cells." Immunity **38**(3): 414-423.
Oldenburg, M., A. Kruger, R. Ferstl, A. Kaufmann, G. Nees, A. Sigmund, B. Bathke, H. Lauterbach, M. Suter, S. Dreher, U. Koedel, S. Akira, T. Kawai, J. Buer, H. Wagner, S. Bauer, H. Hochrein and C. J. Kirschning (2012). "TLR13 recognizes bacterial 23S rRNA devoid of erythromycin resistance-forming modification." Science **337**(6098): 1111-1115.
Pandiyan, P., L. Zheng, S. Ishihara, J. Reed and M. J. Lenardo (2007). "CD4+CD25+Foxp3+ regulatory T cells induce cytokine deprivation-mediated apoptosis of effector CD4+ T cells." Nat Immunol **8**(12): 1353-1362.
Papadaki, O., S. Milatos, S. Grammenoudi, N. Mukherjee, J. D. Keene and D. L. Kontoyiannis (2009). "Control of thymic T cell maturation, deletion and egress by the RNA-binding protein HuR." J Immunol **182**(11): 6779-6788.
Parkin, J. and B. Cohen (2001). "An overview of the immune system." Lancet **357**(9270): 1777-1789.
Pelham, H. R. and D. D. Brown (1980). "A specific transcription factor that can bind either the 5S RNA gene or 5S RNA." Proc Natl Acad Sci U S A **77**(7): 4170-4174.
Peyman, J. A. (1999). "Repression of major histocompatibility complex genes by a human trophoblast ribonucleic acid." Biol Reprod **60**(1): 23-31.
Peyman, J. A. (2001). "Mammalian expression cloning of two human trophoblast suppressors of major histocompatibility complex genes." Am J Reprod Immunol **45**(6): 382-392.
Pioli, P. A., B. J. Hamilton, J. E. Connolly, G. Brewer and W. F. Rigby (2002). "Lactate dehydrogenase is an AU-rich element-binding protein that directly interacts with AUF1." J Biol Chem **277**(38): 35738-35745.
Piskounova, E., C. Polytarchou, J. E. Thornton, R. J. LaPierre, C. Pothoulakis, J. P. Hagan, D. Iliopoulos and R. I. Gregory (2011). "Lin28A and Lin28B inhibit let-7 microRNA biogenesis by distinct mechanisms." Cell **147**(5): 1066-1079.
Qi, M. Y., Z. Z. Wang, Z. Zhang, Q. Shao, A. Zeng, X. Q. Li, W. Q. Li, C. Wang, F. J. Tian, Q. Li, J. Zou, Y. W. Qin, G. Brewer, S. Huang and Q. Jing (2012). "AU-rich-element-dependent translation repression requires the cooperation of tristetraprolin and RCK/P54." Mol Cell Biol **32**(5): 913-928.
Rajkowitsch, L., C. Vilela, K. Berthelot, C. V. Ramirez and J. E. McCarthy (2004). "Reinitiation and recycling are distinct processes occurring downstream of translation termination in yeast." J Mol Biol **335**(1): 71-85.

Read, K. A., M. D. Powell, P. W. McDonald and K. J. Oestreich (2016). "IL-2, IL-7, and IL-15: Multistage regulators of CD4(+) T helper cell differentiation." Exp Hematol **44**(9): 799-808.
Rouse, B. T., P. P. Sarangi and S. Suvas (2006). "Regulatory T cells in virus infections." Immunol Rev **212**: 272-286.
Sadri, N. and R. J. Schneider (2009). "Auf1/Hnrnpd-deficient mice develop pruritic inflammatory skin disease." J Invest Dermatol **129**(3): 657-670.
Saito, I. and T. Matsuura (1985). "Chemical Aspects of UV-induced crosslinking of proteins to nucleic acids. Photoreactions with lysine and tryptophan." Accounts of chemical research **18**(5): 134-141.
Sakaguchi, S., N. Sakaguchi, J. Shimizu, S. Yamazaki, T. Sakihama, M. Itoh, Y. Kuniyasu, T. Nomura, M. Toda and T. Takahashi (2001). "Immunologic tolerance maintained by CD25+ CD4+ regulatory T cells: their common role in controlling autoimmunity, tumor immunity, and transplantation tolerance." Immunol Rev **182**: 18-32.
Sakaguchi, S., T. Yamaguchi, T. Nomura and M. Ono (2008). "Regulatory T cells and immune tolerance." Cell **133**(5): 775-787.
Samstein, R. M., A. Arvey, S. Z. Josefowicz, X. Peng, A. Reynolds, R. Sandstrom, S. Neph, P. Sabo, J. M. Kim, W. Liao, M. O. Li, C. Leslie, J. A. Stamatoyannopoulos and A. Y. Rudensky (2012). "Foxp3 exploits a pre-existent enhancer landscape for regulatory T cell lineage specification." Cell **151**(1): 153-166.
Sandler, H., J. Kreth, H. T. Timmers and G. Stoecklin (2011). "Not1 mediates recruitment of the deadenylase Caf1 to mRNAs targeted for degradation by tristetraprolin." Nucleic Acids Res **39**(10): 4373-4386.
Sawicka, K., M. Bushell, K. A. Spriggs and A. E. Willis (2008). "Polypyrimidine-tract-binding protein: a multifunctional RNA-binding protein." Biochem Soc Trans **36**(Pt 4): 641-647.
Schiering, C., T. Krausgruber, A. Chomka, A. Frohlich, K. Adelmann, E. A. Wohlfert, J. Pott, T. Griseri, J. Bollrath, A. N. Hegazy, O. J. Harrison, B. M. J. Owens, M. Lohning, Y. Belkaid, P. G. Fallon and F. Powrie (2014). "The alarmin IL-33 promotes regulatory T-cell function in the intestine." Nature **513**(7519): 564-568.
Schmidl, C., M. Klug, T. J. Boeld, R. Andreesen, P. Hoffmann, M. Edinger and M. Rehli (2009). "Lineage-specific DNA methylation in T cells correlates with histone methylation and enhancer activity." Genome Res **19**(7): 1165-1174.
Serdar, L. D., D. L. Whiteside and K. E. Baker (2016). "ATP hydrolysis by UPF1 is required for efficient translation termination at premature stop codons." Nat Commun **7**: 14021.
Shevach, E. M. and A. M. Thornton (2014). "tTregs, pTregs, and iTregs: similarities and differences." Immunol Rev **259**(1): 88-102.
Shi, Y. (2012). "Alternative polyadenylation: new insights from global analyses." RNA **18**(12): 2105-2117.
Shi, Y. and J. L. Manley (2015). "The end of the message: multiple protein-RNA interactions define the mRNA polyadenylation site." Genes Dev **29**(9): 889-897.
Skinner, S. O., H. Xu, S. Nagarkar-Jaiswal, P. R. Freire, T. P. Zwaka and I. Golding (2016). "Single-cell analysis of transcription kinetics across the cell cycle." Elife **5**: e12175.
Smith, E. L., H. M. Finney, A. M. Nesbitt, F. Ramsdell and M. K. Robinson (2006). "Splice variants of human FOXP3 are functional inhibitors of human CD4+ T-cell activation." Immunology **119**(2): 203-211.
Sojka, D. K., Y. H. Huang and D. J. Fowell (2008). "Mechanisms of regulatory T-cell suppression - a diverse arsenal for a moving target." Immunology **124**(1): 13-22.
Surh, C. D. and J. Sprent (2008). "Homeostasis of naive and memory T cells." Immunity **29**(6): 848-862.
Sysoev, V. O., B. Fischer, C. K. Frese, I. Gupta, J. Krijgsveld, M. W. Hentze, A. Castello and A. Ephrussi (2016). "Global changes of the RNA-bound proteome during the maternal-to-zygotic transition in Drosophila." Nat Commun **7**: 12128.
Szostak, E. and F. Gebauer (2013). "Translational control by 3'-UTR-binding proteins." Brief Funct Genomics **12**(1): 58-65.

Takahashi, T., Y. Kuniyasu, M. Toda, N. Sakaguchi, M. Itoh, M. Iwata, J. Shimizu and S. Sakaguchi (1998). "Immunologic self-tolerance maintained by CD25+CD4+ naturally anergic and suppressive T cells: induction of autoimmune disease by breaking their anergic/suppressive state." Int Immunol **10**(12): 1969-1980.
Tan, D., M. Zhou, M. Kiledjian and L. Tong (2014). "The ROQ domain of Roquin recognizes mRNA constitutive-decay element and double-stranded RNA." Nat Struct Mol Biol **21**(8): 679-685.
Tang, Q. and J. A. Bluestone (2008). "The Foxp3+ regulatory T cell: a jack of all trades, master of regulation." Nat Immunol **9**(3): 239-244.
Tarique, M., C. Saini, R. A. Naqvi, N. Khanna, A. Sharma and D. N. Rao (2017). "IL-12 and IL-23 modulate plasticity of FoxP3(+) regulatory T cells in human Leprosy." Mol Immunol **83**: 72-81.
Tarun, S. Z., Jr. and A. B. Sachs (1996). "Association of the yeast poly(A) tail binding protein with translation initiation factor eIF-4G." EMBO J **15**(24): 7168-7177.
Taylor, G. A., E. Carballo, D. M. Lee, W. S. Lai, M. J. Thompson, D. D. Patel, D. I. Schenkman, G. S. Gilkeson, H. E. Broxmeyer, B. F. Haynes and P. J. Blackshear (1996). "A pathogenetic role for TNF alpha in the syndrome of cachexia, arthritis, and autoimmunity resulting from tristetraprolin (TTP) deficiency." Immunity **4**(5): 445-454.
Teixeira, D., U. Sheth, M. A. Valencia-Sanchez, M. Brengues and R. Parker (2005). "Processing bodies require RNA for assembly and contain nontranslating mRNAs." RNA **11**(4): 371-382.
Theil, K., M. Herzog and N. Rajewsky (2018). "Post-transcriptional Regulation by 3' UTRs Can Be Masked by Regulatory Elements in 5' UTRs." Cell Rep **22**(12): 3217-3226.
Thornton, A. M. and E. M. Shevach (1998). "CD4+CD25+ immunoregulatory T cells suppress polyclonal T cell activation in vitro by inhibiting interleukin 2 production." J Exp Med **188**(2): 287-296.
Tian, B., J. Hu, H. Zhang and C. S. Lutz (2005). "A large-scale analysis of mRNA polyadenylation of human and mouse genes." Nucleic Acids Res **33**(1): 201-212.
Treiber, T., N. Treiber, U. Plessmann, S. Harlander, J. L. Daiss, N. Eichner, G. Lehmann, K. Schall, H. Urlaub and G. Meister (2017). "A Compendium of RNA-Binding Proteins that Regulate MicroRNA Biogenesis." Mol Cell **66**(2): 270-284 e213.
Turgeon, M. (2012). "Clinical hematology: Theory and procedures." LWW **5th edition**.
Turner, M., A. Galloway and E. Vigorito (2014). "Noncoding RNA and its associated proteins as regulatory elements of the immune system." Nat Immunol **15**(6): 484-491.
Uehata, T. and S. Akira (2013). "mRNA degradation by the endoribonuclease Regnase-1/ZC3H12a/MCPIP-1." Biochim Biophys Acta **1829**(6-7): 708-713.
Utrera, R., L. Collavin, D. Lazarevic, D. Delia and C. Schneider (1998). "A novel p53-inducible gene coding for a microtubule-localized protein with G2-phase-specific expression." EMBO J **17**(17): 5015-5025.
Vahl, J. C., C. Drees, K. Heger, S. Heink, J. C. Fischer, J. Nedjic, N. Ohkura, H. Morikawa, H. Poeck, S. Schallenberg, D. Riess, M. Y. Hein, T. Buch, B. Polic, A. Schonle, R. Zeiser, A. Schmitt-Graff, K. Kretschmer, L. Klein, T. Korn, S. Sakaguchi and M. Schmidt-Supprian (2014). "Continuous T cell receptor signals maintain a functional regulatory T cell pool." Immunity **41**(5): 722-736.
Verhagen, J., L. Gabrysova, E. R. Shepard and D. C. Wraith (2014). "Ctla-4 modulates the differentiation of inducible Foxp3+ Treg cells but IL-10 mediates their function in experimental autoimmune encephalomyelitis." PLoS One **9**(9): e108023.
Vignali, D. A., L. W. Collison and C. J. Workman (2008). "How regulatory T cells work." Nat Rev Immunol **8**(7): 523-532.
Vincent, M. and S. Schnell (2016). "A collection of intrinsic disorder characterizations from eukaryotic proteomes." Sci Data **3**: 160045.
Vinuesa, C. G., M. C. Cook, C. Angelucci, V. Athanasopoulos, L. Rui, K. M. Hill, D. Yu, H. Domaschenz, B. Whittle, T. Lambe, I. S. Roberts, R. R. Copley, J. I. Bell, R. J. Cornall and C. C. Goodnow (2005). "A RING-type ubiquitin ligase family member required to repress follicular helper T cells and autoimmunity." Nature **435**(7041): 452-458.

Viswanathan, S. R., G. Q. Daley and R. I. Gregory (2008). "Selective blockade of microRNA processing by Lin28." Science **320**(5872): 97-100.
Wahle, E. and G. S. Winkler (2013). "RNA decay machines: deadenylation by the Ccr4-not and Pan2-Pan3 complexes." Biochim Biophys Acta **1829**(6-7): 561-570.
Walker, M. R., D. J. Kasprowicz, V. H. Gersuk, A. Benard, M. Van Landeghen, J. H. Buckner and S. F. Ziegler (2003). "Induction of FoxP3 and acquisition of T regulatory activity by stimulated human CD4+CD25- T cells." J Clin Invest **112**(9): 1437-1443.
Wang, E. T., R. Sandberg, S. Luo, I. Khrebtukova, L. Zhang, C. Mayr, S. F. Kingsmore, G. P. Schroth and C. B. Burge (2008). "Alternative isoform regulation in human tissue transcriptomes." Nature **456**(7221): 470-476.
Wei, L., G. Vahedi, H. W. Sun, W. T. Watford, H. Takatori, H. L. Ramos, H. Takahashi, J. Liang, G. Gutierrez-Cruz, C. Zang, W. Peng, J. J. O'Shea and Y. Kanno (2010). "Discrete roles of STAT4 and STAT6 transcription factors in tuning epigenetic modifications and transcription during T helper cell differentiation." Immunity **32**(6): 840-851.
Weischenfeldt, J., I. Damgaard, D. Bryder, K. Theilgaard-Monch, L. A. Thoren, F. C. Nielsen, S. E. Jacobsen, C. Nerlov and B. T. Porse (2008). "NMD is essential for hematopoietic stem and progenitor cells and for eliminating by-products of programmed DNA rearrangements." Genes Dev **22**(10): 1381-1396.
Wessels, H. H., K. Imami, A. G. Baltz, M. Kolinski, A. Beldovskaya, M. Selbach, S. Small, U. Ohler and M. Landthaler (2016). "The mRNA-bound proteome of the early fly embryo." Genome Res **26**(7): 1000-1009.
Wilczynska, A., C. Aigueperse, M. Kress, F. Dautry and D. Weil (2005). "The translational regulator CPEB1 provides a link between dcp1 bodies and stress granules." J Cell Sci **118**(Pt 5): 981-992.
Wittkopp, N., E. Huntzinger, C. Weiler, J. Sauliere, S. Schmidt, M. Sonawane and E. Izaurralde (2009). "Nonsense-mediated mRNA decay effectors are essential for zebrafish embryonic development and survival." Mol Cell Biol **29**(13): 3517-3528.
Workman, C. J., A. L. Szymczak-Workman, L. W. Collison, M. R. Pillai and D. A. Vignali (2009). "The development and function of regulatory T cells." Cell Mol Life Sci **66**(16): 2603-2622.
Xu, J., W. Peng, Y. Sun, X. Wang, Y. Xu, X. Li, G. Gao and Z. Rao (2012). "Structural study of MCPIP1 N-terminal conserved domain reveals a PIN-like RNase." Nucleic Acids Res **40**(14): 6957-6965.
Yoon, J. H., S. De, S. Srikantan, K. Abdelmohsen, I. Grammatikakis, J. Kim, K. M. Kim, J. H. Noh, E. J. White, J. L. Martindale, X. Yang, M. J. Kang, W. H. Wood, 3rd, N. Noren Hooten, M. K. Evans, K. G. Becker, V. Tripathi, K. V. Prasanth, G. M. Wilson, T. Tuschl, N. T. Ingolia, M. Hafner and M. Gorospe (2014). "PAR-CLIP analysis uncovers AUF1 impact on target RNA fate and genome integrity." Nat Commun **5**: 5248.
Yoshida, M., K. Yoshida, G. Kozlov, N. S. Lim, G. De Crescenzo, Z. Pang, J. J. Berlanga, A. Kahvejian, K. Gehring, S. S. Wing and N. Sonenberg (2006). "Poly(A) binding protein (PABP) homeostasis is mediated by the stability of its inhibitor, Paip2." EMBO J **25**(9): 1934-1944.
Yu, M. and S. J. Levine (2011). "Toll-like receptor, RIG-I-like receptors and the NLRP3 inflammasome: key modulators of innate immune responses to double-stranded RNA viruses." Cytokine Growth Factor Rev **22**(2): 63-72.
Zhai, G., M. Iskandar, K. Barilla and P. J. Romaniuk (2001). "Characterization of RNA aptamer binding by the Wilms' tumor suppressor protein WT1." Biochemistry **40**(7): 2032-2040.
Zhao, D. M., A. M. Thornton, R. J. DiPaolo and E. M. Shevach (2006). "Activated CD4+CD25+ T cells selectively kill B lymphocytes." Blood **107**(10): 3925-3932.
Zheng, Y., A. Chaudhry, A. Kas, P. deRoos, J. M. Kim, T. T. Chu, L. Corcoran, P. Treuting, U. Klein and A. Y. Rudensky (2009). "Regulatory T-cell suppressor program co-opts transcription factor IRF4 to control T(H)2 responses." Nature **458**(7236): 351-356.

Zheng, Y., S. Josefowicz, A. Chaudhry, X. P. Peng, K. Forbush and A. Y. Rudensky (2010). "Role of conserved non-coding DNA elements in the Foxp3 gene in regulatory T-cell fate." Nature **463**(7282): 808-812.
Zheng, Y. and A. Y. Rudensky (2007). "Foxp3 in control of the regulatory T cell lineage." Nat Immunol **8**(5): 457-462.
Zhou, X., S. L. Bailey-Bucktrout, L. T. Jeker, C. Penaranda, M. Martinez-Llordella, M. Ashby, M. Nakayama, W. Rosenthal and J. A. Bluestone (2009). "Instability of the transcription factor Foxp3 leads to the generation of pathogenic memory T cells in vivo." Nat Immunol **10**(9): 1000-1007.
Zhou, Y., S. Basu, E. Laue and A. A. Seshia (2016). "Single cell studies of mouse embryonic stem cell (mESC) differentiation by electrical impedance measurements in a microfluidic device." Biosens Bioelectron **81**: 249-258.
Zhu, J., H. Yamane and W. E. Paul (2010). "Differentiation of effector CD4 T cell populations (*)." Annu Rev Immunol **28**: 445-489.
Ziegler, S. F. (2006). "FOXP3: of mice and men." Annu Rev Immunol **24**: 209-226.
Zou, W. (2006). "Regulatory T cells, tumour immunity and immunotherapy." Nat Rev Immunol **6**(4): 295-307.

12. Supplements

12.1 List of Figures

Figure 1: Components of innate and adaptive immunity (modified from Dranoff 2004) 6
Figure 2: Regulatory T cell development (modified from Lee and Lee 2018) 8
Figure 3: Mechanisms of suppression by regulatory T cells (modified from Workman, Szymczak-Workman et al. 2009) 10
Figure 4: Mechanisms of post-transcriptional gene regulation (modified from Kojima, Shingle et al. 2011) 13
Figure 5: Prominent RNA-binding proteins regulating mRNA stability (modified from Kovarik, Ebner et al. 2017) 17
Figure 6: Vector backbone of pMSCVpuro. 33
Figure 7: Experimental setup for total mRNA pull down 36
Figure 8: Verification experiments for total mRNA pull down 44
Figure 9: Quantitative analysis of T_{eff} and T_{Foxp3+} RBPome 45
Figure 10: Semi-quantitative analysis of T_{eff} and T_{Foxp3+} RBPome 45
Figure 11: Validation of mRNA binding of selected proteins identified in the RBPome dataset 46
Figure 12: Classification of $CD4^+$ expressed genes, $CD4^+$ proteome and $CD4^+$ RBPome datasets into known and previously unknown RBPs 47
Figure 13: Functional characterization of $CD4^+$ RBPome 48
Figure 14: Overview of proteins and their domains and regions that are not classified as RNA binding by GO 49
Figure 15: Number of proteins containing classical, non-classical, or unknown RNA binding domains in the $CD4^+$ RBPome 50
Figure 16: Biophysical features of $CD4^+$ RBPome 51
Figure 17: Overlap of the combined $CD4^+$ RBPome (proteins detected in either T_{eff} or T_{Foxp3+} cells) with other previously identified mammalian RBPome datasets. 52
Figure 18: Percentage of proteins of the $CD4^+$ RBPome that are known to be associated to an immune function 53
Figure 19: Overlap of the T_{eff} and T_{Foxp3+} RBPome 53
Figure 20: Classification of T_{eff} and T_{Foxp3+} RBPome datasets into known and previously unknown RBPs 54
Figure 21: Scatterplot of RNA sequencing FPKM values in T_{Foxp3+} versus T_{eff} cells of proteins, which were identified in the combined $CD4^+$ RBPome 55
Figure 22: Integration of the analyses of Figures 17-19 and Figure 21 with a more detailed analysis of the known immune related function of a protein and the PubMed identifier of the respective publication 56
Figure 23: Efficiency of specific mRNA pull down 57
Figure 24: Foxp3 upregulation in response to cytokines 61
Figure 25: Effects of different cytokines on Foxp3 62
Figure 26: Foxp3 qPCR race primers and mRNA isoforms 63

12.2 List of tables

Table 1: Antibodies for cell culture 21
Table 2: Western Blot antibodies 21
Table 3: FACS antibodies 21

Table 4: Cytokines 22
Table 5: Cloning Primers 22
Table 6: qPCR Primers 23
Table 7: Oligonucleotides for specific mRNA pull down 23
Table 8: Chemicals 26
Table 9: Enzymes 27
Table 10: Kits 27
Table 11: Devices 28
Table 12: Software 28
Table 13: Two-step PCR 32
Table 14: One-step PCR 32
Table 15: Distribution of isoforms of *Foxp3* mRNA in different cell types. 63

12.3 List of supplementary tables

Supplementary Table 1: Gene names and Ensemble IDs of proteins identified in the $CD4^+$ RBPome 95
Supplementary Table 2: Gene names and Ensemble IDs of proteins not previously identified in other mammalian RBPome datasets (T cell unique) 99
Supplementary Table 3: Gene names and Ensemble IDs of proteins preferentially identified in the T_{eff} RBPome 99
Supplementary Table 4: Gene names and Ensemble IDs of proteins preferentially identified in the T_{Foxp3+} RBPome 101
Supplementary Table 5: Gene names and Ensemble IDs of proteins identified in the $CD4^+$ RBPome but in neither total proteome dataset 101

12.4 List of abbreviations and scientific notation

The following format was used for genes, RNAs or proteins:

Gene *RNA* Protein

Murine gene – *Zfp36*
Human gene – *ZFP36*

In principle the terms Treg and T_{Foxp3+} cell can be used interchangeably as they both refer to regulatory T cells. In this thesis we use 'T_{Foxp3+} cells' to specifically denote cells differentiated *in vitro* towards regulatory T cells, while 'Treg cells' denotes cells differentiated in an *in vivo* system.

%	Percent
°C	Degree Celsius
(v/w)	Volume per weight

(w/w)	Mass per weight
APA	Alternative polyadenylation
ARE	AU-rich element
Bp	Basepairs
BSA	Bovine serum albumin
CD4	Cluster of differentiation
cDNA	Complementary DNA
CDS	Coding sequence
ChIRP	Chromatin isolation by RNA purification
DNA	Deoxyribonucleic acid
DTT	Dithiothreitol
ER	Endoplasmatic reticulum
eYFP	Enhanced yellow fluorescent protein
FL	Full length
FPKM	Fragments per kilobase of transcript per million mapped reads
GAPDH	Glyceraldehyde-3-phosphate dehydrogenase
GFP	Green fluorescent protein
GO	Gene ontology
h	Hours
Iap	Intracisternal particle A
ICOS	Inducible T cell co-stimulatory molecule
IDR	Intrinsically disordered protein region
IRES	Internat ribosomal entry site
kDa	Kilo Dalton
LC-MS/MS	Liquid chromatography with tandem mass spectrometry
lncRNA	Long non-coding RNA
MFI	Mean fluorescence intensity
min	Minute
miRNA	microRNA
mRNA	Messenger RNA
MS	Mass spectrometry
ms	Millisecond
NAD(H)	Nicotinamide adenine dinucleotide
PAGE	Polyacrylamide gel electrophoresis
PBS	Phosphate-buffered saline
PCR	Polymerase chain reaction
pH	Potentio hydrogenii
Poly(A) tail	Polyadenylated 3´end of mRNA
ppm	Parts per million
PVDF	polyvinylidenfluoride
RBP	RNA-binding protein
RBPome	RNA-binding proteome
RFP	Red fluorescent protein
RNA	Ribonucleic acid
RNase	Ribonuclease
rRNA	Ribosomal RNA
rpm	Revolutions per minute
RT	Room temperature
s	Seconds
SDS	Sodium dodecyl sulfate
snRNA	Small nuclear RNA
SSC	Saline-sodium citrate
STAT	Signal transducer and activator of transcription

TCR	T cell receptor
TF	Transcription factor
TLR	Toll-like receptor
Treg	Regulatory T cell
U	Enzyme unit
UTR	Untranslated region
UV	Ultraviolet
V	Volt
ZF	Zinc finger

Supplementary Table 1: Gene names and Ensemble IDs of proteins identified in the CD4$^+$ RBPome

Gene name	Ensembl Gene ID
A230050P20Rik	ENSMUSG00000038884
Ago2	ENSMUSG00000036698
Akap8	ENSMUSG00000024045
Ankhd1	ENSMUSG00000024483
Ankrd17	ENSMUSG00000055204
Anxa2	ENSMUSG00000032231
Api5	ENSMUSG00000027193
Apobec3	ENSMUSG00000009585
Atxn2	ENSMUSG00000042605
Atxn2l	ENSMUSG00000032637
Boll	ENSMUSG00000025977
Caprin1	ENSMUSG00000027184
Casc3	ENSMUSG00000078676
Ccar2	ENSMUSG00000033712
Ccdc9	ENSMUSG00000041375
Celf1	ENSMUSG00000005506
Celf2	ENSMUSG00000002107
Cirbp	ENSMUSG00000045193
Cnbp	ENSMUSG00000030057
Cnot1	ENSMUSG00000036550
Cnot2	ENSMUSG00000020166
Cnot4	ENSMUSG00000038784
Cpeb4	ENSMUSG00000020300
Crip1	ENSMUSG00000006360
Csde1	ENSMUSG00000068823
Cstf2	ENSMUSG00000031256
Dazap1	ENSMUSG00000069565
Ddx1	ENSMUSG00000037149
Ddx17	ENSMUSG00000055065
Ddx21	ENSMUSG00000020075
Ddx3y	ENSMUSG00000069045
Ddx5	ENSMUSG00000020719
Ddx6	ENSMUSG00000032097
Dhx29	ENSMUSG00000042426
Dhx30	ENSMUSG00000032480
Dhx36	ENSMUSG00000027770
Dhx57	ENSMUSG00000035051
Dhx9	ENSMUSG00000042699
Dis3l2	ENSMUSG00000053333

Edf1	ENSMUSG00000015092
Eif2a	ENSMUSG00000027810
Eif3a	ENSMUSG00000024991
Eif3c	ENSMUSG00000030738
Eif3d	ENSMUSG00000016554
Eif3g	ENSMUSG00000070319
Eif3l	ENSMUSG00000033047
Eif4a1	ENSMUSG00000059796
Eif4a3	ENSMUSG00000025580
Eif4b	ENSMUSG00000058655
Eif4enif1	ENSMUSG00000020454
Eif4g1	ENSMUSG00000045983
Eif4g2	ENSMUSG00000005610
Eif4g3	ENSMUSG00000028760
Eif4h	ENSMUSG00000040731
Elavl1	ENSMUSG00000040028
Ewsr1	ENSMUSG00000009079
Fam120a	ENSMUSG00000038014
Fam120c	ENSMUSG00000025262
Fam98a	ENSMUSG00000002017
Fmr1	ENSMUSG00000000838
Fubp1	ENSMUSG00000028034
Fubp3	ENSMUSG00000026843
Fus	ENSMUSG00000030795
Fxr1	ENSMUSG00000027680
Fxr2	ENSMUSG00000018765
Fyttd1	ENSMUSG00000022800
G3bp1	ENSMUSG00000018583
G3bp2	ENSMUSG00000029405
Grsf1	ENSMUSG00000044221
Hdlbp	ENSMUSG00000034088
Helz	ENSMUSG00000020721
Hnrnpa0	ENSMUSG00000007836
Hnrnpa1	ENSMUSG00000046434
Hnrnpa2b1	ENSMUSG00000004980
Hnrnpa3	ENSMUSG00000059005
Hnrnpab	ENSMUSG00000020358
Hnrnpc	ENSMUSG00000060373
Hnrnpd	ENSMUSG00000000568
Hnrnpdl	ENSMUSG00000029328
Hnrnpf	ENSMUSG00000042079
Hnrnph1	ENSMUSG00000007850
Hnrnph2	ENSMUSG00000045427
Hnrnph3	ENSMUSG00000020069
Hnrnpk	ENSMUSG00000021546
Hnrnpl	ENSMUSG00000015165
Hnrnpll	ENSMUSG00000024095
Hnrnpm	ENSMUSG00000059208
Hnrnpr	ENSMUSG00000066037
Hnrnpul2	ENSMUSG00000071659
Igf2bp3	ENSMUSG00000029814
Ilf2	ENSMUSG00000001016
Ilf3	ENSMUSG00000032178
Khdrbs1	ENSMUSG00000028790
Khsrp	ENSMUSG00000007670
Kif1c	ENSMUSG00000020821
Larp1	ENSMUSG00000037331
Larp1b	ENSMUSG00000025762

Larp4	ENSMUSG00000023025
Larp4b	ENSMUSG00000033499
Ldha	ENSMUSG00000063229
Lrpprc	ENSMUSG00000024120
Lsm14a	ENSMUSG00000066568
Lsm14b	ENSMUSG00000039108
Map4	ENSMUSG00000032479
Marf1	ENSMUSG00000060657
Mbnl1	ENSMUSG00000027763
Mbnl3	ENSMUSG00000036109
Mov10	ENSMUSG00000002227
Mrps31	ENSMUSG00000031533
Mrps35	ENSMUSG00000040112
Mrps5	ENSMUSG00000027374
Mrps7	ENSMUSG00000046756
Msi2	ENSMUSG00000069769
Msn	ENSMUSG00000031207
Mtdh	ENSMUSG00000022255
Mtpap	ENSMUSG00000024234
Myef2	ENSMUSG00000027201
Myh9	ENSMUSG00000022443
Ncl	ENSMUSG00000026234
Nfx1	ENSMUSG00000028423
Nono	ENSMUSG00000031311
Nufip2	ENSMUSG00000037857
Nxf1	ENSMUSG00000010097
Pabpc1	ENSMUSG00000022283
Pabpc4	ENSMUSG00000011257
Pabpn1	ENSMUSG00000022194
Patl1	ENSMUSG00000046139
Pcbp1	ENSMUSG00000051695
Pcbp2	ENSMUSG00000056851
Poldip3	ENSMUSG00000041815
Ppia	ENSMUSG00000071866
Prdx1	ENSMUSG00000028691
Prrc2b	ENSMUSG00000039262
Pspc1	ENSMUSG00000021938
Ptbp1	ENSMUSG00000006498
Ptbp3	ENSMUSG00000028382
Ptcd2	ENSMUSG00000021650
Ptcd3	ENSMUSG00000063884
Puf60	ENSMUSG00000002524
Pum1	ENSMUSG00000028580
Pum2	ENSMUSG00000020594
Pura	ENSMUSG00000043991
Purb	ENSMUSG00000094483
R3hdm1	ENSMUSG00000056211
R3hdm2	ENSMUSG00000025404
Rack1	ENSMUSG00000020372
Raly	ENSMUSG00000027593
Raver1	ENSMUSG00000010205
Rbm10	ENSMUSG00000031060
Rbm14	ENSMUSG00000006456
Rbm15	ENSMUSG00000048109
Rbm22	ENSMUSG00000024604
Rbm3	ENSMUSG00000031167
Rbm45	ENSMUSG00000042369
Rbm6	ENSMUSG00000032582

Rbms1	ENSMUSG00000026970
Rbms2	ENSMUSG00000040043
Rbmxl1	ENSMUSG00000037070
Rc3h1	ENSMUSG00000040423
Rpl4	ENSMUSG00000032399
Rpl8	ENSMUSG00000003970
Rps10	ENSMUSG00000052146
Rps11	ENSMUSG00000003429
Rps12	ENSMUSG00000061983
Rps14	ENSMUSG00000024608
Rps15	ENSMUSG00000063457
Rps18	ENSMUSG00000008668
Rps20	ENSMUSG00000028234
Rps23	ENSMUSG00000049517
Rps24	ENSMUSG00000025290
Rps25	ENSMUSG00000009927
Rps26	ENSMUSG00000025362
Rps28	ENSMUSG00000067288
Rps3	ENSMUSG00000030744
Rps3a1	ENSMUSG00000028081
Rps5	ENSMUSG00000012848
Rps7	ENSMUSG00000061477
Rps8	ENSMUSG00000047675
Rpsa	ENSMUSG00000032518
Rsl1d1	ENSMUSG00000005846
Rtcb	ENSMUSG00000001783
Sarnp	ENSMUSG00000078427
Secisbp2	ENSMUSG00000035139
Secisbp2l	ENSMUSG00000035093
Serbp1	ENSMUSG00000036371
Sf1	ENSMUSG00000024949
Sf3b1	ENSMUSG00000025982
Sf3b4	ENSMUSG00000068856
Sfpq	ENSMUSG00000028820
Slirp	ENSMUSG00000021040
Smg6	ENSMUSG00000038290
Smg7	ENSMUSG00000042772
Snd1	ENSMUSG00000001424
Srsf1	ENSMUSG00000018379
Srsf2	ENSMUSG00000034120
Srsf3	ENSMUSG00000071172
Srsf5	ENSMUSG00000021134
Srsf6	ENSMUSG00000016921
Srsf7	ENSMUSG00000024097
Ssb	ENSMUSG00000068882
Stau1	ENSMUSG00000039536
Syncrip	ENSMUSG00000032423
Taf15	ENSMUSG00000020680
Tardbp	ENSMUSG00000041459
Tbrg4	ENSMUSG00000000384
Tdrd3	ENSMUSG00000022019
Tia1	ENSMUSG00000071337
Tial1	ENSMUSG00000030846
Tnrc6a	ENSMUSG00000052707
Tnrc6b	ENSMUSG00000047888
Tnrc6c	ENSMUSG00000025571
Trim25	ENSMUSG00000000275
Trim56	ENSMUSG00000043279

U2af1	ENSMUSG00000061613
U2af2	ENSMUSG00000030435
Ubap2	ENSMUSG00000028433
Ubap2l	ENSMUSG00000042520
Unk	ENSMUSG00000020770
Upf1	ENSMUSG00000058301
Usp10	ENSMUSG00000031826
Xrn1	ENSMUSG00000032410
Xrn2	ENSMUSG00000027433
Ybx1	ENSMUSG00000028639
Ybx3	ENSMUSG00000030189
Ythdc1	ENSMUSG00000035851
Ythdc2	ENSMUSG00000034653
Ythdf1	ENSMUSG00000038848
Ythdf2	ENSMUSG00000040025
Ythdf3	ENSMUSG00000047213
Zc3h11a	ENSMUSG00000102976
Zc3h14	ENSMUSG00000021012
Zc3h7a	ENSMUSG00000037965
Zc3h7b	ENSMUSG00000022390
Zc3hav1	ENSMUSG00000029826
Zcchc11	ENSMUSG00000034610
Zcchc6	ENSMUSG00000035248
Zfp326	ENSMUSG00000029290
Zfp36l2	ENSMUSG00000045817
Zfr	ENSMUSG00000022201
Znfx1	ENSMUSG00000039501

Supplementary Table 2: Gene names and Ensemble IDs of proteins not previously identified in other mammalian RBPome datasets (T cell unique)

With human ortholog	
Gene name	**Ensembl Gene ID**
Adamts12	ENSMUSG00000047497
Aven	ENSMUSG00000003604
Boll	ENSMUSG00000025977
Capzb	ENSMUSG00000028745
Chtf8	ENSMUSG00000046691
Crip1	ENSMUSG00000006360
Gtse1	ENSMUSG00000022385
Ptpn6	ENSMUSG00000004266
Stat1	ENSMUSG00000026104
Stat4	ENSMUSG00000062939
Vav1	ENSMUSG00000034116
Without human ortholog	
Gene name	**Ensembl Gene ID**
Cnn2	ENSMUSG00000004665
Rps27	ENSMUSG00000090733
Iap	

Supplementary Table 3: Gene names and Ensemble IDs of proteins preferentially identified in the T_{eff} RBPome

Gene name	**Ensembl Gene ID**

Adar	ENSMUSG00000027951
Ahnak	ENSMUSG00000069833
Akap1	ENSMUSG00000018428
Alkbh5	ENSMUSG00000042650
Aqr	ENSMUSG00000040383
Ascc3	ENSMUSG00000038774
Aven	ENSMUSG00000003604
Bclaf3	ENSMUSG00000044150
Capzb	ENSMUSG00000028745
Ccdc124	ENSMUSG00000007721
Chtf8	ENSMUSG00000046691
Cnn2	ENSMUSG00000004665
Cnot9	ENSMUSG00000026174
Coro1a	ENSMUSG00000030707
Dap	ENSMUSG00000039168
Dhx8	ENSMUSG00000034931
Eif2s1	ENSMUSG00000021116
Eif3b	ENSMUSG00000056076
Eif3h	ENSMUSG00000022312
Fastkd2	ENSMUSG00000025962
Grb2	ENSMUSG00000059923
Gtse1	ENSMUSG00000022385
Hcls1	ENSMUSG00000022831
Iap	
Lcp1	ENSMUSG00000021998
Mbnl2	ENSMUSG00000022139
Mkrn2	ENSMUSG00000000439
Mybbp1a	ENSMUSG00000040463
Ncbp3	ENSMUSG00000020783
Pa2g4	ENSMUSG00000025364
Parp12	ENSMUSG00000038507
Ppig	ENSMUSG00000042133
Ppil4	ENSMUSG00000015757
Prrc2a	ENSMUSG00000024393
Ptpn6	ENSMUSG00000004266
Rbm15b	ENSMUSG00000074102
Rbm47	ENSMUSG00000070780
Rnf213	ENSMUSG00000070327
Rpl37	ENSMUSG00000041841
Rps13	ENSMUSG00000090862
Rps19	ENSMUSG00000040952
Rps27	ENSMUSG00000090733
Snw1	ENSMUSG00000021039
Spen	ENSMUSG00000040761
Srpk1	ENSMUSG00000004865
Srsf9	ENSMUSG00000029538
Ssbp1	ENSMUSG00000029911
Stat1	ENSMUSG00000026104
Stat4	ENSMUSG00000062939
Strap	ENSMUSG00000030224
Strbp	ENSMUSG00000026915
Tnpo1	ENSMUSG00000009470
Tpi1	ENSMUSG00000023456
Vav1	ENSMUSG00000034116
Zcchc17	ENSMUSG00000028772
Zfp36l1	ENSMUSG00000021127
Zfp598	ENSMUSG00000041130

Supplementary Table 4: Gene names and Ensemble IDs of proteins preferentially identified in the T_{Foxp3+} RBPome

Gene name	Ensembl Gene ID
Adamts12	ENSMUSG00000047497
Cfl1	ENSMUSG00000056201
Edc4	ENSMUSG00000036270
Rbm4	ENSMUSG00000094936
Rpl26	ENSMUSG00000060938
Thrap3	ENSMUSG00000043962

Supplementary Table 5: Gene names and Ensemble IDs of proteins identified in the $CD4^+$ RBPome but in neither total proteome dataset

Gene name	Ensembl Gene ID
A230050P20Rik	ENSMUSG00000038884
Boll	ENSMUSG00000025977
Cnot2	ENSMUSG00000020166
Cpeb4	ENSMUSG00000020300
Dhx57	ENSMUSG00000035051
Fam120c	ENSMUSG00000025262
Kif1c	ENSMUSG00000020821
Larp1b	ENSMUSG00000025762
Nfx1	ENSMUSG00000028423
R3hdm1	ENSMUSG00000056211
R3hdm2	ENSMUSG00000025404
Rbms2	ENSMUSG00000040043
Rc3h1	ENSMUSG00000040423
Secisbp2	ENSMUSG00000035139
Secisbp2l	ENSMUSG00000035093
Tnrc6a	ENSMUSG00000052707
Tnrc6c	ENSMUSG00000025571
Ybx3	ENSMUSG00000030189
Ythdc2	ENSMUSG00000034653
Zc3h7b	ENSMUSG00000022390
Zcchc11	ENSMUSG00000034610
Zfp36l2	ENSMUSG00000045817
Znfx1	ENSMUSG00000039501